

Department of Mechanical and Aerospace Engineering

**A Feasibility Study on Active Solar Space Heating  
Technology for Office Buildings in Greece**

Author: Evangelos Kyrou

Supervisor: Dr. Daniel Cóstola

A thesis submitted in partial fulfilment for the requirement of the degree

Master of Science

Sustainable Engineering: Renewable Energy Systems and the Environment

2016

## Copyright Declaration

This thesis is the result of the author's original research. It has been composed by the author and has not been previously submitted for examination which has led to the award of a degree.

The copyright of this thesis belongs to the author under the terms of the United Kingdom Copyright Acts as qualified by University of Strathclyde Regulation 3.50. Due acknowledgement must always be made of the use of any material contained in, or derived from, this thesis.

Signed: Evangelos Kyrou

Date: 31/08/16

A handwritten signature in blue ink, appearing to be 'EK', with a long horizontal line extending to the right.

## Abstract

This study explores the feasibility of using solar thermal collector systems with storage capacity and conventional radiators to support space heating applications of office buildings in Greece. A dynamic simulation model in ESP-r tool is employed to analyse the performance of the building-integrated solar collector system for different demand profiles in all the climatic zones of Greece.

The impact of the storage system capacity, the collector area and the tilt angle are investigated as to what extent the overall system performance is influenced. The offices in Greece are approximated within various yearly demand scenarios, determined by the building orientation, the location and the exposure to the outer environment.

Finally, an attempt is made to extrapolate the findings to the whole office building stock of Greece, after the essential fabric upgrades have been implemented. From that point, using the proposed active solar space heating system, further thermal energy savings of 29 % are achievable in total due to solar coverage, leading to significant CO<sub>2</sub> emissions abatement of approximately 184 kt per year for the offices throughout the country.

## Acknowledgements

Firstly, I would like to thank my supervisor Dr. Daniel Cóstola for his continuous guidance and support throughout the project execution. Also, for appreciating my efforts and encouraging me to the fulfilment of my research targets, despite the difficulties.

I am also grateful to all my teachers this year, who have imparted their knowledge to us with remarkable dedication and enthusiasm.

I would specially like to extend my gratitude to all my friends here in Glasgow who have always been so supportive during this demanding year, as well as those who have encouraged me to my efforts from far away, or to take up my Master's studies in the first place.

Finally and most importantly, I would like to express my deepest thanks to my family for their constant and unfailing support. Thank you for having faith in me and doing everything possible to help me succeed. Without your love and encouragement, I never would have come this far.

## Table of contents

Abstract.....	3
Acknowledgements.....	4
Table of contents.....	5
Nomenclature.....	8
List of Figures.....	9
List of Tables.....	12
1. Introduction.....	15
1.1. Background – Motivation/Problem to be addressed.....	15
1.2. Scope/Phasing.....	17
1.3. Project Aim.....	19
1.4. Approach/Methods.....	19
1.4.1. Dynamic Modelling Tool (ESP-r).....	20
1.5. Deliverables/Outcomes.....	21
2. Review of solar energy utilisation.....	23
2.1. Introduction.....	23
2.2. Low temperature solar thermal.....	23
2.2.1. Solar thermal system overview.....	24
2.2.2. Solar collector types.....	26
2.3. Flat plate collector.....	28
2.3.1. Thermal vector fluid.....	29
2.3.2. Absorber plate.....	30
2.3.3. Insulating layer.....	30
2.3.4. Covering plate.....	31
2.3.5. Collector case.....	32

2.3.6.	Efficiency of the collector.....	32
2.3.7.	Hydraulic connection of panels .....	34
2.3.8.	Synopsis .....	35
2.4.	Typology of solar system .....	35
2.4.1.	Open and closed systems .....	36
2.4.2.	Natural and forced circulation systems.....	37
2.4.3.	Final typology selection.....	39
2.5.	Storage tank.....	41
2.6.	Solar circuit .....	45
2.7.	Conclusion.....	48
3.	Modelling of active solar system.....	49
3.1.	Introduction .....	49
3.2.	ESP-r model description.....	49
3.2.1.	Dimensioning and geometry .....	52
3.2.2.	Construction materials .....	56
3.2.3.	Operational details .....	60
3.2.4.	Surface connections and boundary conditions.....	61
3.2.5.	Control loops.....	62
3.2.6.	Integrated simulation parameters .....	64
3.3.	Climatic data .....	65
4.	Energy performance of model and system selection .....	68
4.1.	Introduction .....	68
4.2.	Initial design of the model.....	70
4.3.	Impact of specific storage tank volume.....	72
4.4.	Impact of collector area with standard specific storage size.....	75

4.5.	Impact of collector tilt angle .....	78
4.6.	Conclusion.....	83
5.	Energy performance at different building exposure .....	84
5.1.	Introduction .....	84
5.2.	Building orientation.....	84
5.3.	Climatic zones .....	89
5.4.	Exposure of building surfaces .....	91
5.5.	Conclusion.....	95
6.	Extrapolation to office building stock in Greece .....	97
6.1.	Introduction / Disclaimer .....	97
6.2.	Overview of office sector in Greece .....	97
6.2.1.	Analysis and assumptions for the estimation of share by fuel for the thermal energy used for space heating of offices in Greece.....	99
6.3.	Realisation of active solar system for space heating of offices in Greece ..	101
6.4.	Environmental performance appraisal and conclusions.....	104
7.	Final discussion .....	108
8.	Proposals for further investigation .....	109
9.	References .....	110
10.	Appendix.....	116

## Nomenclature

**$\eta$** : efficiency of collector

**$q_{av}$** : heat acquired from the thermal vector fluid at a certain time unit (available heat)

**$q_{in}$** : heat received on the surface of the collector at a certain time unit (input heat)

**$R$** : thermal resistance in  $m^2 \cdot K/W$

**U-value**: thermal transmittance in  $W/(m^2 \cdot K)$

**ac/h**: air changes per hour

**CIBSE**: Chartered Institution of Building Services Engineers

**$k$** : thermal conductivity in  $W/(m \cdot K)$

**$\rho$** : density in  $kg/m^3$

**$c_p$** : specific heat in  $J/(kg \cdot K)$

**$Q_{aux}$** : thermal energy delivered from the auxiliary (conventional) heating system, in kWh per year, while the solar system provides energy to the building

**$Q_{total}$** : total thermal energy required for space heating from the conventional system without the solar system, in kWh per year

**PJ**: petajoules ( $10^{15}$  joules)

**kt**: kilotonnes ( $10^3$  tonnes or  $10^6$  kg)

## List of Figures

Figure 1: Climatic zones of Greek territory (Source: Papamanolis, 2015).....	18
Figure 2: Overview of a typical low temperature solar thermal building application (Source: Thoubboron, 2015).....	25
Figure 3: Typical layout of an active/pumped solar heating system (Source: Solar Sense, 2013).....	26
Figure 4: Flat plate collector elements (Source: GreenSpec, 2016) .....	29
Figure 5: Heat transfer processes occurring in a typical flat plate solar collector (Source: Quaschnig, 2004).....	33
Figure 6: Forced circulation closed loop solar heating system with radiators, including an additional heating source (Source: Solar King, 2016) .....	39
Figure 7: Storage tank in a typical combined system for space heating and hot water supply (Source: Solar365, 2016).....	42
Figure 8: Typical cylindrical tall and narrow storage tank (Source: ArchiEXPO, 2016) .....	44
Figure 9: ESP-r model cellular_expl_sdhw of two adjacent cellular offices with zone- based SDHW (GitHub, 2016) .....	50
Figure 10: Base case model of two adjacent cellular offices (cellular_bc) .....	51
Figure 11: Office manager_a overview .....	52
Figure 12: Corridor zone overview .....	53
Figure 13: Solar collector in ESP-r model.....	54
Figure 14: Storage tank in ESP-r model .....	55
Figure 15: Radiator in ESP-r model.....	56
Figure 16: Casual gains in a typical weekday for each office .....	61

Figure 17: Heating and cooling schedules for the two offices in different day types .	63
Figure 18: Location of simulated climates in Greece (Source: Papamanolis, 2015)...	65
Figure 19: Yearly graphs of dry bulb temperatures in each area.....	67
Figure 20: Monthly solar fractions for the initial scenario in Kastoria.....	72
Figure 21: Yearly and monthly solar fraction comparisons with different specific storage tank volumes.....	74
Figure 22: Yearly and monthly solar fraction comparisons with different combinations of collector area – tank size (70 L/m <sup>2</sup> ).....	76
Figure 23: Yearly convection losses through transparent covering (glazing) of collectors and through opaque surface of tank with different combinations of collector area – tank size (70 L/m <sup>2</sup> ) .....	77
Figure 24: Yearly and monthly solar fraction comparisons with different tilt angles .	80
Figure 25: Monthly solar fractions for different tilt angles and collation with heating demands .....	81
Figure 26: Solar panel inclination depending on the sun’s position (Source: BeNature, 2015) .....	82
Figure 27: Specific heating demands before and after the implementation of the active solar system and respective yearly solar fractions with different orientations of building for Kastoria.....	86
Figure 28: ESP-r model with north-facing windows .....	87
Figure 29: ESP-r model with west-facing windows .....	88
Figure 30: Specific heating demands before and after the active solar system implementation and respective yearly solar fractions for all the climatic zones of Greece with west orientation of building (low demand) .....	90

Figure 31: Yearly mean values of temperature and direct solar radiation in each climatic zone .....	91
Figure 32: Yearly solar fraction comparisons between the two office rooms in all the climatic zones of Greece for the west orientation of building .....	92
Figure 33: Specific heating demands before and after the implementation of the active solar system and respective yearly solar fractions for all the climatic zones of Greece with west orientation of building (high demand).....	94
Figure 34: Estimation (based on assumptions) of share by fuel for the energy used for space heating of the offices in Greece .....	101
Figure 35: Specific heating demands before and after the active solar system implementation and respective yearly solar fractions for each climatic zone and total of Greece in the final combined scenario after extrapolation to the whole office sector .....	104
Figure 36: CO <sub>2</sub> emissions abatement in kilotonnes (kt) per year compared to the office floor area distribution in each climatic zone, after the implementation of the active solar system in the total number of offices .....	106

## List of Tables

Table 1: Breakdown of barriers to solar space heating applications in Greece .....	17
Table 2: Main benefits and shortcomings of different solar collector types.....	27
Table 3: Breakdown of zones defined in ESP-r model cellular_expl_sdhw (GitHub, 2016) .....	50
Table 4: Parameters of the active solar system included at the initial design of the model.....	50
Table 5: Geometry attributes of each office (manager_a, manager_b) .....	53
Table 6: Geometry attributes of the corridor .....	54
Table 7: Collector plates dimensions and resulting collector area in the model (initially) .....	55
Table 8: Double glazing construction details.....	56
Table 9: Insulation frame construction details (spandral, window frame, collector case frame).....	57
Table 10: Office walls construction details .....	57
Table 11: Ceiling construction details .....	57
Table 12: Floor construction details .....	58
Table 13: Corridor back wall construction details.....	58
Table 14: Absorber plates construction details.....	59
Table 15: Transparent covering (single glazing) construction details.....	59
Table 16: Storage tank construction details.....	60
Table 17: Level of exposure of office building in the “low demand” scenario .....	62
Table 18: Yearly stats for climatic characteristics in each area.....	66
Table 19: Yearly heating demands for the two offices in Kastoria before and after the implementation of the active solar system.....	70

Table 20: Monthly and annual simulated demands and solar fractions for the two offices in Kastoria for the initial scenario.....	72
Table 21: Yearly simulated results comparison with different specific storage tank volumes.....	73
Table 22: Yearly simulated results comparison with different combinations of collector area – tank size (70 L/m <sup>2</sup> ).....	75
Table 23: Yearly simulated results comparison with different tilt angles.....	79
Table 24: Yearly simulated results comparison with different orientations of building for Kastoria.....	85
Table 25: Yearly simulated results comparison between the climatic zones of Greece for west orientation of building (low demand).....	89
Table 26: Yearly simulated results comparison between the two office rooms in all the climatic zones of Greece for the west orientation of building.....	92
Table 27: Yearly simulated results comparison between the climatic zones of Greece for west orientation of building (high demand).....	94
Table 28: Low demand office building.....	95
Table 29: High demand office building.....	96
Table 30: Distribution of office buildings in Greece (2002–2010) by climatic zone (Source: Gaglia et al., 2007: 1163).....	98
Table 31: Summary of total energy share by fuel (based on assumption and data) and by use (based on data) for the office sector in Greece.....	100
Table 32: Final combined scenario for the average office demands and the performance of the active solar system in Greece (average of low and high demand scenarios).....	102

Table 33: Percentage share by fuel for office space heating and specific CO <sub>2</sub> emissions factors used.....	105
Table 34: Final total thermal energy demand reduction and CO <sub>2</sub> emissions abatement per year after the implementation of the active solar system in the offices of whole Greece .....	106
Table 35: Coordinates of vertices for collec_low zone .....	116
Table 36: Coordinates of vertices for collec_mid zone .....	116
Table 37: Coordinates of vertices for collec_hi zone .....	117
Table 38: Coordinates of vertices for col_casee zone .....	117

# 1. Introduction

## 1.1. Background – Motivation/Problem to be addressed

Solar thermal systems are used nowadays for a wide range of applications; domestic hot water (DHW), swimming pools heating, space heating (SH), district heat, process heat, solar cooling and electricity production from solar thermal power plants (Streicher, 2016). Capturing free energy from the sun, these systems generate low-cost and environmentally friendly thermal energy. While solar energy markets have been established worldwide over the past decades (Streicher, 2016), particularly Mediterranean countries of southern Europe, have come up with very well-developed solar thermal markets (ESTIF, 2014), managing to take advantage of their high levels of solar irradiation (OME, 2012).

Focusing on Greece, solar thermal collectors have been popular mostly for domestic applications for hot water provision systems. The main solar thermal product in the country has been the thermosiphon water heater. Greece's solar thermal market has been active for well above 30 years, allowing the country to have one of the highest solar thermal capacities within Europe for many years (Giakoumi and Iatridis, 2009).

Giakoumi and Iatridis (2009) also state that domestic hot water (DHW) production constitutes the impressive 98 % of the total installed solar thermal collector area in Greece. On the other hand, little consideration has been given to the utilisation of the solar thermal technology for space heating (SH), which comprised not nearly as much as 1% of the installed collector area in the country in 2009.

Moreover, according to the general trend in Greece, Renewable Energy Sources (RES) have been mostly associated with the electricity generation rather than the heating sector. Thusly, apart from the hot water supply, for which the solar integration was at 31.4 % in 2004 among other sources, space heating in Greece is basically provided by non-RES with negligible solar integration (Giakoumi and Iatridis, 2009).

There has been a number of independent studies on the development of active solar space heating systems for different countries worldwide. The design of an experimental solar energy facility for Spanish housing (Marcos, Izquierdo and Parra, 2011) as well as the TRNSYS model-based sensitivity analysis of a solar heating

system for a Greek multi-storey building (Stegou-Sagia, Koronaki and Sagia, 2010) have made considerable efforts to assess the applicability and viability of active solar thermal technology for Mediterranean countries.

However, as depicted from the lack of sufficient data in the national statistics services of Greece, as well as from the absence of relevant policy schemes for the support of the renewables heating sector (Giakoumi and Iatridis, 2009), it is apparent that the focus has remained on electricity rather than the heating from RES. This partly explains why the results of the above and other relevant works on solar heating systems (Sobhy, Brakez and Benhamou, 2015) have not been applied to a greater extent for the case of Greece.

Among the lack of policies, plans and programmes (PPPs) to support solar space heating applications, financial barriers have also restrained the growth of this sector in Greece. During a time period when the aftermath of the financial crisis has strongly affected Greek economy, initial capital cost investments as well as potential increased maintenance requirements have deterred people from replacing old heating systems with new ones. While high investment costs compared to conventional systems are common to most renewable energy technologies (OME, 2012), additionally there are technical difficulties that arise regarding solar space heating, for example when it comes to refurbishing older buildings and integrating underfloor heating systems. In each case, specific incentive programmes need to be implemented in order to reduce the gap between the solar thermal and the traditional technologies and help overcome the aforementioned financial and technical barriers (OME, 2012).

Another important barrier relevant to most renewable technologies, including solar thermal, is the lack of certain knowledge combined with the underlying distrust of people to new technologies. To put it more clearly, not enough effort has been made to prove the feasibility, reliability and competitiveness of solar heating technology in case the right signals are given to market operators (OME, 2012).

After all, most people in Greece have not even been aware of the potential benefits from the exploitation of solar energy to fuel their space heating (SH) circuits, except for providing domestic hot water (DHW). Therefore, campaigns raising public awareness, accompanied with stringent certification schemes for quality assurance of new technologies, could help overcome existing hurdles and progressively lead to reliable commercial solutions for solar space heating applications in the country.

This study will endeavor to provide a technical solution for the office/commercial building stock of Greece. The aforementioned barriers, as listed in Table 1, which have kept solar thermal market sluggish for space heating applications in the country, need to be overcome. Focus needs to be maintained to offering insight into reliable solar space heating technology as well as examining the conditions under which this technology would gain ground and be adopted to a greater extent for heating up Greek buildings.

<i>Barriers</i>	
#1	<b>Regulatory</b> (lack of PPPs or incentive schemes)
#2	<b>Financial</b> (financial crisis, high investment costs)
#3	<b>Technical</b> (gaps between old and new technologies)
#4	<b>Lack of knowledge</b> (mistrust to new technologies)
#5	<b>Lack of public awareness</b> (lack of campaigns)

*Table 1: Breakdown of barriers to solar space heating applications in Greece*

## 1.2. Scope/Phasing

During this study, the validity of relevant previous works shall be enhanced, by using a model which effectively describes a non-domestic active solar space heating system and how it would perform as integrated to an exemplar office building. This model could also be valid for other Mediterranean countries with similar climatic characteristics to the areas under investigation, for example Spain or Italy. The benchmark for assessing the validity of the model could rely on the comparison between current results and previously measured or simulated results.

The model describing a typical commercial solar thermal application for space heating in Greece will take into account already popular technologies, as for example flat plate solar collectors. This study will also exploit the conventional heating system configuration of radiators to deliver the energy of the solar system into the building.

Nevertheless, different system configurations such as an underfloor or a wall-integrated heating system could perform more efficiently and are proposed for further investigation (Peuser et al., 2002: 29).

The Greek territory is divided into four climatic zones based on heating degree days (from the warmest zone A to the coldest D), according to the Greek legislation scheme KENAK (YPEKA, 2010). These zones are displayed in Figure 1. It is important to note that during this work the presentation of results will be more extensive for climatic zone D, which has a harsher climate in relation to the rest of the country, according to the climatic data of regions in Greece (TEE, 2012). Hence, an investigation on the potential and feasibility of active solar space heating technology would be scientifically and practically more interesting for this part of northern Greece, adding value to previous studies where this area has not been particularly examined. However, results for all the climatic zones will eventually be integrated and compared to each other.

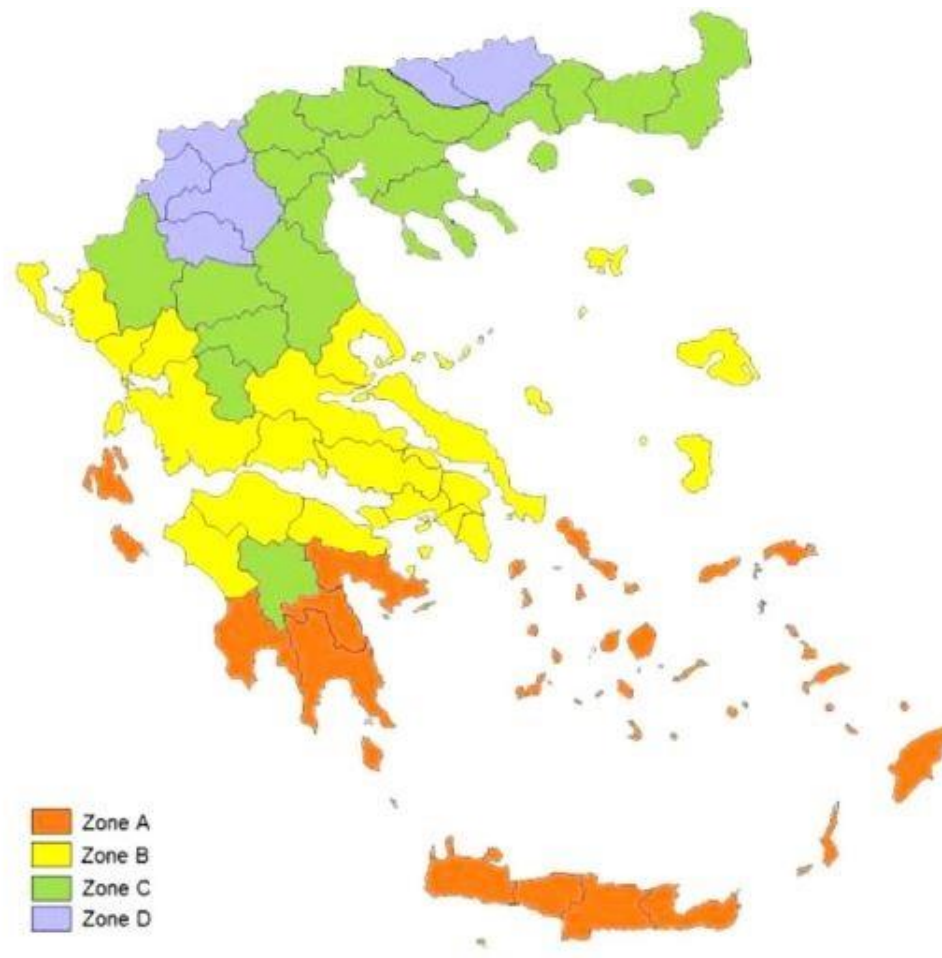


Figure 1: Climatic zones of Greek territory (Source: Papamanolis, 2015)

The storage tank size, the collector area and tilt angle of the panels will be investigated regarding their impact on the overall performance, and the resulting solar fraction will then be identified for the typical office/commercial application in Greece. A reliable system design, covering a proportion of the annual heating demands of the building, would be the outcome of this study, whilst providing a useful way to overcome the previously mentioned barriers. The energy and environmental performance of the designed system will finally be appraised in terms of thermal energy savings and CO<sub>2</sub> emissions abatement for the office sector in Greece.

Nevertheless, it is anticipated that the required equipment, in order to achieve a considerable demand reduction and make the building less dependent on other heating sources, would lead to potential issues with the generation of excessive heat in the summer (Chwieduk, 2016). While this project will not focus on dealing with the excess generation in the summer, useful solutions could be proposed for further investigation within future projects, such as underground heat storage for the winter (Chwieduk, 2016) or utilisation of heat for solar cooling (Angrisani et al., 2016).

### 1.3. Project Aim

The overall aim of the project is to evaluate the technical feasibility and assess the energy and environmental performance of active solar thermal technology with storage capacity and conventional radiators for space heating applications to the office buildings in Greece.

The assessment of the thermal energy savings and CO<sub>2</sub> emissions abatement will be extrapolated to the office sector of the country as a whole, as well as separating each climatic zone for inter-climatic comparisons.

### 1.4. Approach/Methods

The methodology is composed of the following key steps to be followed throughout the project:

- Provide design guidelines for the active solar thermal system, through the review of existing literature.
- Use a building model and adjust it to describe a typical office/commercial application for solar space heating in Greece. ESP-r software is a useful tool

for simulating the building-integrated active solar space heating system through dynamic modelling, as analysed later.

- Study the impact of storage capacity, collector area and, most importantly, tilt angle on the energy performance inside the model. Then, decide on the solar system capacity and collector angle to be solidly applied to the whole of Greece.
- Investigate how the selected active solar system performs in different building orientations, climatic zones and structural exposures, resulting in final “average” energy performance for each climatic zone.
- Extrapolate the “average” energy performance to the whole office/commercial building stock of Greece, so that the energy and environmental performance is ultimately appraised. Thermal energy savings and CO<sub>2</sub> emissions abatement result for the whole country, as well as for each climatic zone separately, as regards the offices, as part of the non-residential sector.
- Propose ideas for further investigation, such as how to deal effectively with potential issues or to increase the efficiency of the designed system.

#### 1.4.1. Dynamic Modelling Tool (ESP-r)

The modelling tool that has been selected for carrying out the dynamic simulation of active solar space heating systems for this research project is ESP-r, an integrated building/plant simulation tool. It is appropriate for modelling building performance and undertaking energy assessments, regarding heat, air flow, water flow, light and electrical calculations (ESRU, n.d.).

One of the absolute benefits of ESP-r tool that particularly fits this project is its suitability for the design of a building-integrated system, while all modelled elements mentioned above are possible to be incorporated into the same building domain. This holistic approach allows the well-informed user to be able to make improvements to the building model, taking advantage of the software’s range of features and performing an in-depth appraisal of the factors which affect the energy and environmental performance of the building. Its flexibility in building modelling makes ESP-r a powerful tool for research purposes like this, in addition to uses in teaching and consultancy contexts (ESRU, n.d.).

A potential drawback in the use of ESP-r could be that it requires specific or expert knowledge from the user so as to perform complex tasks. However, a worldwide development community, called GitHub, has been formed to manage the distribution of ESP-r source code and share specific knowledge among users. Especially, the efforts that have already been made in developing and distributing the ESP-r code for solar thermal applications though this community could definitely contribute to the successful accomplishment of this project (GitHub, 2016).

Furthermore, the availability of ESP-r tool under the open source licence (GitHub, 2016) and its confirmed validity through various studies and theses (Strachan, 2000), considering the high degree of expertise in the tool within the Mechanical & Aerospace Engineering Department of the University of Strathclyde, are additional reasons for choosing ESP-r for the modelling purposes of this study. Last but not least, since there are not any previous studies on active solar space heating systems that are based on ESP-r as a simulation tool, the novelty of this study is completely ensured.

### 1.5. Deliverables/Outcomes

After introducing an effective way to overcome existing barriers to active solar technology for office/commercial space heating applications in Greece, this study will endeavor to approach the problem from the engineering point of view and deal with underlying technical challenges. As a result, a reliable active solar system, meeting a proportion of the typical heating requirements of an office building in Greece, will be a useful outcome of this study, including suggestions on (Peuser et al., 2002: 305):

- The quality of system components (solar collectors, storage unit).
- The actual design, namely the solar system capacity (storage tank size, solar collector area) and orientation of the collector field (tilt and azimuth angles).

Consequently, these factors will influence the solar coverage fraction, namely the percentage of yearly space heating demands covered by solar energy, which will be determined for the proposed system in various orientations of the building, locations and exposures. Thusly, the energy performance of the solar system will be assessed in different yearly demand profiles. Lastly, the designed system will be evaluated in terms of its energy and environmental performance, estimating the energy savings and

CO<sub>2</sub> emissions abatement, associated with the office sector in every climatic zone of Greece and totally.

The analysis will start with an elaboration on the existing literature review on solar systems, providing details on system types, operating principles, materials and common design guidelines.

## 2. Review of solar energy utilisation

### 2.1. Introduction

Solar energy can be exploited in two main different ways:

- Heat production for domestic, commercial and industrial purposes (solar thermal energy).
- Electricity production by directly converting solar into electrical energy (photovoltaic solar energy).

The focus in this thesis is maintained on solar thermal energy utilisation. There are three basic types of solar thermal energy systems; low, medium and high temperature technologies (Wang and Ge, 2016).

Firstly, low temperature systems are used to heat fluids at temperatures usually less than 100 °C, by employing devices such as solar thermal collectors. The most common uses of low temperature systems is for sanitary hot water production, space heating for domestic or non-domestic purposes, swimming pool heating and industrial heating utilisation (Chwieduk, 2016).

On the contrary, medium temperature systems are able to heat fluids reaching temperatures higher than 100 °C but lower than 250 °C. One of the most common applications of these systems is the solar ovens, which are simple devices utilising solar radiant energy to cook food. Furthermore, there are high temperature technologies which usually concentrate solar radiation to thermal receivers; the so-called concentrating solar power (CSP) systems. These systems can reach temperatures of the working fluid higher than 250 °C and have numerous applications in electricity generation (Lorenzini et al., 2010).

This study focuses on the utilisation of low temperature solar thermal technology for space heating applications, which is described in detail in the following sections.

### 2.2. Low temperature solar thermal

Economic and environmental reasons usually justify the utilisation of low temperature solar thermal systems. Given the fact of significant energy bills reduction and pollutant emissions abatement, there is a solid advantage emerging for the communities, obtained from the use of solar energy.

Solar systems applications can also be financially justified by the payback period of the investment. For example, for the case of a solar thermal installation for the hot water production for a single family, the system cost will be around 1500-2600 €, being able to be paid back within 3-5 years on average. At the same time, the useful technical lifespan of the system is nearly 20 years, while its maintenance costs are 1% of the initial capital investment (Lorenzini et al., 2010).

The main working principles of low temperature solar thermal systems are basically the same, except for minor changes depending on the application. First of all, the solar collectors absorb the solar radiation and produce heat, which is then transferred to the fluid that crosses them, referred to as thermal vector fluid. After the fluid crosses the solar circuit, arrives at the accumulator where thermal energy is stored for future needs (Lorenzini et al., 2010).

An overview of a typical low temperature solar thermal installation is presented in the following section.

### 2.2.1. Solar thermal system overview

The general overview of a solar thermal system to heat water for space heating as well as hot water provision is shown in Figure 2 below for a typical building application. The system features hot water storage and controllers for the operation of the active solar water heating system, which will be explained as well as simulated later in this work for the specific space heating application in the Greek offices.

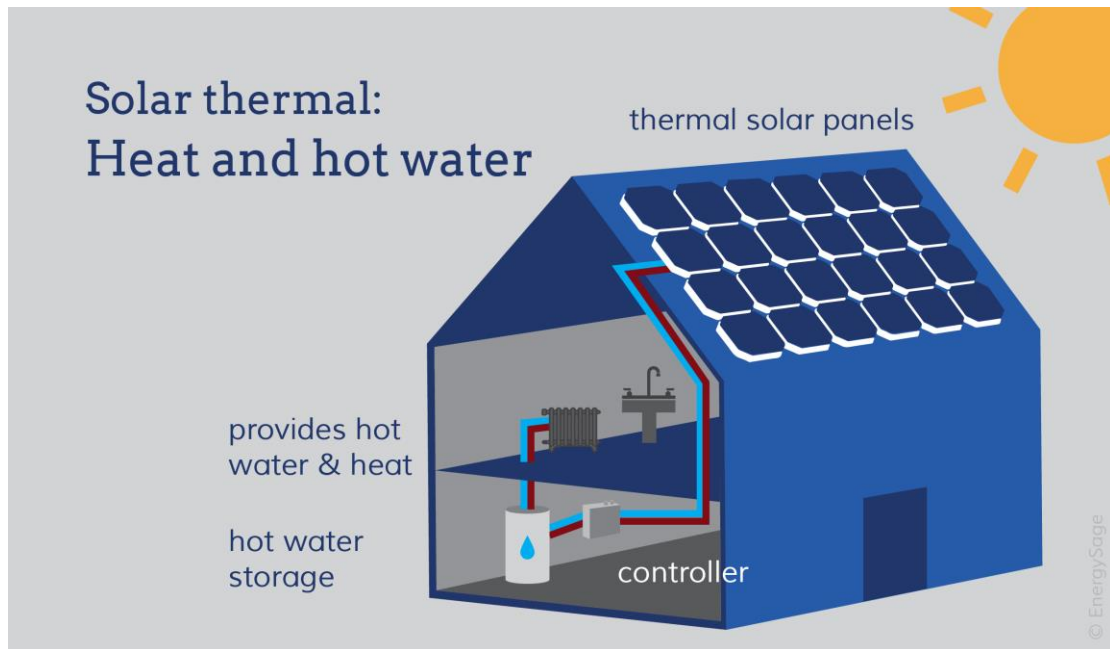


Figure 2: Overview of a typical low temperature solar thermal building application (Source: Thoubboron, 2015)

Solar space heaters (solar collector systems to provide space/room heating) utilise the energy of the sun to warm up a building. They commonly require a larger collector area, and subsequently more roof space, in relation to solar thermal for the provision of hot water only. Thermal energy is harnessed from the collectors and heats the working fluid, which is circulated to distribute the absorbed heat to the building zones (Thoubboron, 2015).

Solar thermal heating systems are classified into active and passive systems. While in passive systems collectors harness energy, which is then trapped and the heat is circulated naturally like in greenhouses, active solar systems use pumps and controllers to circulate heat within the system components. A typical configuration of an active/pumped solar heating system is displayed in Figure 3 below. Most buildings also require an auxiliary/back-up heating system, while solar space heaters can be integrated within the existing heating system of the building (DOE, 2016).

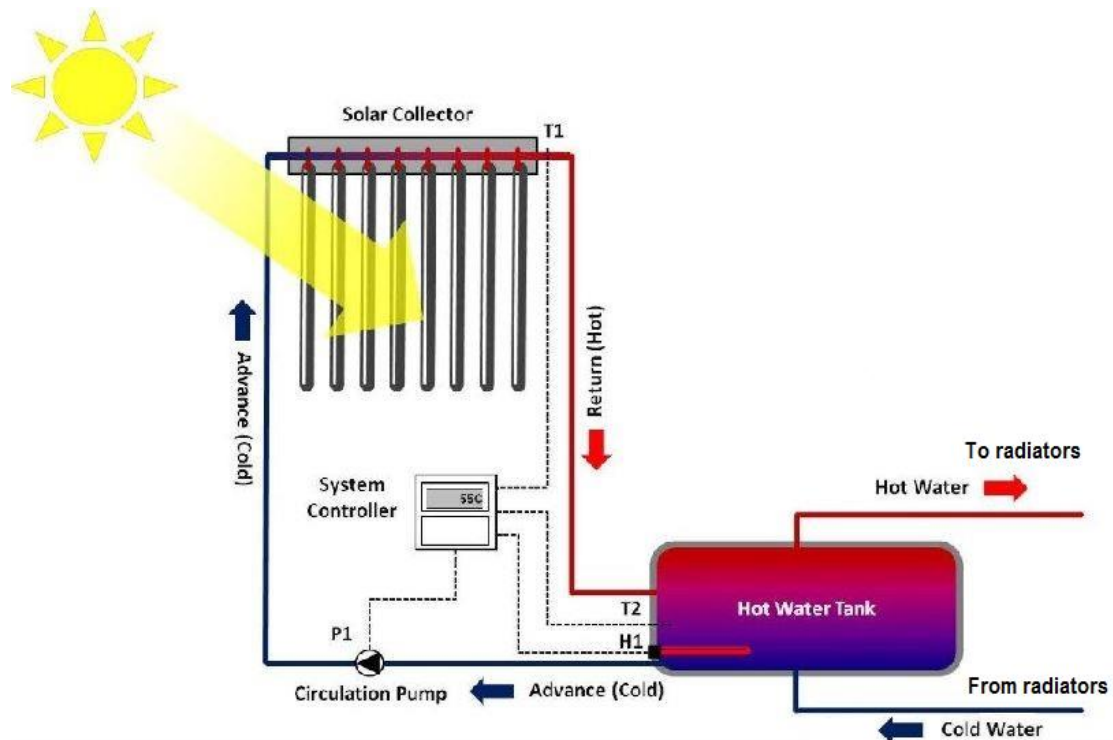


Figure 3: Typical layout of an active/pumped solar heating system (Source: Solar Sense, 2013)

Certainly, solar space heaters are more cost-effective when they replace an expensive fuel at the existing heating system, for example electricity, oil or propane. Cold climates with sufficient solar resources provide an energy- and cost-effective option for the application of active solar space heating systems (DOE, 2016). This is an inexpensive solution in areas where the building can be heated up from solar energy throughout the year, which is mostly the case in the above mentioned climate type. Solar space heating systems are very resistant and their life expectancy is estimated at nearly 20 years or above (Thoubboron, 2015).

The analysis of the low temperature solar thermal systems will start with their most important component, which is the solar collector.

### 2.2.2. Solar collector types

Several types of solar collectors have been developed depending on the application and possible uses. The main collector types captured within the respective bibliography (Peuser et al., 2002; Lorenzini et al., 2010; Chwieduk, 2016; The Renewable Energy Hub, 2016), as well as their advantages and disadvantages are

presented in Table 2 below, before deciding on the most appropriate collector type for the purposes of this study.

Type	Benefits	Downsides
<b>Flat plate collectors</b>	<ul style="list-style-type: none"> <li><input checked="" type="checkbox"/> Simple, robust structure</li> <li><input checked="" type="checkbox"/> Versatile</li> <li><input checked="" type="checkbox"/> Very common / technically perfected</li> <li><input checked="" type="checkbox"/> Medium cost</li> <li><input checked="" type="checkbox"/> Reasonable efficiency</li> <li><input checked="" type="checkbox"/> Excellent performance over price ratio</li> </ul>	<ul style="list-style-type: none"> <li><input checked="" type="checkbox"/> Not as efficient as evacuated tube collectors</li> </ul>
<b>Evacuated tube collectors</b>	<ul style="list-style-type: none"> <li><input checked="" type="checkbox"/> High efficiency</li> <li><input checked="" type="checkbox"/> Useful throughout the year</li> </ul>	<ul style="list-style-type: none"> <li><input checked="" type="checkbox"/> Expensive</li> </ul>
<b>Unglazed / pool collectors</b>	<ul style="list-style-type: none"> <li><input checked="" type="checkbox"/> Very economical</li> </ul>	<ul style="list-style-type: none"> <li><input checked="" type="checkbox"/> Useful only in the hot season</li> <li><input checked="" type="checkbox"/> Suitable for swimming pools or bathing establishments</li> </ul>
<b>Integrated storage collectors</b>	<ul style="list-style-type: none"> <li><input checked="" type="checkbox"/> Decreased cost of solar system</li> </ul>	<ul style="list-style-type: none"> <li><input checked="" type="checkbox"/> Useful mostly for mild climate zones</li> </ul>

*Table 2: Main benefits and shortcomings of different solar collector types*

The collector types most commonly used for active solar room heating applications are the flat plate and the evacuated tube collectors. Especially in Europe, the flat plate collector is very popular (Chwieduk, 2016). Since this study focuses on the development of a useful and inexpensive solution of a low temperature solar thermal system, which would ideally be applicable for wider office/commercial uses in the building sector in Greece, therefore the flat plate collector is deemed the most appropriate starting point for this development.

Certainly, improvements to different parts of the solar system, thus to the collector type as well, are always possible for further investigation. However, the flat plate collector type is characterised by the best performance over price ratio among the different collector types and, thereby, as for now focus will be maintained on the flat plate collector, which will firstly be analytically described and then incorporated into the active solar system design.

### 2.3. Flat plate collector

The basic aim of a generic solar collector is to convert the largest possible amount of the electromagnetic energy received from the solar radiation into useful thermal energy for the users by heating a working fluid (Duffie and Beckman, 2013). To achieve this, a flat plate collector needs to exploit the capacity of materials, which can be metals such as copper, or alloys such as steel, so as to heat up quickly from the incident solar radiation and to easily dispense the stored thermal energy. These are the fundamental characteristics of the absorber plate, which is crossed by tubes through which the working fluid flows and is warmed up (Lorenzini et al., 2010).

All the heat exchanges occurring between the plate-tube elements to elements other than the working fluid have to be minimum. Thusly, the parts of the plate which are not directly exposed, namely the posterior and the side parts, are covered with insulating materials to reduce conductive losses, while the temperature inside the collector is maintained at the highest level by virtue of the covering transparent plates which reduce convective and radiant losses to the atmosphere (Duffie and Beckman, 2013).

The structure of the flat plate collector is lined with an inflexible container case with insulation on the inside. The role of the transparent covering is to limit heat losses to the outer side and keep the inside temperature of the collector at its highest level, as mentioned before. At the same time, the transparent covering plate allows easy penetration of the incident solar radiation, which is thereafter intercepted by the absorber plate, a black metal plate lying below. In contact with the absorber plate surface, there are pipes where the thermal vector fluid flows and removes the absorbed heat (Lorenzini et al., 2010).

To better understand the structure and operation of the flat plate solar collector, its elements are displayed in Figure 4 below, as previously described.



Figure 4: Flat plate collector elements (Source: GreenSpec, 2016)

### 2.3.1. Thermal vector fluid

As regards the water mixtures for the thermal vector fluid, antifreeze solutions are important to prevent these mixtures from freezing. Actually, in areas where days and especially nights are very cold, combined with the lack of solar radiation, the freezing of the liquid will cause expansion and might damage the pipes or the collectors and, as a result, the operation of the solar circuit.

The common solution for the thermal vector fluid is a mixture of water with propylene glycol, which is a good antifreeze and generally non-toxic (Shojaeizadeh et al., 2014). However, either water alone or mere saline solutions can be used depending on the application. The main problems associated with the use of plain water as the thermal vector fluid are the limescale accumulation and its relatively high freezing point. To name the most important properties required for the thermal vector fluid (Lorenzini et al., 2010), these are:

- High density and high specific heat, so as to be used within pipes of small dimensions.
- Unable to cause corrosion in pipes and walls of the solar circuit.
- Stability and chemical inertia at temperatures lower than 100 °C.
- Restrained hardness to reduce limescale accumulation.

- Low freezing point.
- Low viscosity.
- Non-toxicity, when supplying sanitary hot water.

However, in the case of space heating applications like in the current study, the requirement of non-toxicity can be overridden (Lorenzini et al., 2010). In this case, a solution of water and ethylene glycol, which is a toxic antifreeze with higher specific heat capacity than propylene glycol, can also be used as long as it is confirmed there are no leakages out of the closed loop system (Marken and Olson, 2003).

### 2.3.2. Absorber plate

The metal plate which actually constitutes the absorber plate should have high thermal conductivity. The commonly used metals for this purpose are copper, which is the best option albeit heavy and expensive, aluminium, which is the most popular choice, or steel (Lorenzini et al., 2010; REUK, 2015). The outer surface of the absorber plate is covered by a dark absorbing coating, usually black chrome finish coating, to maximise heat collecting efficiency (GreenSpec, 2016). Solar radiation hitting the metal plate is mostly absorbed, whilst only a small percentage is reflected. As a result, heat is produced which is thereafter transferred to the copper pipe through the metal sheet (REUK, 2015). Finally, the thermal vector fluid, flowing inside the pipe, absorbs this heat. Apparently, the amount of radiation reflected back to the atmosphere has to be limited as much as possible for achieving higher utilisation of the incident solar radiation.

Plates made of steel have the disadvantages of the high thermal resistance and high thermal capacity, which make them less efficient when harnessing the thermal transitories associated with the passing of the clouds. On the other hand, aluminium plates need to be supplemented with dielectric joints, between the aluminium and the copper elements of the hydraulic circuit, to avoid corrosion caused by the formation of aluminium-copper piles (Lorenzini et al., 2010).

### 2.3.3. Insulating layer

It is important that there is an insulating layer which prevents conductive losses to the sides and the back of the panel (Streicher, 2016). Another way to limit heat

transmission to the outside of the panel is the existence of microscopic air spaces in between the internal insulating materials. This is the reason why the commonly utilised materials, such as polyurethane, polyester wool, stone wool or fiberglass, usually have a porous or alveolar structure. Moreover, a thin aluminium sheet can be used to cover insulating materials for two reasons. Firstly, to avoid humidity to be absorbed by these materials and, secondly, to reflect back to the absorber plate the energy received by radiation that would otherwise be lost (Lorenzini et al., 2010).

#### 2.3.4. Covering plate

As regards the covering plate of the collector, it has to be transparent to the wavelengths of the incident solar radiation, which are between 0.2 to 0.5  $\mu\text{m}$  on average, and opaque to the wavelengths of the infrared radiation coming from the plate and pipes when their temperatures increase, which are generally over 4  $\mu\text{m}$  (Lorenzini et al., 2010; Streicher, 2016). This is because the penetration of the received radiation needs to be increased as much as possible and, at the same time, energy losses to the atmosphere need to be limited.

These requirements for the covering plate can be met using glass, particularly after being treated to increase its transparency and resistance. Commonly, two sheets of tempered, prismatic and antireflection glass are used. Otherwise, sheets of plastic materials such as polycarbonate may be preferred, since they are lighter and less fragile than glass (Lorenzini et al., 2010). Nevertheless, the transparent covering plate could be characterized as the chink in the armor when trying to reduce the thermal losses of the collector to the atmosphere. Indeed, it is a surface which cannot be insulated properly due to its transparency requirements.

In contrast with the conductive losses which can easily be reduced by choosing a good insulating material towards the back and the sides of the panel, the convective losses through the air space between the absorber and the covering plate cannot easily be restricted. To make it clearer, as regards the convective losses, the air that comes into contact with the hot plate is heated up quickly moving up and transferring a significant part of its thermal energy to the cover. As previously analysed, the latter cannot have a proper thermal insulation, hence heat is lost towards the lower-temperature environment following its natural flow. This has an adverse impact on the performance of the collector (Kalidasan and Srinivas, 2014).

There are different ways to limit the convective heat losses through the air gap. One solution is the use of double glazing for the covering plate; the still (insulating) air space between the two glazings can effectively contain heat losses and make the collector more efficient than the single-glazed (Ozsoy, Demirer and Adam, 2014).

Another alternative would be the use of alveolar-structured polycarbonate for the transparent covering plate, which would create microscopic air spaces preventing heat losses and, additionally, would be lighter and cheaper. However, this material has optical properties which tend to deteriorate more quickly than those of glass, having a detrimental effect to the transparency of the covering plate and, therefore, to the amount of solar radiation entering the panel (Lorenzini et al., 2010).

### 2.3.5. Collector case

The role of collector case/housing is to make the collector structure compact and mechanically solid, while protecting it from atmospheric particles and dust. However, most importantly, the container case has to be completely waterproof, so as to prevent moisture from entering the collector (Peuser et al., 2002). If humidity enters the inner structure, it evaporates after contacting the hot plate and soon after it condenses onto the inner side of the transparent covering, when the outside temperature is low. This condensation ends up to reducing the transparency of the covering plate, which could have detrimental effects to the efficiency of the collector. Another effect humidity could have is raising the thermal conductivity of insulating materials inside the panels (Peuser et al., 2002).

The collector housing can be made of stainless steel (Lorenzini et al., 2010: 34) or galvanised steel (GreenSpec, 2016), which is usually zinc-plated. A common material choice for the casing includes aluminium, while plastic with fiberglass reinforcement can also be used (Lorenzini et al., 2010; GreenSpec, 2016).

### 2.3.6. Efficiency of the collector

To epitomize, the heat transfer processes, which occur in a flat plate solar collector and were analytically described above, are clearly depicted in Figure 5 below:

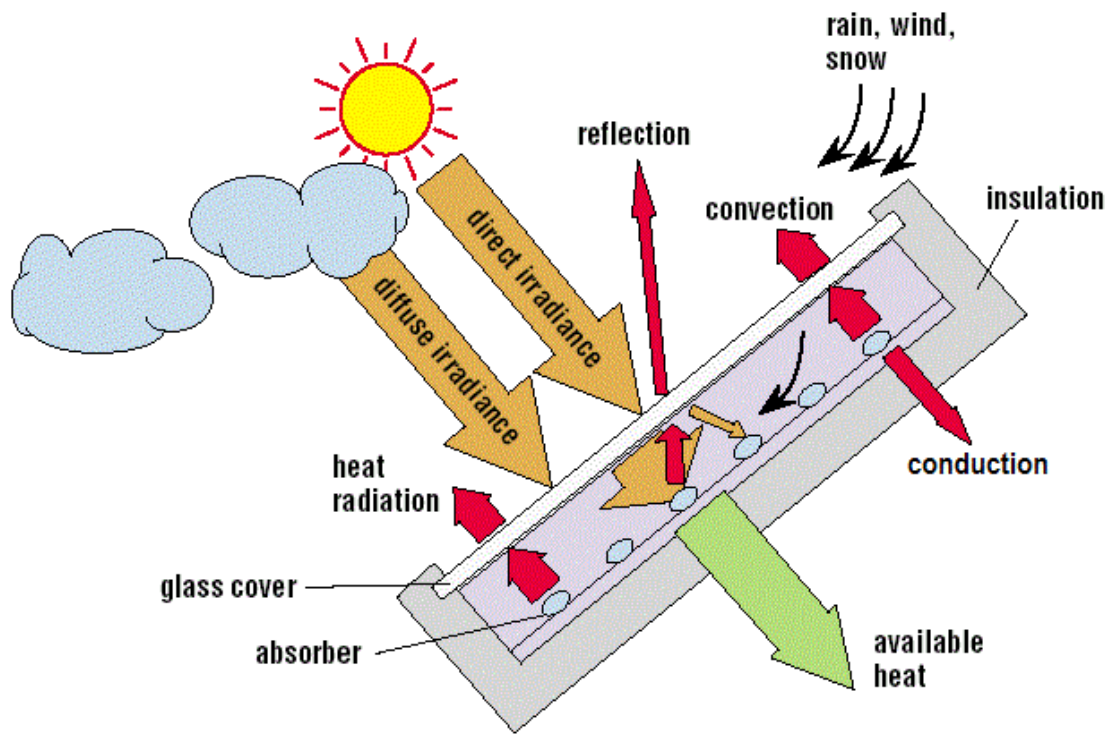


Figure 5: Heat transfer processes occurring in a typical flat plate solar collector (Source: Quaschnig, 2004)

These heat transfer processes determine the heat losses of the collector and, therefore, its overall efficiency.

The collector's efficiency ( $\eta$ ) is defined as the ratio of the amount of heat obtained from the thermal vector fluid ( $q_{av}$ : available heat) over the amount of heat received on the collector's surface ( $q_{in}$ : input heat) at a certain time scale:

$$\eta = q_{av} / q_{in}$$

The efficiency of the collector depends on several different factors and showcases its ability to exploit the incident solar radiation to meet the user's needs. Specifically, the collector's efficiency is a function of:

- The outside temperature and radiation conditions. For example, when the outer temperature becomes lower, the collector's losses are higher due to the difficulty to hold back the heat against the natural heat transmission processes.
- The temperature of the thermal vector fluid. For instance, when the temperature difference between the pipes and the fluid is greater, the heat exchange is quicker and more efficient.

- The characteristics of the collector's structure. Namely, the materials, the optical properties of the covering plate, the absorber plate as well as the connection between the plate and the pipes where the thermal vector fluid flows, all of these affect the collector's ability to limit the outward energy losses, hence to increase its efficiency.

In practice, the formula below can be used to represent an estimation of the collector's efficiency ( $\eta$ ), since the analytical formula is much more complex than this:

$$\eta = A - B \cdot \Delta T^*$$

$$\Delta T^* = (T_{fm} - T_a) / G$$

(Lorenzini et al., 2010)

Where:

A: constant, represents the maximum solar radiation which can actually enter the panel and reach the fluid, taking into account the material's optical properties.

B: constant, represents the collector's ability to hold back the acquired heat.

G: global radiation per  $m^2$  which is received by an intercepting surface in a time unit ( $W/m^2$ ).

$T_{fm}$ : average temperature of the thermal vector fluid flowing inside the panel.

$T_a$ : ambient temperature.

### 2.3.7. Hydraulic connection of panels

There are several different specific hydraulic connection plans for solar collectors, described as follows (Lorenzini et al., 2010):

- The parallel connection involves panels working with the same sending and return temperatures.
- There is the parallel connection with inverse return, which requires longer pipe length.

- The series connection is usually applied to a maximum of five panels while the temperature progressively increases, resulting in a higher final temperature.
- Lastly, the series/parallel connection is the most inexpensive to achieve, so that it is mostly used in small-scale systems with only two solar panels.

### 2.3.8. Synopsis

Ultimately, what makes the glazed flat plate collector so popular in the worldwide market is its versatility. Particularly, the various ways it can be used as well as the different working conditions under which it performs efficiently. The most common use of the flat plate collector is definitely for sanitary hot water production.

After all, the main reason to choose the flat plate solar collector for the space heating application in this study is its excellent performance over price ratio, which makes it stand out from all the other available commercial solutions in Greece. The average lifespan of this collector exceeds 20 years, while the temperatures of the water it provides are usually between 30 °C and 90 °C (Lorenzini et al., 2010).

Not only the flat plate collector can exploit the solar source effectively in most climate types and respond satisfactory at various latitudes and altitudes, but also it can provide a year round hot water output. The possible uses of this collector vary from small solar installations for sanitary hot water production to medium or large scale systems for space heating schemes in residential or commercial applications, like in this particular study. Another possible use of the flat plate collectors could be for low temperature solar heating applications in industrial contexts.

## 2.4. Typology of solar system

After elaborating on the solar collector, which is the most important element of the active solar system, the description will continue with a number of necessary parts of the system that can make it compact and reliable to the end users. This section will result in the basic typologies used in commercial solar systems, their benefits and the typology selected for the current system installation.

Firstly, the principal elements of the solar system, in addition to the collectors, will be introduced (Duffie and Beckman, 2013):

- The storage tank, whose role is to store the hot water produced by the collectors and supply it to the system at different times and weather conditions, when needed. Except for storing the heated water, its role also involves maintaining its temperature at a constant level, if possible, or at least without significant temperature fluctuations.
- The auxiliary or back-up system is essential in every kind of installation so as to provide its energy to the building since the solar source is intermittent and not always available, especially during the winter months. It is usually a central-heating boiler working on fossil fuels, such as an oil or gas boiler, or an electric-powered heater. Otherwise, oversizing of the solar system would be required leading the system to huge costs and without guaranteeing 100 % solar energy coverage by any means.
- The expansion tube is an important element for protecting the system from overpressures by absorbing any excessive expansions of the working fluid.
- System check valves and safety bolts include the intercepting valve, the “jolly” valve, thermostats and other devices, analysed later in this chapter.
- Circulator pumps, control station and other elements can only be met in specific types of systems.

A fundamental classification of solar energy systems is analysed below, based on a number of criteria.

#### 2.4.1. Open and closed systems

As regards the typology of solar energy systems, the first distinction comes in regard to the relation between the working fluid and the service to the end users, and there are two types of systems (Lorenzini et al., 2010):

- Open loop systems, in which the working fluid inside the collector is the same water provided to the end service after acquiring the desired temperature. This system type is mostly used for the direct provision of hot water to the users.

- Closed loop systems, where a heat exchanger comes between the thermal vector fluid inside the collector and the fluid (usually water) connected to the end user side, transferring heat from the former to the latter.

The main advantages of the open circuit system are the avoidance of heat dispersions occurring when thermal energy is transferred through different circuits, as well as the simplicity of the circuit connections. On the contrary, there can be some serious issues with the use of open systems, most importantly the freezing of the water at negative temperatures and the limescale accumulation on the inner surface of the piping system, which would both lead to the damage of the collector and the hydraulic circuit. For these reasons, the use of open loop systems is mostly confined to unglazed collector systems such as swimming pool heating systems used only during the hot season, as well as integrated storage collector systems in mild climates for sanitary hot water production (Lorenzini et al., 2010). However, none of these applications match the criteria for the system design proposal of this study.

Consequently, the type of system for the solar room heating application proposed in the current study will be the **closed circuit system**. This is also the most common and reliable solution for commercial solar thermal systems. In a closed system, two separate hydraulic circuits are involved in the heat exchange process; the closed primary circuit for the thermal vector fluid (either water or antifreeze solution) flowing through the solar collectors and the secondary circuit for the water flowing to the end service, such as to the radiator closed system loop in the case of room heating or directly to the end users in an open secondary loop in the case of sanitary hot water production (Chwieduk, 2016). The efficiency of the heat exchange process taking place between the two circuits inside the heat exchanger will eventually affect and determine the efficiency of the entire active solar system.

#### 2.4.2. Natural and forced circulation systems

A second criterion to distinguish the solar energy systems is the way the working fluid is circulated, from which two system categories derive:

- Natural circulation systems, in which spontaneous fluid motions subject to convective forces determine the flow laws. These systems, utilising the action of the so-called buoyancy forces, feature an elevated storage tank in relation to the collector position. The physical phenomenon that takes

place is that the heated fluid from the collector tends to move up to the tank since it becomes less thick. Therefore, more free space is created inside the collector for cooler fluid to fill and be heated up afterwards from the exposed plate following the same procedure (Zerrouki, Boumédien and Bouhadef, 2002).

- Forced circulation systems, where automated devices such as circulator pumps, control units and thermostats are employed in order to adjust and regulate the fluid flows (Duffie and Beckman, 2013).

Despite the benefits of the spontaneous self-regulation of the natural circulation systems that offer simplicity and low installation / maintenance costs, there might be some significant issues associated with natural fluid flow systems that limit their utilisation. Firstly, the continuous exposure of the storage tank to every seasonal variation and weather condition lead to unavoidable energy losses even for well-insulated tanks. Secondly, the elevated position of the storage tank also imposes heavy weights to the structures located below this, essentially the roof or the loft. Lastly, this can result in visual impacts of the system's structures, namely the bulky structures of the natural circulation system located on the roof may not be the best from an aesthetic point of view (Lorenzini et al., 2010).

All in all, a natural circulation system is not the most appropriate solution for the purposes of this study and the basic problem remains the inability of the user to take control of the fluid flows inside the piping system. Therefore, the type of system selected for the design proposal of the current study, regarding the circulation of the working fluid, is the **forced circulation system** described below.

The forced flow system is used when the storage tank cannot be placed in a position above the collectors and, therefore, a natural circulation could not be possible. For the circulation of the working fluid opposite to the natural flow, it is necessary for the system to employ additional devices; a circulation pump to move the fluid towards the storage tank located below, a non-return valve to prevent reverse flow in every case, as well as a control station to regulate and determine the fluid flow laws, so as to improve the system performance (Lorenzini et al., 2010).

Notwithstanding the complexity and cost of the forced circulation system, the architectural integration of the collectors and their separation from the storage tank adds to the flexibility of the system design (Lorenzini et al., 2010). Moreover, the suitability of this system for any seasonal variations of the weather by virtue of the

flexible placement of the storage tank, as well as the ability offered to the user to gain control and accurately regulate the system, eventually led to the selection of the forced circulation system type for the purposes of this study.

### 2.4.3. Final typology selection

Consequently, the typology employed by the design of this study is the **forced circulation closed system**, used for the office space heating application described later in this work in detail. A general overview of this typology is presented in Figure 6 below.

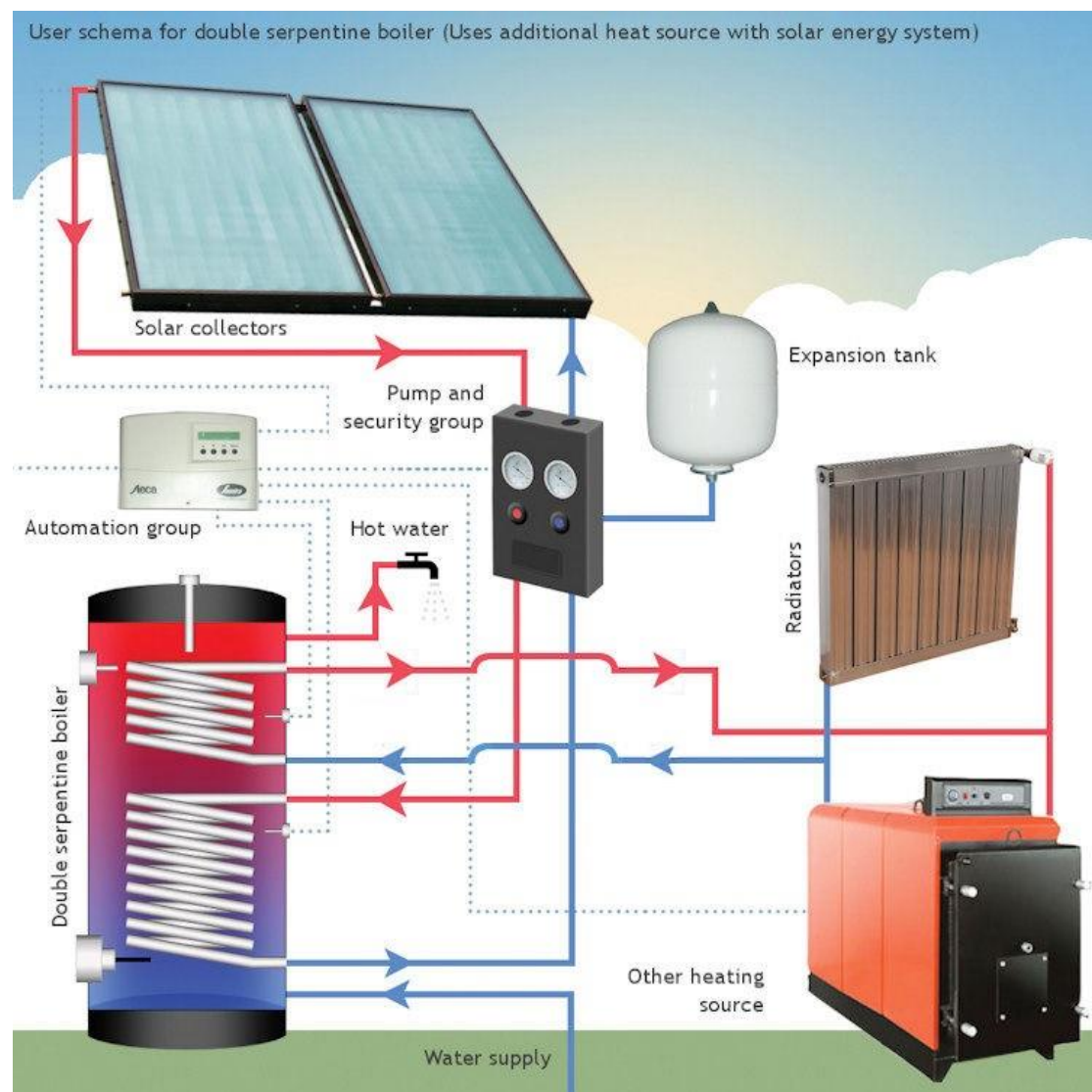


Figure 6: Forced circulation closed loop solar heating system with radiators, including an additional heating source (Source: Solar King, 2016)

The circulation pump is a centrifugal unit responsible for the fluid flow within the primary circuit connected to the collectors. At the same time, it has to ensure that the heat transfer process between the primary and secondary circuits remains efficient. That is, there must be sufficient temperature difference between the two circuits for effective heat transmission to take place through the heat exchanger, which is usually located inside the storage tank (Chwieduk, 2016).

For this reason, the circulator pump employs a differential thermostat which measures the temperature difference between the fluid at the top of the collector and the water at the bottom of the storage tank. When the measured temperature difference exceeds a specific limit, the regulating power unit sends a signal to the circulator to move the fluid inside the primary circuit. The heat exchange between the two circuits occurs as long as the difference remains above the set limit; otherwise the pump is turned off by the regulating unit. This control, as captured through the bibliography (Lorenzini et al., 2010), is implemented into the active solar model of this study in ESP-r, described in Chapter 3.

Although this study concerns solar room heating exclusively, in most real cases a combined system is used, which is capable of providing space heating and hot water at the same time. As indicated by Lorenzini et al. (2010), a combined solar system would generally be fitted so as to provide 10-40 % of the annual energy required for the space heating only. They also argue that any solar coverage percentage higher than this would not be favorable from a technical as well as from an economic perspective.

The basic technical complication would be the excessive amount of heat that would be produced in the summer from the surfaces required to produce considerable amount of energy in the winter. If there were not any additional heating requirements then, such as consistent summer thermal loads, this surplus energy would mostly be wasted.

In this case, a possible way to make the system more energy-efficient would be the storage of the excess energy in the summer for utilisation during the winter, a method referred to as seasonal energy storage (Lorenzini et al., 2010). This would however require huge storage capacity, which would make the system economically unaffordable for small combined active solar systems.

## 2.5. Storage tank

As plenty of the renewable energy sources, the solar source is intermittent and often unpredictable, while demand and supply mismatch during a remarkable amount of the time, which makes the use of thermal energy storage necessary. Heat produced in low demand periods needs to be stored so that it can be available later when the demand is higher again. As already mentioned, seasonal storage would be the most energy-efficient solution, which would however cause technical and economic complications, especially for small-scale solar thermal systems. Hence, the common storage solution is the one which stores the heat for use in the same or the next day (Peuser et al., 2002).

As regards the materials used for commercial pressurized storage tanks, they can be made of stainless steel, enameled steel or plastic-covered steel. Stainless steel is lighter and more resistant over time, albeit more expensive than the other materials (Peuser et al., 2002; Lorenzini et al., 2010). Corrosion by water with high chlorine content is a potential problem with stainless steel tanks, which would basically concern the current space heating application if the same tank was aimed to be used in a combined system to provide sanitary hot water as well. In this case, stainless steel tanks can be provided with a magnesium anode which needs to be regularly replaced. The less costly solution from the three would be the non-porous plastic-covered steel tank, yet not being resistant at temperatures above 80°C. They are generally less reliable than the other solutions (Lorenzini et al., 2010).

As already mentioned, a combined system could be employed in many kind of applications, so as to provide both space heating and sanitary hot water. Although this project regards only space heating load calculations, the presentation of the solar system and its components can sometimes be uniform for the case of a combined system.

The storage tank typically used in such combined systems would be of a general configuration as the one presented in Figure 7 below. There are two heat exchangers immersed into this storage device (Solar365, 2016):

- The solar heat exchanger, which commonly has a dipped worm-pie configuration, is connected to the solar loop/circuit and allows the heat exchange between the thermal vector fluid and the fluid at the lower part of the tank (Lorenzini et al., 2010).

- An additional heat exchanger at a higher part of the tank is connected to the closed space heating loop of the installed heating system, for example a closed radiator loop. If the storage tank is used within a combined scheme for space heating and hot water, then there is also a secondary open loop for the hot water provision, which flows through the exchanger at the higher part of the tank. For the purposes of this project though, the latter loop for the hot water is omitted since our focus is kept on space heating exclusively, concerning the energy calculations and the solar coverage fraction.

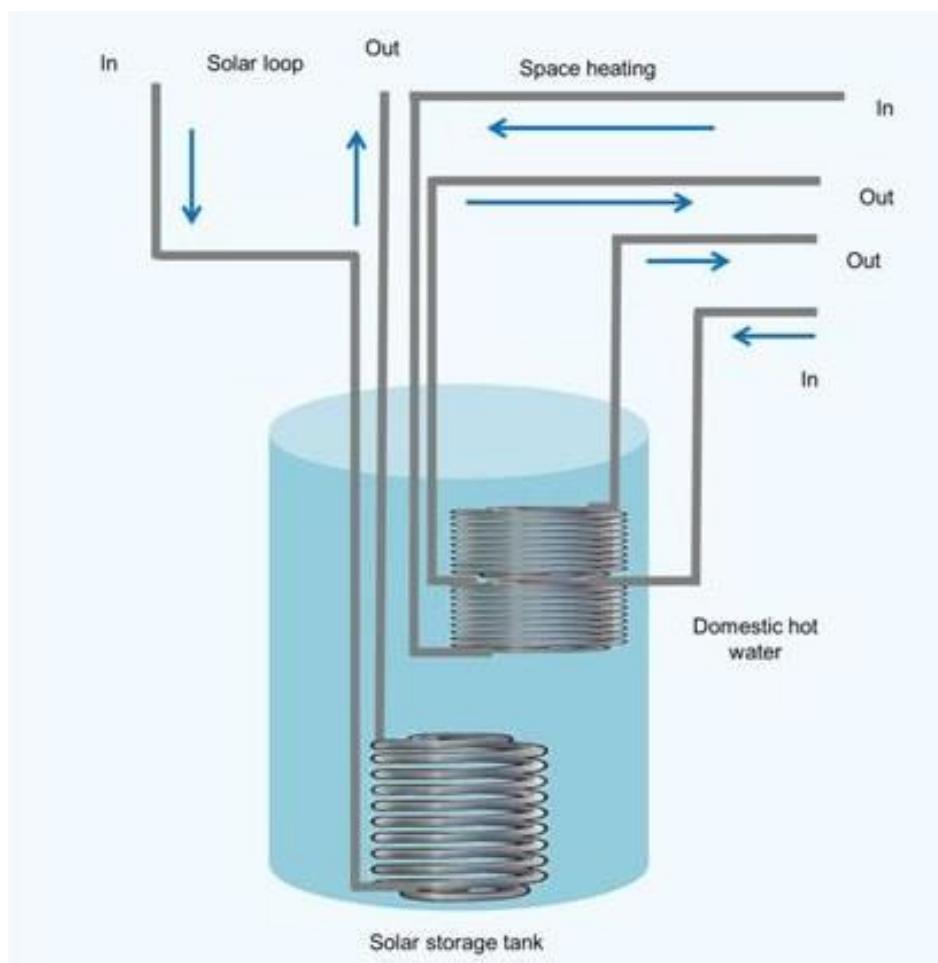


*Figure 7: Storage tank in a typical combined system for space heating and hot water supply (Source: Solar365, 2016)*

It is important to note that in the current project it is considered that there is also a central pre-existing heating system, such as oil or gas-fired boiler or electricity-fueled system, which is not however incorporated into the solar system design study. This means that for the model calculations (Chapter 3) it is assumed that the central-heating system is separated from the active solar system and it is not within this

project's scope to investigate the way the central heating system delivers energy to the building.

Nevertheless, there could be a system realisation, which would incorporate the central-heating system into the same storage tank and, thereafter, to the same radiator heating loop. In that case, an extra heat exchanger would be immersed into the same storage tank, which would allow the heat exchange between the integrative heating system (coming from the central-heating boiler loop) and the fluid stored inside the tank (Lorenzini et al., 2010).

Pressurized storage tanks usually operate at a pressure between 4-6 bars. Regarding the sizing of the storage tank, the general directions suggest a volume of 40-100 L per  $\text{m}^2$  of flat plate collector area (Lorenzini et al., 2010), falling in line with other sources as well (Peuser et al., 2002; Weiss, 2003). There is a dependence of the tank's volume value within the above suggested range on the size of the active solar system. Large-scale solar systems may have values closer to the lower limit of the above range, while this is the other way around for smaller systems. As can also be seen later on this project (Chapter 4), the value finally chosen for the current solar application is in the middle of the above range; 70  $\text{l/m}^2$  of flat plate collector area.

As regards the storage tank shape, there is a good reason why in most cases the storage tank is a tall cylindrical structure. During the normal operation of the storage tank, separate water layers are created inside it due to the difference of the fluid density at various temperatures. The low-density hot water naturally flows and, therefore, is stored at the upper part of the tank, while the high-density cold water stays at the bottom (Streicher, 2016). This effect, referred to as the layering or stratification effect, is fundamental for the effective operation of the active solar system (Weiss, 2003; Chwieduk, 2016).

The warmer water at the top provides its heat to the closed space heating loop through the additional heat exchanger, while the colder water at the bottom is heated from the solar loop through the solar exchanger. In every case, the larger the temperature difference between the two sides of the heat exchanger the more efficient the heat transfer process, which is apparently favored by the temperature layering inside the storage tank. For example, the storage of the coldest water at the lower part of the tank ensures that the heat exchange occurs in the maximum possible efficiency, even when the fluid inside the solar loop is not the warmest (Duffie and Beckman, 2013).

Consequently, the tall and narrow cylindrical structure, which is in favor of the stratification effect, is the most common for commercial storage tanks. These conditions are realised through a vertical storage tank with a ratio of height over diameter of at least 2.5:1 (Lorenzini et al., 2010), as the one displayed in Figure 8 below. Before the installation and fitting of this type of tank to its final place, its height needs to be checked to be compatible with the storage room height.



*Figure 8: Typical cylindrical tall and narrow storage tank (Source: ArchiEXPO, 2016)*

Lastly, as far as the storage tank insulation is concerned, it is very important for the storage tank to be insulated properly, so as to limit heat dispersions from the inside to the outside environment as much as possible. The basic characteristic of the tank insulation to minimise heat losses are (Peuser et al., 2002; Lorenzini et al., 2010):

- It should be thick on the sides, as well as to the upper and bottom surfaces of the tank.
- It should be consistent when covering the sides of the tank without gaps or discontinuities, so as to limit thermal dispersions. Coverings connected with flanges and pipe fittings should be hermetically sealed.
- It should be completely adherent to the sides of the tank, so as to limit convective losses.
- The materials should not include PVC or CFC, while their thermal conductivity should be lower than  $0.035 \text{ W}/(\text{m}\cdot\text{K})$ .

Common options for tank insulation include flexible materials such as expanded polyurethane foam or fiberglass, and inflexible materials capable to be used either outside of the tank for retrofit works or directly injected such as metal or plastic coverings (Lorenzini et al., 2010).

## 2.6. Solar circuit

This section will endeavour to put more emphasis on the connection circuit between the collectors and the storage tank, referred to as the solar circuit. The material commonly used for the pipes of the circuit can be either copper or stainless steel. Certainly, the heat losses throughout the circuit have to be minimised, which is the reason why the piping system has to be as short in length as possible, as well as insulated to the maximum. Comparing copper with stainless steel pipes, the former have a smoother inner surface, which result in less heat losses, besides preventing encrustation (Lorenzini et al., 2010).

The insulation of the solar circuit needs to have been implemented with special care and attention. In addition to an adequate insulation layer, the compactness of the insulation is very important without gaps or escapes, even at the circuit's "elbows". Insulating materials need to be very resistant to high temperatures, which can temporarily occur inside the pipes. Furthermore, resistance to atmospheric particles and ultraviolet rays is necessary as well. The choices of insulating materials include mineral fibers or brands such as Armaflex HT and Aeroflex. The outside protection of the insulation can be a steel or zinc-plated layer covering the pipes (Lorenzini et al., 2010).

Another essential factor that needs to be considered for the solar circuit components is the nature of the working fluid flowing through them. For instance, antifreeze mixtures make it necessary to use taps, fittings and sets resilient to corrosion from specific chemical contents (Lorenzini et al., 2010).

Most of the fundamental hydraulic components required for the solar circuit, as well as its control instruments, such as thermometers and manometers, are offered as pre-set by many manufacturers. Now, we will elaborate on the basic hydraulic components used in a forced circulation system:

- Circulation pump, which is responsible for regulating the fluid flow between the solar collectors and the storage tank (Chwieduk, 2016). The hot fluid flows

from the collectors to the tank through the piping line which is called “lot”, while the cooler fluid flows from the tank to the collectors through the “return” line. Following design directions (Lorenzini et al., 2010), the installation of the pump should be on the “return” line while having its shaft horizontally. No insulation should be placed around the pump.

- Check or non-return valve. Since the collectors are elevated in relation to the storage tank in forced circulation systems, there might be a problem when the temperature of the fluid inside the collectors drops lower than the temperature inside the tank, which can happen more often during the cold nights. In that case, according to the natural circulation forces, the warmer fluid tends to move up from the tank to the colder collectors. The check valve is between the pump and the collectors to prevent this natural circulation, which would cause dispersion of the stored heat from the tank to the collectors and the other parts of the circuit when the circulation pump is off (Duffie and Beckman, 2013).
- Regulating power unit, which aims to utilise the solar energy to its maximum potential by controlling the operation of the circulation pump, based on a simple temperature difference. Standard forced circulation systems, which usually have collectors on the roof and storage tank in the cellar (Solar King, 2016), employ two temperature sensors; one at the top of the collectors and one at the bottom of the tank, commonly connected to the heat exchanger (Duffie and Beckman, 2013).

A control device compares the measured temperature difference from the sensors and activates the relay which turns the circulation pump on as soon as the intervention temperature difference is obtained. The set of the intervention temperature difference depends on different factors of the installed system, such as the length of the circuit tubes; the longer they are, the larger the set temperature difference. Common definitions suggest a difference of 5-8 °C to be sufficient to make the pump work effectively. Contrariwise, the pump is turned off below a difference of 3 °C (Lorenzini et al., 2010).

- The expansion vessel is a necessary component to absorb the dilatation of the thermal vector fluid throughout the working temperature range (commonly between 4 °C and 90 °C). The total amount of the fluid inside the solar circuit determines the size of the expansion vessel, which should be able to

accommodate the working fluid in its expanded state (Duffie and Beckman, 2013). There should not be insulation to the pipes connecting the expansion vessel to the circuit (Lorenzini et al., 2010).

- The pressure relief valve or security valve is responsible for protecting the circuit from overpressures which can be caused, for example, from overheating (Duffie and Beckman, 2013). Typical occasions when this might happen include a black-out to the power supply of the pump or a broken pump. In such cases, the temperature inside the collectors might significantly increase, leading to steam formation, which then has to be released through the security valve. The key is to set the operation of the security valve at a higher pressure in relation to the maximum circuit pressure during normal operation, so as for the security valve not to intervene during normal circumstances (Lorenzini et al., 2010). For instance, if the pressure of the circuit is adjusted at 5.5 bar to its maximum, then the security valve is set to operate at 6 bar.
- A “jolly” valve is a vent-hole usually installed at the upper parts of the solar circuit near the top of the collectors, so as to let air out of the piping system. Air storage would lead to decreased fluid concentration inside the circuit and, therefore, decreased heat exchange (Lorenzini et al., 2010).
- Flow regulating valves are more common in medium- and large-scale solar thermal systems, used to evenly distribute the fluid flow to the different parallel branches of the circuit. They are placed in every collector’s or group of collectors’ row to ensure compact and stable performance from different parts of the same system. In the current study, they could be useful in the case of medium- or large-sized systems to provide space heating to blocks of offices.
- The intercepting valves are used in order to interrupt the fluid flow when maintenance work is required or for security reasons. They are usually employed at the upper and lower side of each element of the circuit.
- Manual emptying taps are incorporated at different points of the system for the emptying of the contained fluid inside the solar circuit, when required. In this case, the emptying tap between two intercepting valves is employed.

- Lastly, there might be a number of three-port valves included into the system design, which can either mix two flows (mixing valves) or divide a flow into two parts (diverting valves).

(Lorenzini et al., 2010).

## 2.7. Conclusion

To sum up, the literature review of the low temperature solar thermal systems has concluded to the use of the flat plate collector type, within a closed loop forced circulation solar circuit, which is connected to a closed radiator heating loop through a storage unit, to provide space heating to office buildings in Greece.

After the key points of each part of the solar system have been captured, it is now time to continue with the modelling of the building-integrated solar system, as a crucial part of the project's methodology.

### 3. Modelling of active solar system

#### 3.1. Introduction

For the design of an active solar space heating system for office buildings in Greece, it is important to use a model which clearly describes and simulates the building-integrated solar system. The code for the used model in ESP-r software is distributed through the GitHub community and incorporates two adjacent cellular offices with zone-based SDHW (Solar Domestic Hot Water).

It actually simulates the use of an active solar heating system with solar collectors and storage tank for the space heating of the offices through hot water radiators (GitHub, 2016). The model and its adjusted parameters are described in more detail in the next section.

#### 3.2. ESP-r model description

The model in ESP-r includes two adjacent offices, connected with a corridor, featuring an active solar water system for space heating. It incorporates a water-based solar collector, an insulated hot water storage tank, which is located in the left corner of the corridor zone, and two water filled radiators, one in each office (GitHub, 2016).

The above mentioned components are represented by thermal zones filled with water. In addition to the water filled zones, there are also separate air filled zones to represent the two offices, the corridor and the collector case. In total, there are ten different zones defined in the model, as shown in Table 3. This model is referred to as *cellular\_expl\_sdhw* from now on.

	#	Zone name	Zone description
<b>Air filled zones</b>	1	manager_a	Office A
	2	manager_b	Office B
	3	corridor	Corridor between the two offices
	4	col_casee	Collector case/housing
<b>Water filled zones</b>	5	collec_low	Lower part of solar collector
	6	collec_mid	Middle part of solar collector

	7	collec_hi	Higher part of solar collector
	8	tank_117	Storage tank
	9	radiator	Radiator in office A
	10	rad_right	Radiator in office B

Table 3: Breakdown of zones defined in ESP-r model *cellular\_expl\_sdhw* (GitHub, 2016)

The *cellular\_expl\_sdhw* model overview, as can be seen within ESP-r tool, is displayed in Figure 9 below. In this model, both windows as well as the solar collectors are facing to the south (azimuth angle  $180^\circ$  from the north).

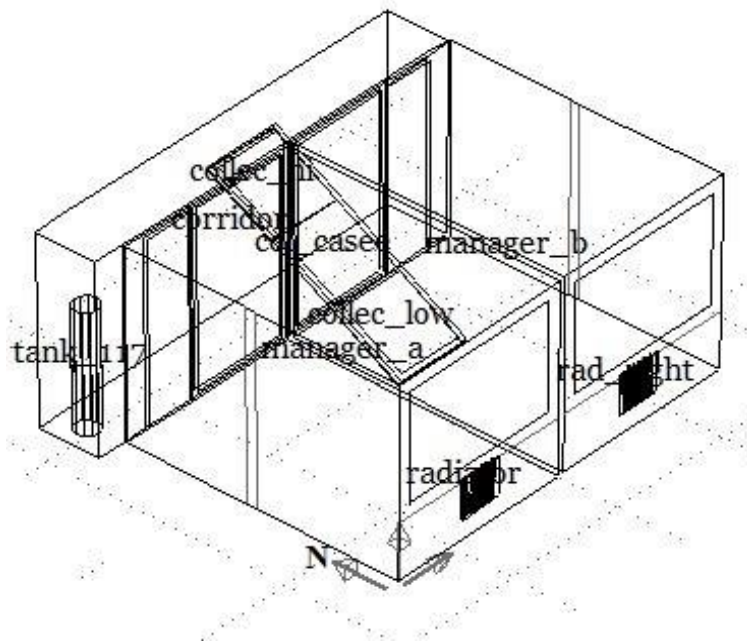


Figure 9: ESP-r model *cellular\_expl\_sdhw* of two adjacent cellular offices with zone-based SDHW (GitHub, 2016)

The model initially incorporates a solar collector area of  $4.32 \text{ m}^2$  and a storage tank capacity of 205.2 L, while the tilt angle is adjusted at  $30^\circ$  from horizontal. The capacity of each radiator is around 8 L of water. These initial design parameters for the dynamic simulations of ESP-r model are presented in Table 4 below.

Initial design parameters of the active solar system in the model	
Solar collector area	$4.32 \text{ m}^2$
Tilt angle	$30^\circ$
Storage tank size	205.2 L

Table 4: Parameters of the active solar system included at the initial design of the model

The nodes of the active solar system in the model are connected through the components of the flow network. The collector pump is placed in line with the solar loop, between the nodes of `collec_low` and `tank`, while the rest of the solar circuit is realised with conduit linkages between the `collec_low`, `collec_mid`, `collec_hi` and `tank` nodes. A similar realisation is achieved in the radiator loops, where each of the radiator pumps is placed between the `tank` and each of the radiators of the offices.

When the top of the solar collector (`collec_hi`) is 3 °C warmer than the storage tank temperature, the collector pump in the solar loop is activated. Nevertheless, each of the radiator pumps is kept on as long as the temperature of the respective office is below 22 °C, regardless of the storage tank temperature. Moreover, a very low flow (trickle) circulator is operating between the `tank` and the collector to reduce extreme conditions in the latter (GitHub, 2016).

The *cellular\_expl\_sdhw* model, shown in Figure 9, is compared to an identical building model except the inclusion of the active solar system, which constitutes the basis for the comparisons in the current work. This is the base case model of two adjacent cellular offices, referred to as *cellular\_bc* (GitHub, 2016), as depicted in Figure 10 below.

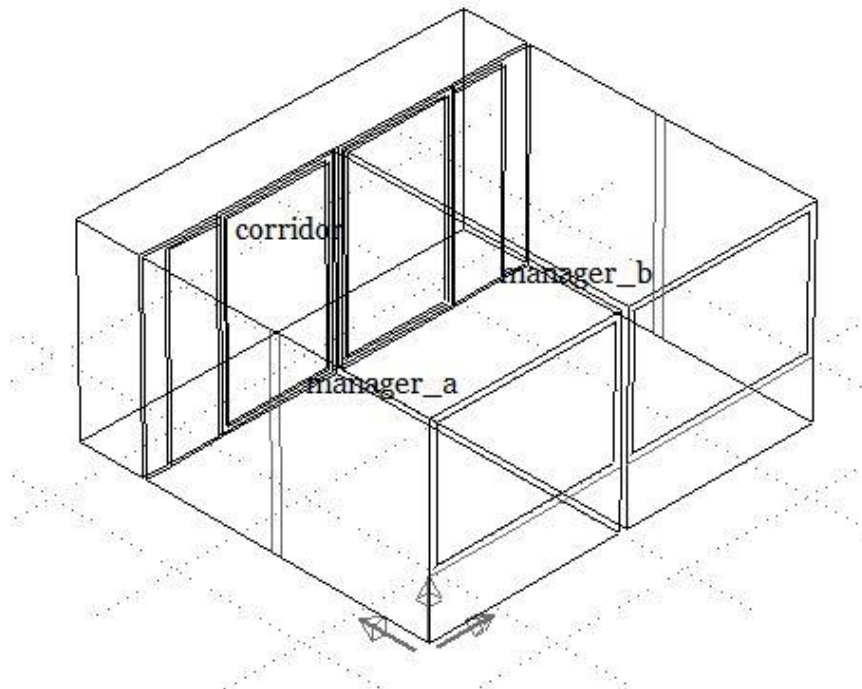


Figure 10: Base case model of two adjacent cellular offices (*cellular\_bc*)

The base case model has to be exactly the same to the main model used for the active solar space heating (*cellular\_expl\_sdhw*), which means they both have the

same office dimensions, window sizes, construction materials, ideal controls and operational details, namely same casual gains and scheduled air flows. The only differentiation of the *cellular\_bc* model is the absence of the active solar system. Therefore, the amount of energy calculated from the *cellular\_expl\_sdhw* model is equal to the energy that needs to be provided from the conventional heating system of the office to complement the active solar system operation. As a result, it is valid to calculate the actual amount of energy delivered from the active solar system, by estimating the **difference** of the delivered energy between the two models.

More details about the inputs to the models are analytically presented in the following sections.

### 3.2.1. Dimensioning and geometry

The typical office building represented by the model in ESP-r incorporates two adjacent office rooms linked together with a corridor at one side and having large windows at the opposite side for exploiting daylight harvesting.

The two office rooms have exactly the same dimensions and geometry characteristics with each other, as presented in Table 5 below. The manager\_a office zone separated from the rest of the building is displayed in Figure 11.

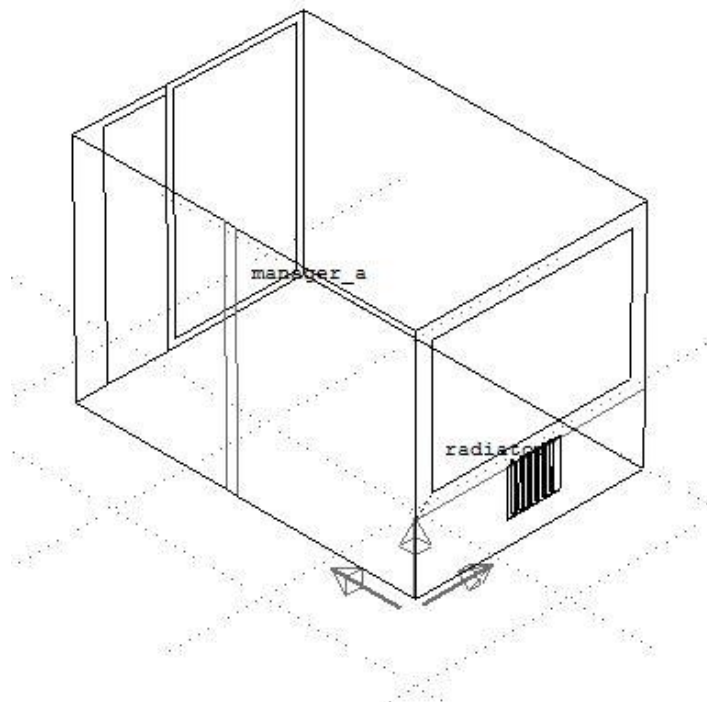


Figure 11: Office manager\_a overview

<b>Office dimensions</b>	(3 m) x (4.5 m) x (3 m)
<b>Base/floor area</b>	13.5 m <sup>2</sup>
<b>Volume</b>	40.5 m <sup>3</sup>
<b>Opaque construction</b>	64.2 m <sup>2</sup>
<b>Façade area</b>	9 m <sup>2</sup>
<b>Window dimensions</b>	(2.6 m) x (1.7 m)
<b>Window area</b>	4.42 m <sup>2</sup>
<b>Window over façade area</b>	49 %

Table 5: Geometry attributes of each office (*manager\_a*, *manager\_b*)

It is important to point out that the corridor in the model (Figure 12) represents a small walking hall/passage leading to the offices and it does not assume part of the heating system. Furthermore, in the *cellular\_expl\_sdhw* model the corridor offers the space for the hot water storage tank, as part of the active solar heating system. However, the focus regarding the heating demands is maintained on the two office rooms, rather than the corridor which underlies to free floating conditions. Some basic geometry attributes for the corridor zone are introduced in Table 6 below.

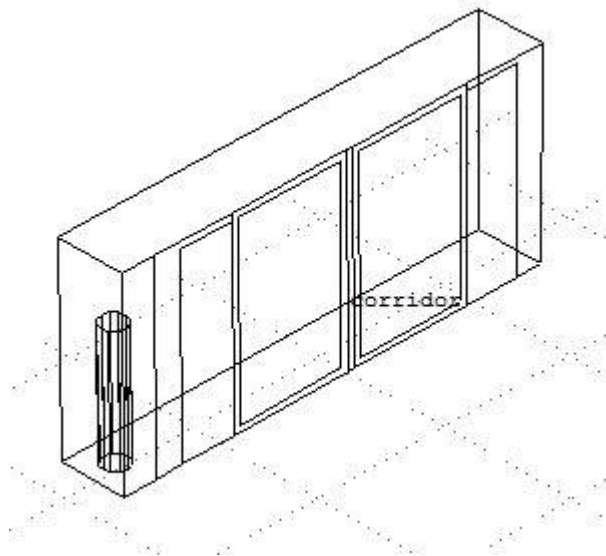


Figure 12: Corridor zone overview

<b>Base/floor area</b>	9.03 m <sup>2</sup>
<b>Volume</b>	19.6 m <sup>3</sup>
<b>Opaque construction</b>	52.3 m <sup>2</sup>

Table 6: Geometry attributes of the corridor

The active solar heating system consists of three basic elements represented by thermal zones in the model; the solar collector, the storage tank and the radiators. Before presenting the geometry characteristics of these basic features, it is important to understand their structure and correspondence to thermal zones.

The solar collector is composed of four parts which correspond to four different thermal zones defined in the model; col\_casee (collector casing), collec\_low (lower part of the panel), collec\_mid (middle part of the panel) and collec\_hi (top part of the panel), as displayed in Figure 13.

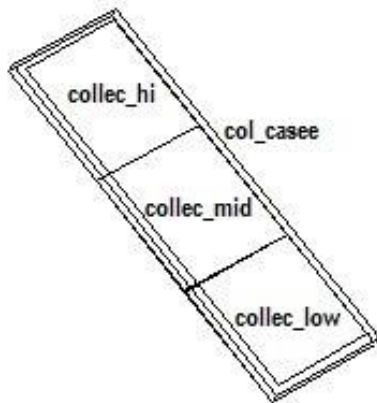


Figure 13: Solar collector in ESP-r model

As presented in Table 4 before, the initial value of the total collector area is set at 4.32 m<sup>2</sup> which occupies nearly  $4.32 \text{ m}^2 / (13.5 + 13.5) \text{ m}^2 = 16 \%$  of the equivalent to the offices roof space area. The dimensions and the resulting area of the collector plates in the model are shown in Table 7 below.

Collector plates	Dimensions (m)	Area (m <sup>2</sup> )	Total collector area	Roof space coverage
collec_low	1.2 x 1.2	1.44	4.32 m <sup>2</sup>	16 %
collec_mid	1.2 x 1.2	1.44		
collec_hi	1.2 x 1.2	1.44		

Table 7: Collector plates dimensions and resulting collector area in the model (initially)

As far as the volumes of the collector elements is concerned, each of the collector plates has initially a volume of 14 L (water filled zones), while the volume of the collector case in the model is equal to 432 L (air filled zone). This results from the collector case having a width of 0.1 m over its surface area of 4.32 m<sup>2</sup>.

The storage tank for the hot water in the model is approximated as a cylindrical structure (Figure 14), located inside the corridor zone. At the initial design stage of the active solar thermal system, the volume of the tank in the model is equal to 205.2 L, resulting from a base/floor area of 0.108 m<sup>2</sup> and a height of 2 – 0.1 = 1.9 m. Its opaque construction area is equal to around 2.46 m<sup>2</sup>.

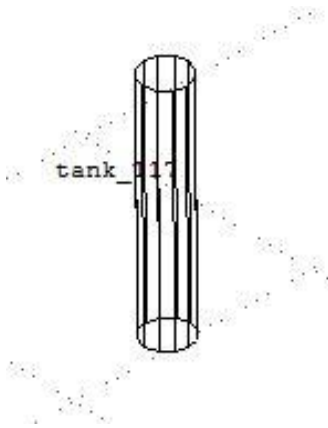


Figure 14: Storage tank in ESP-r model

Lastly, the radiators of the heating system installation in ESP-r model are located inside each of the office rooms and are identical to each other. The dimensions of the radiator are 0.7 m x 0.6 m, while the maximum width reaches 0.05 m, since there are several slots to increase the heat exchange area, as appeared in Figure 15 below. Its capacity is nearly 8 L of water, deriving from a base/floor area of 0.013 m<sup>2</sup> and its height of 0.6 m as mentioned above. Finally, its opaque construction area is equal to 1.08 m<sup>2</sup>, which corresponds to the heat transfer area between the water inside the radiator and the air of the office room.

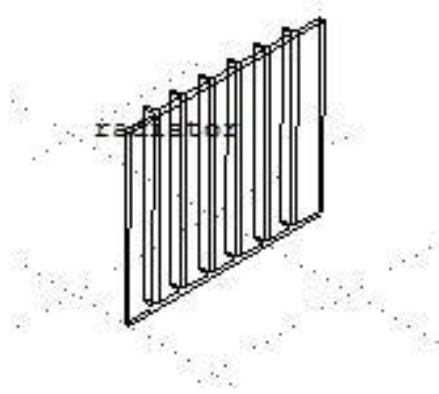


Figure 15: Radiator in ESP-r model

### 3.2.2. Construction materials

Both models (*cellular\_bc*, *cellular\_expl\_sdhw*) have been adjusted so as to have the same construction materials. The offices feature double glazing windows, insulated spandral as well as insulated window frames on the façade. The spandral in the models is the façade surface below each of the windows.

The **double glazing** windows have an overall thickness of 24 mm and a total horizontal U-value of 2.811 W/(m<sup>2</sup>·K). They consist of three layers in total, two layers of plate glass with air gap insulation between them. Detailed construction attributes of the materials for the double glazing are presented in Table 8.

Layer	Description	Thickness (mm)	Conductivity (W/m·K)	Emissivity	Absorptivity	Specific heat (J/kg·K)
<b>Ext</b>	Plate glass	6	0.760	0.83	0.05	837
<b>2</b>	Air gap	12	0	R=0.17 m <sup>2</sup> ·K/W		0
<b>Int</b>	Plate glass	6	0.760	0.83	0.05	837

Table 8: Double glazing construction details

Both the spandral and the window frame, which are elements of the façade, are composed of **insulation frame** with overall thickness of 88 mm and a total horizontal U-value of 0.461 W/(m<sup>2</sup>·K). Two layers of grey coated aluminium are separated with glass fiber insulation in between. The construction details of the insulation frame are presented in Table 9 below.

Layer	Description	Thickness (mm)	Conductivity (W/m·K)	Emissivity	Absorptivity	R (m <sup>2</sup> ·K/W)	Specific heat (J/kg·K)
Ext	Grey coated aluminium	4	210	0.82	0.72	0	880
2	Glass fibre quilt (non-hygroscopic)	80	0.040	0.90	0.65	2	840
Int	Grey coated aluminium	4	210	0.82	0.72	0	880

Table 9: Insulation frame construction details (spandral, window frame, collector case frame)

The rest of the **office walls** are composed of two layers of gypsum board partitions with air gap insulation in between (Table 10). The overall thickness of the wall is 74 mm and the horizontal U-value is 2.144 W/(m<sup>2</sup>·K).

Layer	Description	Thickness (mm)	Conductivity (W/m·K)	Emissivity	Absorptivity	Specific heat (J/kg·K)
Ext	White painted gypsum board	12	0.190	0.91	0.22	840
2	Air gap	50	0	R=0.17 m <sup>2</sup> ·K/W		0
Int	White painted gypsum board	12	0.190	0.91	0.22	840

Table 10: Office walls construction details

The offices also feature well-insulated **ceiling** and **floor** constructions. The ceiling construction has an overall U-value of 0.333 W/(m<sup>2</sup>·K), while the respective U-value for the floor is 1.5 W/(m<sup>2</sup>·K). The Tables 11 and 12 below present more details on the construction layers of the ceiling and the floor respectively and their thermal properties.

Layer	Description	Thickness (mm)	Conductivity (W/m·K)	Emissivity	Absorptivity	R (m <sup>2</sup> ·K/W)	Specific heat (J/kg·K)
Ext	Glass wool	100	0.040	0.90	0.30	2.5	840
Int	Ceiling acoustic tile (mineral fibre based)	10	0.030	0.90	0.60	0.33	2000

Table 11: Ceiling construction details

Layer	Description	Thickness (mm)	Conductivity (W/m·K)	Emissivity	Absorptivity	R (m <sup>2</sup> ·K/W)	Specific heat (J/kg·K)
Ext	Steel	4	50	0.12	0.20	0	502
2	Heavy mix concrete	140	1.4	0.90	0.65	0.1	653
3	Air gap	50	0	0.99	0.99	0.17	0
4	Chipboard	19	0.150	0.91	0.65	0.13	2093
Int	Wilton weave wool carpet	6	0.060	0.90	0.60	0.10	1360

Table 12: Floor construction details

Lastly, as for the building elements, the **corridor back wall** has a different composition than the rest of the office walls, which leads to the better U-value of 1.186 W/(m<sup>2</sup>·K). Two air gaps for thermal insulation are inserted between the different material layers, as displayed in Table 13 below.

Layer	Description	Thickness (mm)	Conductivity (W/m·K)	Emissivity	Absorptivity	Specific heat (J/kg·K)
Ext	White painted gypsum board (inorganic-porous)	13	0.190	0.91	0.22	840
2	Air gap	50	0	R=0.17 m <sup>2</sup> ·K/W		0
3	Block inner (3% mc)	100	0.51	0.90	0.65	1000
4	Air gap	50	0	R=0.17 m <sup>2</sup> ·K/W		0
Int	White painted gypsum board (inorganic-porous)	13	0.190	0.91	0.22	840

Table 13: Corridor back wall construction details

As regards the active solar system construction materials, firstly the **collector plates** are composed of black coated copper, suitable for the effective absorption of the solar thermal energy. The collector plate elements represent the absorber plates of

the flat plate collector, as described in the section 2.3.2 of the literature review. The physical properties of the copper layer are presented in Table 14, from which the high thermal conductivity of the copper is of great importance for the efficient operation of the absorber plate.

Layer	Description	Thickness (mm)	Conductivity (W/m·K)	Emissivity	Absorptivity	R (m <sup>2</sup> ·K/W)	Specific heat (J/kg·K)
1	Black coated copper (coated for absorption)	3	200	0.72	0.85	0	418

Table 14: Absorber plates construction details

Secondly, the **collector case frame** providing insulation to the back and the sides of the panels is composed of the same **insulation frame** materials as in Table 9. Grey coated aluminium layers are separated with glass fiber insulation, resulting in a total U-value of 0.461 W/(m<sup>2</sup>·K). These materials can also be referenced back in the section 2.3.3 of the literature review for the insulating layer.

The **transparent covering** of the panels is consisted of single glazing clear float glass, the details of which can be seen in Table 15 below. The U-value of the single glazing is equal to 5.691 W/(m<sup>2</sup>·K).

Layer	Description	Thickness (mm)	Conductivity (W/m·K)	Emissivity	Absorptivity	R (m <sup>2</sup> ·K/W)	Specific heat (J/kg·K)
1	Clear float glass	6	1.050	0.83	0.05	0.01	750

Table 15: Transparent covering (single glazing) construction details

Moreover, the base, top and all side surfaces of the **storage tank** are consisted of three layers, having Urea-formaldehyde foam insulation between the external (steel) and internal (copper) layer, as presented in Table 16 below. As has been pointed out in section 2.5 of the literature review, the storage tank insulation is a very important aspect of the system. The overall horizontal U-value of the surfaces here is equal to 0.748 W/(m<sup>2</sup>·K).

Layer	Description	Thickness (mm)	Conductivity (W/m·K)	Emissivity	Absorptivity	R (m <sup>2</sup> ·K/W)	Specific heat (J/kg·K)
Ext	White painted steel	3	40	0.82	0.30	0	502
2	UF foam (non-hygroscopic)	35	0.030	0.90	0.50	1.17	1764
Int	Copper	3	200	0.72	0.65	0	418

Table 16: Storage tank construction details

Lastly, the **radiators** are made of white painted steel (3 mm), as the external layer in Table 16 above, having a horizontal U-value of 5.880 W/(m<sup>2</sup>·K). This relatively high U-value is important for the effective thermal exchange between the surface of the radiators and the air inside the office rooms.

### 3.2.3. Operational details

The operational details of the model include the casual gains from occupants, lighting and equipment, as well as the scheduled air flows.

Standard occupancy patterns for both offices and the corridor have been used according to the day type, namely weekday, Saturday or Sunday. The occupancy pattern for a typical weekday in each of the offices can be seen with the blue line in Figure 16. This represents a typical occupancy pattern figure, similar to the quoted patterns in relevant works for office buildings (Duarte et al., 2013). Between 09:00-12:00 and 14:00-17:00 the maximum amount of heat gains is coming from almost two people in average inside each office, while typically there is one person at each office most of the time.

Lights operate in both the offices and the corridor, while gains from equipment are considered in the offices zones only. During a typical weekday in each office, the profile of casual gains from lighting and equipment is considered the same and is represented by the orange line in Figure 16. Specifically, between 08:00-18:00, each of the lighting and equipment gain is set at 5 W/m<sup>2</sup>, or 67.5 W for each office.

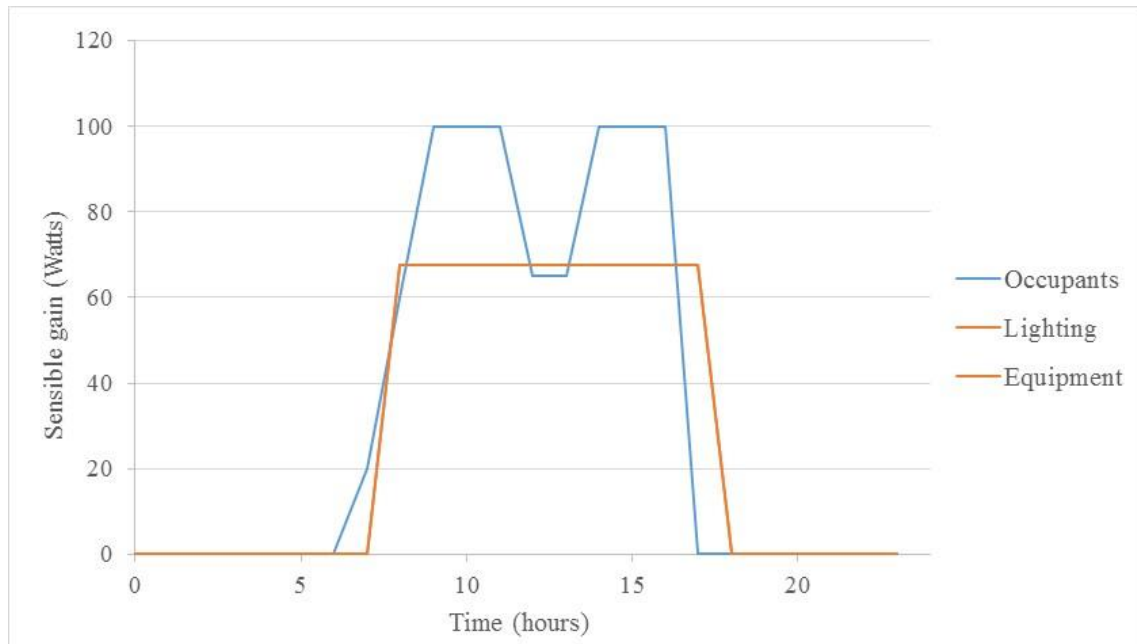


Figure 16: Casual gains in a typical weekday for each office

As regards the scheduled air flows, the values of the infiltration rates are adjusted, which in ESP-r account for the air movement and exchanges with the outside. Whether unintentional or mechanically forced, the air exchanges with the outside of the building are necessary for the proper ventilation of the inside space and must be taken into account in the model since they directly affect the heating demands.

The infiltration rates in our model are set at 0.33 air changes per hour (ac/h) for each office. This means that ESP-r accounts for fresh air entering each office zone (volume = 40.5 m<sup>3</sup>) at a rate of:

$$(0.33 \text{ ac/h}) \cdot (40.5 \text{ m}^3) = 13.365 \text{ m}^3/\text{h} \approx 3.7 \text{ L/s}$$

This infiltration rate is considered sufficient for limiting CO<sub>2</sub> concentration levels to 0.5% for two people working inside the office performing “light work” (office work) according to CIBSE standards for acceptable indoor air quality (CIBSE, 2001).

### 3.2.4. Surface connections and boundary conditions

The level of exposure of the office to the outer environment can be adjusted in the model from the connections between surfaces which determine the boundary conditions of the zones.

Initially, our case study includes an office as part of a block of offices, which generally represents a *low demand* case for Greece. This is the reason why the floors of the offices are set to be connected with an identical environment on the respective lower floor of the building. The well-insulated ceilings are set as external. However, it is considered that one of the offices is internal from both sides and the back, having only its façade exposed to the outer environment, while the other office has one side exposed as well as its façade.

This represents a common case study scenario for an office as part of an office block. This case resembles the typical *low demand* office building in Greece, according to the results presented in Chapter 4. A higher demand scenario regarding the exposure of the office to the external environment is executed later in section 5.4.

Table 17 below summarizes the main surface connections that determine the exposure of the office to the environment in the *low demand* scenario.

<b>Surfaces</b>	<b>Exposure</b>
<b>Side wall of manager_a office, Side wall of corridor (west)</b>	External
<b>Façade (spandral, window frame)</b>	External
<b>Ceiling</b>	External
<b>Floor</b>	Identical/Internal
<b>Side wall of manager_b office, Side wall of corridor (east)</b>	Identical/Internal
<b>Back wall of corridor</b>	Identical/Internal

Table 17: Level of exposure of office building in the “low demand” scenario

### 3.2.5. Control loops

The model uses one control loop to heat up the two offices. The control loop represents the conventional auxiliary heating system, which is responsible for keeping the temperature inside the offices at the desired level, regardless of the solar source availability. This means that the auxiliary system will be in operation for as long as it is needed in order to provide adequate heating load for the building to reach the set temperature, while complementing the operation of the active solar system.

The control loop is linked to zones manager\_a and manager\_b, namely to the two offices, which constitute the main space that needs to be heated up in our model. The total floor area for which space heating is required is 27 m<sup>2</sup>. Heating load is requested at regular office hours on weekdays and reduced hours on Saturdays. Finally, on Sundays the auxiliary heating system is on stand-by and it is set at a low reference temperature.

The sensor for the control loop senses the current zone dry bulb temperature, while the actuator is located at the air point of the respective zone featuring a purely convective injection of heat.

The schedules for the heating control loops (as well as the cooling loops which are not of importance in this project) during the different day types of the year in the models are presented in Figure 17 below for the two offices.

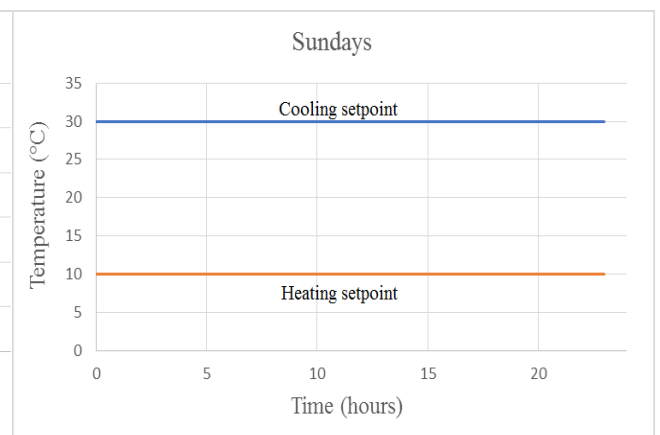
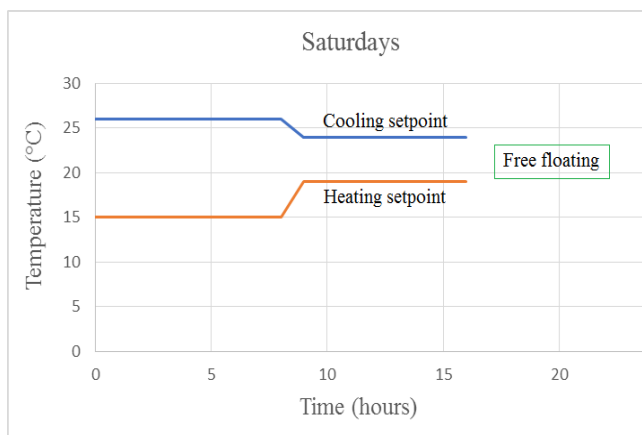
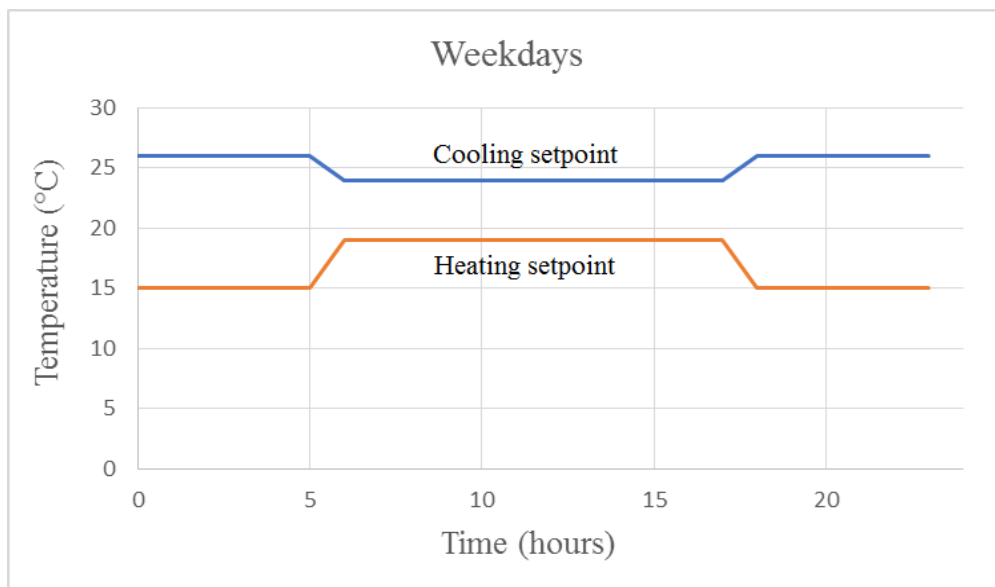


Figure 17: Heating and cooling schedules for the two offices in different day types

### 3.2.6. Integrated simulation parameters

The integrated simulation of the *cellular\_expl\_sdhw* model needs to run interactively, while adjusting the simulation toggles accordingly. The non-air filled zones, namely the water filled zones appeared in Table 3, need to be selected and then the following properties of the fluid, which is water in this case, are entered:

- *Thermal Conductivity*:  $k = 0.598 \text{ W}/(\text{m}\cdot\text{K})$  (at 20 °C)
- *Density*:  $\rho = 998 \text{ kg}/\text{m}^3$  (at 20 °C)
- *Specific Heat*:  $c_p = 4182 \text{ J}/(\text{kg}\cdot\text{K})$  (at 20 °C)
- *Absorptivity*:  $\alpha = 0$

The mass flow stack pressure method value (IPSMOD) needs to be changed from 1 (sending node) to 2 (average of nodes). Afterwards, the mass flow parameters need to be reentered. More specifically, there is a number of parameters which control the iterative fluid flows calculation process (GitHub, 2016). These are set to:

- *MAXITF* = 200 (maximum number of iterations allowed for one time step).
- *FERREL* = 1 % (largest percentage residual flow error allowed in any node).
- *FERMFL* = 0.0005 kg/s (largest absolute residual flow error allowed in any node).
- *PMAX* = 100 Pa (maximum absolute pressure correction applied to any node).
- *STEFFR* = -0.5 (when the ratio of successive pressure corrections for a node is lower than *STEFFR* value, then Steffensen's relaxation is applied to that node).

### 3.3. Climatic data

A significant input to ESP-r modelling tool is the climate file used for the building side simulations. As has been mentioned in the scope/phasing section before, there are four climatic zones in the Greek territory, according to the legislation scheme KENAK (YPEKA, 2010), as shown in Figure 18 below. The key was to find available weather data for each region, which could be representative of the respective climatic zone. Four different cities in Greece have been chosen to represent each climatic zone, as appeared in Figure 18:

- **Iraklion** (latitude 35° 20', longitude 25° 11') for climatic zone A
- **Athens** (latitude 37° 54', longitude 23° 45') for climatic zone B
- **Thessaloniki** (latitude 40° 31', longitude 22° 58') for climatic zone C
- **Kastoria** (latitude 40° 27', longitude 21° 17') for climatic zone D

(TEE, 2012)

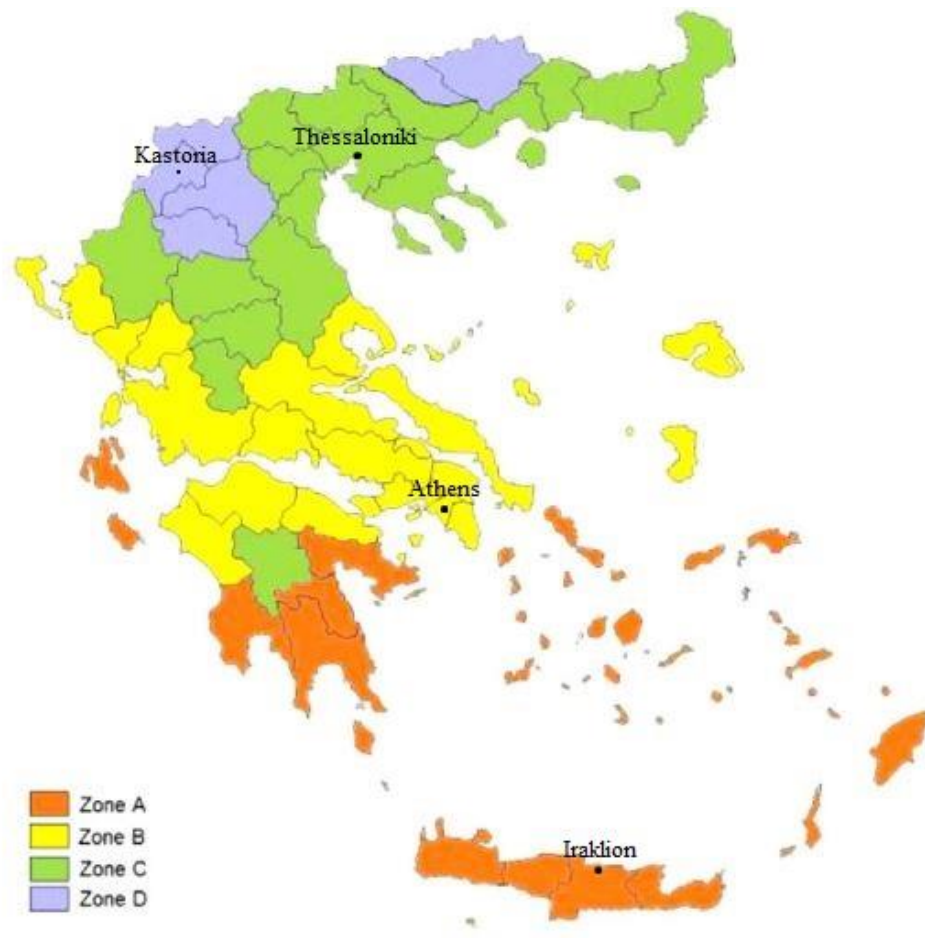


Figure 18: Location of simulated climates in Greece (Source: Papamanolis, 2015)

The weather data for Athens and Thessaloniki have been available on EnergyPlus website (EnergyPlus, n.d.) and for Kastoria and Iraklion in Meteonorm weather files category at the EnergyPlus Support yahoo group (EnergyPlus Support, 2016). All the weather files were available in .epw file format and needed to be converted into binary weather files, readable from the simulator module of ESP-r. The conversions were made using the user defined climate database facility of the clm weather module of ESP-r.

There are significant differences in the climatic characteristics between the climatic zones. As stated in the “Climatic Data of regions in Greece” technical directive (TEE, 2012), regions are classified into climatic zones from the warmest to the coldest, following the order from zone A to D. This can also be verified from the climatic data presented in Table 18 below, by looking for example at the mean values of dry bulb temperature over the year in different zones. The data were extracted from the downloaded weather files using the ESP-r clm module.

However, the order of climatic zones from warmer to colder is not straightforwardly correlated with the mean values of the direct solar radiation, as can be seen in Table 18. Although these values are reduced from zone A to C, a very interesting differentiation from this pattern occurs for the coldest zone D. The fact that Kastoria area (zone D), albeit the coldest, has higher mean direct solar radiation even from Athens (zone B) can lead to very interesting results regarding the performance of the active solar thermal system there, which are presented later in section 5.3. In Figure 19, the yearly graphs of dry bulb temperature for each area can be seen, as exported from the ESP-r climate module.

City	Climatic Zone	Year of data	Dry bulb temperature (°C)			Direct normal radiation (W/m <sup>2</sup> )		
			Min	Max	Mean	Min	Max	Mean
<b>Iraklion</b>	A	2005	5.1	35.7	<b>18.6</b>	0	982	<b>217.3</b>
<b>Athens</b>	B	1999	2	37.2	<b>17.9</b>	0	942	<b>173.1</b>
<b>Thessaloniki</b>	C	1984	- 4.2	34.8	<b>15.3</b>	0	894	<b>156.8</b>
<b>Kastoria</b>	D	2005	- 8.9	39.2	<b>12.8</b>	0	1025	<b>193.2</b>

Table 18: Yearly stats for climatic characteristics in each area

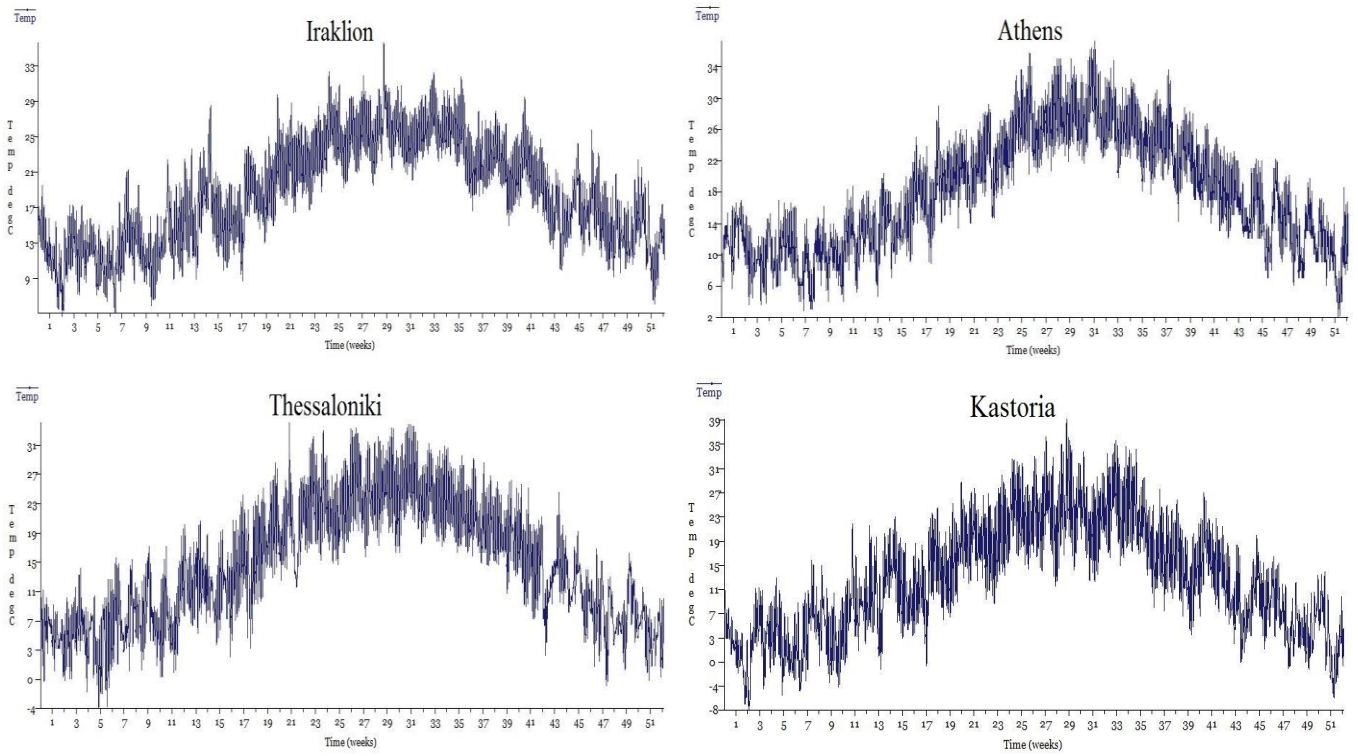


*Figure 19: Yearly graphs of dry bulb temperatures in each area*

Finally, the site exposure in the model is set at “Urban (normal)”, since urban areas usually accommodate a considerable amount of office buildings, while the ground reflectivity factor is regarded constant at 0.2, which represents a dry, bare ground surface.

## 4. Energy performance of model and system selection

### 4.1. Introduction

After elaborating on the ESP-r model inputs which determine the active solar system performance for the described office building, the model is tested in regard to its energy performance. To make it clearer, the simulation results from two described models (*cellular\_bc*, *cellular\_expl\_sdhw*) which have exactly the same inputs apart from the inclusion of the active solar collector system, are compared taking into account the delivered energy from the heating control loops for each model.

Based on these results, the solar coverage fraction is calculated and assessed for each study case. More specifically, the equation used to estimate the solar fraction reached with a specific building and active system configuration is the following (Jaehnig and Weiss, 2007):

$$\text{Solar fraction} = 1 - Q_{\text{aux}} / Q_{\text{total}} \quad (4.1)$$

Where:

$Q_{\text{aux}}$  = energy delivered from the auxiliary (conventional) heating system, in kWh per annum, while the active solar system provides its energy to the building.

$Q_{\text{total}}$  = total energy required for space heating from the conventional system without the active solar system, in kWh per annum.

In our case, there is the following correspondence between the variables of equation (4.1) and the results from the two models:

- $Q_{\text{aux}}$  is the energy delivered, predicted from the *cellular\_expl\_sdhw* model, which includes the active solar system.
- $Q_{\text{total}}$  is the energy delivered, predicted from the *cellular\_bc* model, which is the base case model for the respective case study each time.

Thereupon, the resulting solar fraction is estimated for each case.

It is important to understand that, during the series of simulations, there are parameters of the building which are kept stable for each case. For this chapter, the stable / standard parameters are, as described in the previous chapter:

- Building dimensioning and geometry, namely the geometric attributes of the office rooms, the corridor and the windows.

- Construction materials used for all zones.
- Operational details for building zones.
- Building exposure to the outside, defined by the boundary conditions and connections of the surfaces. However, this parameter changes later in the case study scenarios of section 5.4.
- Heating control loops.
- Controls of the flow network for the active solar system (as mentioned in section 3.2).
- Integrated simulation parameters.
- Site exposure (urban) as well as ground reflectance factor.

As regards the climatic data, the simulation results presented in this chapter are all for the climatic zone D with the weather of Kastoria, which resembles a harsher climate than the rest of Greece.

The *cellular\_expl\_sdhw* model is tested in regard to the active solar system design parameters. Thereafter, the effect of these parameters on the yearly performance of the system is assessed. The first investigation concerns the specific storage tank volume, namely the storage tank volume per m<sup>2</sup> of the collector area. This is an important aspect captured within various sources of the existing literature (Peuser et al., 2002; Weiss, 2003; Lorenzini et al., 2010). After choosing the specific storage size, the impact of the changing collector area is studied, which obviously affects the storage tank at the same time. When having concluded to the pair of storage tank and collector area for the designed system, the impact of the collector tilt angle on the energy performance is finally assessed. It is important that the changes in the above mentioned parameters are also updated to the nodes of the flow network inside the model, in addition to the updates of the geometry attributes in the respective zones.

This chapter results in the final active solar system selection, which will thereafter be implemented in the case study scenarios of Chapter 5. It is important to note that the selected active solar system will be compact and solid for implementation in the Greek offices regardless of the climatic zone. The resulting active solar system is the most important output after this chapter ends.

## 4.2. Initial design of the model

### Initial scenario

**4.32 m<sup>2</sup> collector area (16% roof space)**

**30° tilt angle**

**205.2 L tank (47.5 L/m<sup>2</sup>)**

**Kastoria (Zone D)**

The heating demand loads predicted from the building-integrated simulations of the two models, using the initial design parameters mentioned in chapter 3.2 for the climate of Kastoria airport, which belongs to the climatic zone D of Greece, are summarised in Table 19 below. The estimations of the models concern the yearly energy delivered from the heating control loops in ESP-r, which represents the delivered energy from the conventional heating system of the offices.

Model	Heating energy (kWh)	Specific heating energy (kWh/m <sup>2</sup> ·a)	Total heating hours
<i>cellular_bc</i>	Q <sub>total</sub> = 1115.7	41.32	3702
<i>cellular_expl_sdhw</i>	Q <sub>aux</sub> = 718.6	26.61	2844

Table 19: Yearly heating demands for the two offices in Kastoria before and after the implementation of the active solar system

The base case heating demands deriving from the *cellular\_bc* model for Kastoria, having all constructional and operational details as described in Chapter 3, are equal to 1115.7 kWh annually or **41.32 kWh/m<sup>2</sup>·a**, considering the total heating area of 27 m<sup>2</sup> of the two offices where the heating control loops apply.

This value represents a generally *low demand* office building profile for the climate of Kastoria (Zone D). It constitutes an average low demand base case, which includes one office internal from both sides and one office external from the one side, while both are part of an office block and they both have external façades as well, as presented in section 3.2.4. Later on (section 5.4), a higher demand office building profile will be explored, so as to finally result in a better approximation for the whole office building stock in Greece (Chapter 6).

According to the difference from the heating control loop calculations between the two described models, the active solar system in this case contributes to around 1115.7

– 718.6 = 397.1 kWh annually, which is interpreted as a solar coverage fraction of  $397.1 / 1115.7 \approx 35.6 \%$ .

Alternatively, using the equation (4.1):

$$\text{Solar fraction} = 1 - 718.6 / 1115.7 \approx 35.6 \%$$

This means that the implementation of the initial scenario for the active solar system in Kastoria leads to potential annual thermal energy savings of around 35.6 %. This results in a final specific thermal energy demand of **26.61 kWh/m<sup>2</sup>·a**, which is a significant improvement for the *low demand* office building in Kastoria. This improvement is also depicted in the total number of required heating hours for the two offices yearly (Table 19), which is reduced by  $1 - 2844 / 3702 \approx 23.2 \%$ . It is important to note that the number of total heating hours refers to the sum of the heating hours required for each office, even if some of these coincide.

The breakdown of the monthly total heating demand ( $Q_{\text{total}}$ ) for the two offices in Kastoria, as well as the monthly residual heating demand ( $Q_{\text{aux}}$ ) after the implementation of the active solar system, are presented in Table 20 below for the initial scenario, resulting from the simulations of the models *cellular\_bc* and *cellular\_expl\_sdhw* respectively. Consequently, the solar coverage fraction is estimated on a monthly basis as well, using the equation (4.1).

<b>Kastoria</b>	<b><math>Q_{\text{total}}</math> (kWh)</b>	<b><math>Q_{\text{aux}}</math> (kWh)</b>	<b>Solar fraction (%)</b>
<b>January</b>	289.9	205.6	29.1
<b>February</b>	225.5	157.3	30.2
<b>March</b>	152.6	84.5	44.6
<b>April</b>	53.7	22	59.0
<b>May</b>	7.6	2	73.7
<b>June</b>	0.6	0	100
<b>July</b>	0.1	0	100
<b>August</b>	0	0	100
<b>September</b>	3.7	0.5	86.5
<b>October</b>	27.8	15.3	45.0
<b>November</b>	125.7	74.8	40.5
<b>December</b>	228.5	156.6	31.5
<b>Year</b>	<b>1115.7</b>	<b>718.6</b>	<b>35.6 %</b>

Table 20: Monthly and annual simulated demands and solar fractions for the two offices in Kastoria for the initial scenario

As can be observed in Table 20, the solar fraction is the lowest in the coldest month of the year (January) and thereafter becomes higher as moving toward the summer months, where the heating demands are negligible, leading to 100 % solar coverage by any means. Afterwards, the solar coverage percentages are reduced as approaching to the winter, with December however having a higher solar fraction than January and February. This described trend appears better in Figure 20 below.

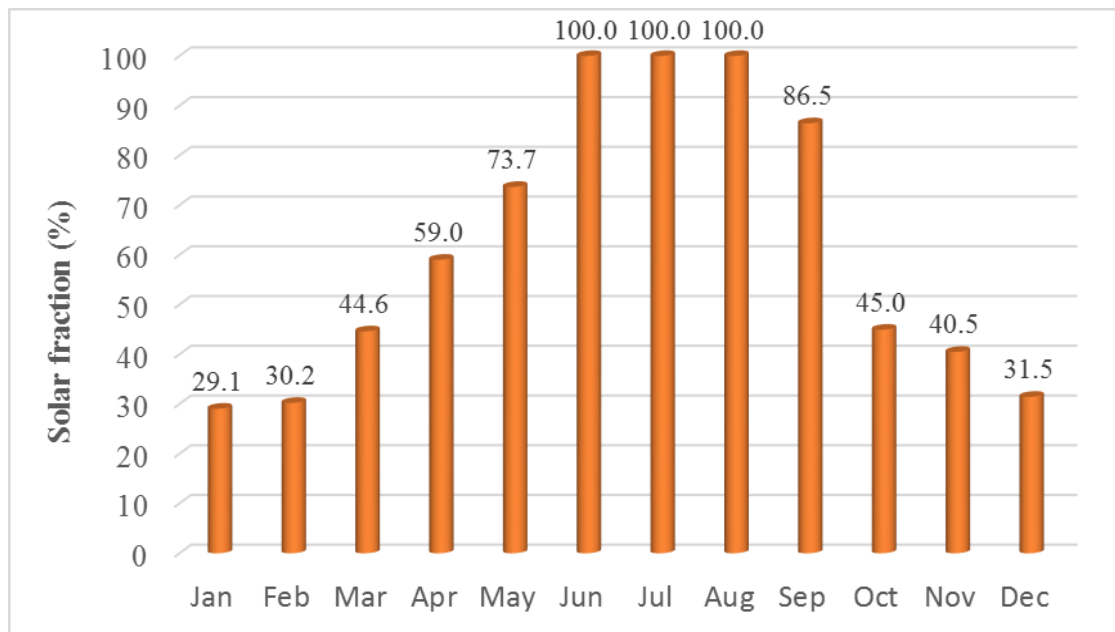


Figure 20: Monthly solar fractions for the initial scenario in Kastoria

Thence, the analysis of the model is carried out, regarding its sensitivity to the parameters of the active solar system. The model is tested for different values of the initial design parameters, consecutively the specific storage tank size (storage volume per  $m^2$  of collector area), the collector area and the tilt angle, so as for the impact of these parameters on the model to be assessed. During each step, the final value of the respective parameter is decided, resulting in the final selection of the active solar system which will afterwards be used for the whole office building stock of Greece.

#### 4.3. Impact of specific storage tank volume

Based on the initial scenario of section 4.2, the collector area of  $4.32 m^2$  (16 % roof space) is kept stable while changing the specific storage volume downwards and

upwards from the initial value of 47.5 L/m<sup>2</sup> of collector area. Hence, two scenarios come up with a specific storage volume of 22.5 L/m<sup>2</sup> and 70 L/m<sup>2</sup> respectively. The resulting absolute storage volumes of 97.2 L and 302.4 L are implemented into the model by setting the height in all vertices of the top surface of the tank to 1 m and 2.9 m respectively. The second case leaves enough space to accommodate the insulation of the top surface of the tank under the ceiling (height = 3 m).

Consequently, the simulated scenarios and the results comparison with the initial scenario, while changing the specific storage tank volume, turn up as follows:

**Scenario 4.3.1.**

4.32 m <sup>2</sup> collector area (16% roof space)	30° tilt angle
<b>97.2 L tank (22.5 L/m<sup>2</sup>)</b>	Kastoria (Zone D)

**Scenario 4.3.2.**

4.32 m <sup>2</sup> collector area (16% roof space)	30° tilt angle
<b>302.4 L tank (70 L/m<sup>2</sup>)</b>	Kastoria (Zone D)

Kastoria (Zone D)	Specific tank volume (L/m <sup>2</sup> )	Q <sub>total</sub>		Q <sub>aux</sub>		Solar fraction	Solar fraction difference
		kWh	kWh/m <sup>2</sup> ·a	kWh	kWh/m <sup>2</sup> ·a		
<b>Initial scenario</b>	<b>47.5</b>	1115.7	41.32	718.6	26.61	35.6 %	0 %
<b>Scenario 4.3.1.</b>	<b>22.5</b>	1115.7	41.32	743.6	27.54	33.4 %	- 2.2 %
<b>Scenario 4.3.2.</b>	<b>70</b>	1115.7	41.32	693.6	25.69	37.8 %	+ 2.2 %

Table 21: Yearly simulated results comparison with different specific storage tank volumes

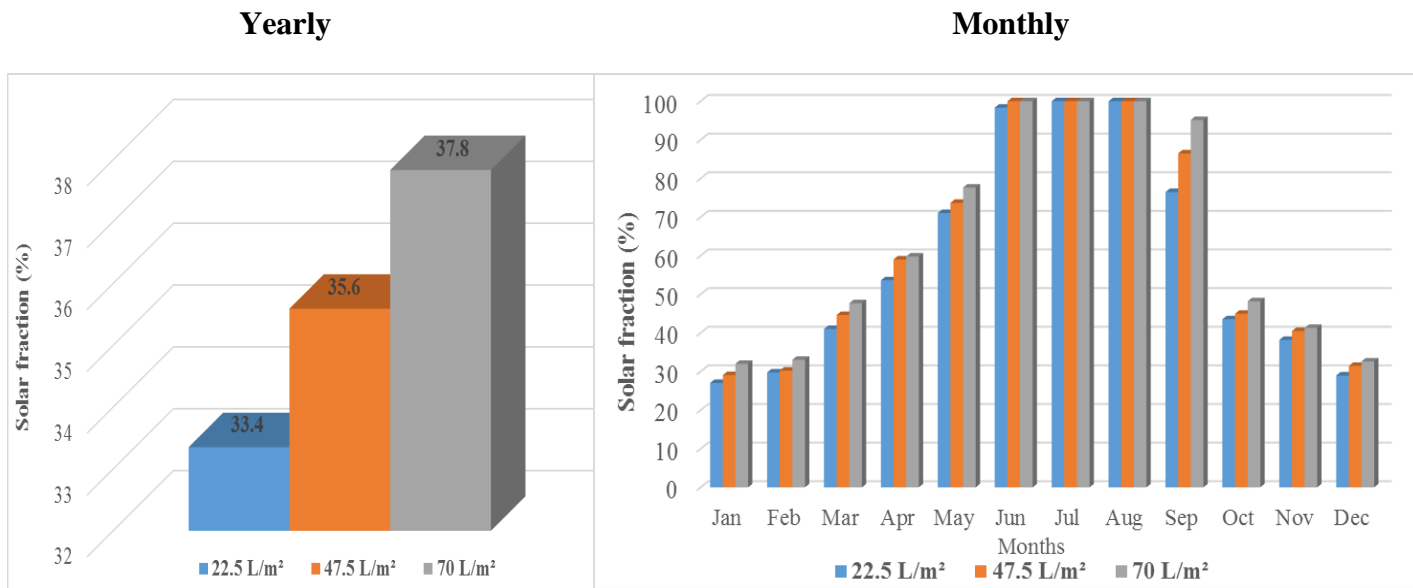


Figure 21: Yearly and monthly solar fraction comparisons with different specific storage tank volumes

As can be observed from the yearly simulations with variable specific storage tank volume, there is a fair impact of the storage size on the building-integrated active solar system performance. It was anticipated that the yearly solar coverage fraction increases as the specific storage size increases, showing the importance of a sufficient storage system as highlighted in section 2.5 of the literature review.

The same occurs with the monthly solar fractions, as can be seen in Figure 21, where the impact of changes is higher during the autumn and spring months, and slightly lower during the winter months. During the summer months, the heating demands of the office building are negligible by any means, so that the solar coverage fraction from almost all systems reaches 100 %.

After this analysis, the selected value for the specific storage tank volume is **70 L/m<sup>2</sup>** of collector area, which results in satisfactory results from the simulations for the harsher climate of Kastoria and it is therefore expected to be sufficient storage capacity for the rest of the climates in Greece, as presented in section 3.3. This selection is also in line with the directives suggested for common solar systems in the respective literature review (Peuser et al., 2002; Weiss, 2003; Lorenzini et al., 2010).



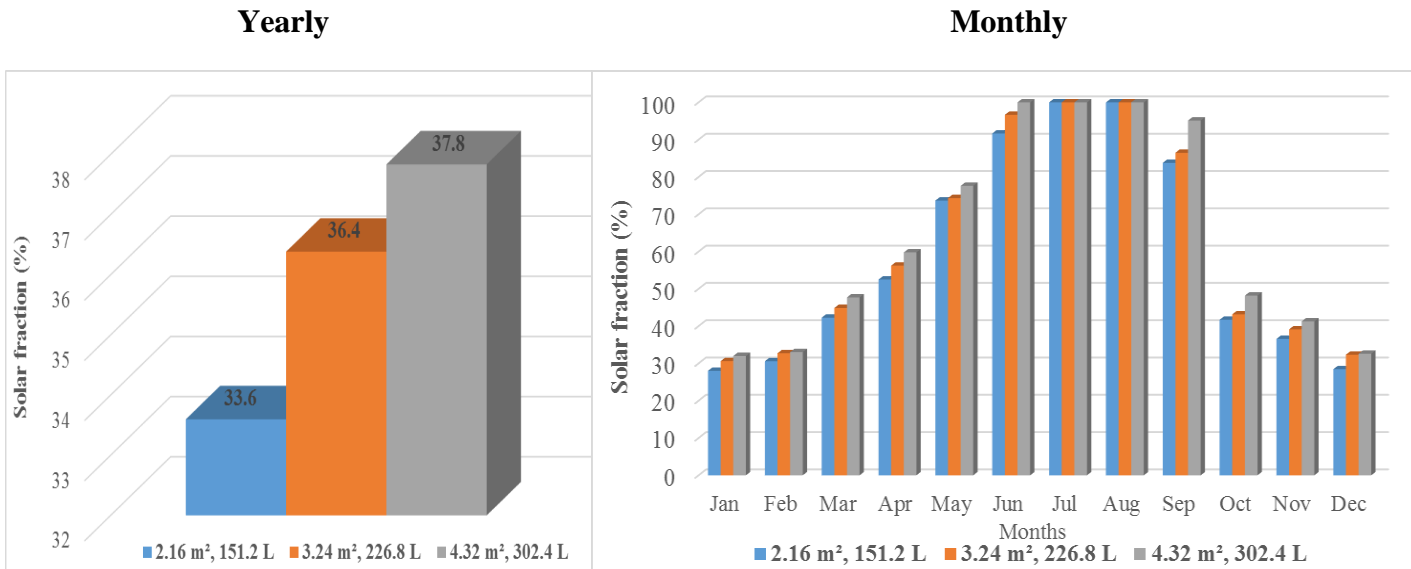


Figure 22: Yearly and monthly solar fraction comparisons with different combinations of collector area – tank size (70 L/m<sup>2</sup>)

As can be derived from the results in Table 22 and Figure 22, there is an anticipated impact of the combination collector area – storage tank volume on the energy performance of the building-integrated active solar system. The yearly as well as the monthly solar coverage fraction increases as both the collector area and the storage volume increase in magnitude. As regards the monthly increases, there is a clearer impact of the larger system during the spring and autumn months than the winter months. From the summer months, only in June the solar fraction does not reach 100 % with the two smaller systems, albeit remaining above 90 %.

The fact that the impact of the applied system alterations is not extensive to the final energy performance can be explained by taking a look at the energy losses of the system. It is known that energy losses occur in almost every part of the system; the transparent covering (glazing) of the collectors, the sides and back of the collector case, the tubes, the storage tank surfaces are some examples of particular areas where heat losses can occur. In Figure 23, the yearly convective losses through the transparent covering of the panels to the outside and through the opaque surface of the storage tank is depicted for the three tested system combinations.

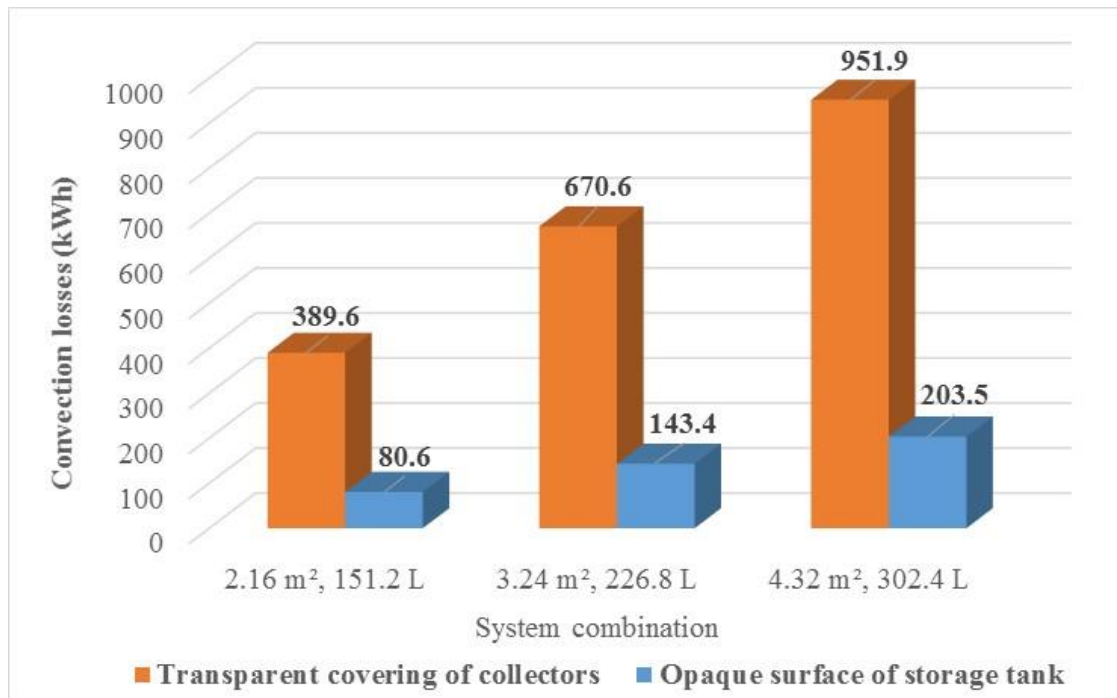


Figure 23: Yearly convection losses through transparent covering (glazing) of collectors and through opaque surface of tank with different combinations of collector area – tank size (70 L/m<sup>2</sup>)

As can be derived from the energy losses presented in Figure 23:

- Moving from the (2.16 m<sup>2</sup>, 151.2 L) to the (3.24 m<sup>2</sup>, 226.8 L) system, thus increasing the size of each aspect of the system by 1.5 or 150 %, leads to:
  - An increase of the transparent covering convective losses by  $670.6 / 389.6 \approx 172$  %.
  - An increase of the storage tank convective losses by  $143.4 / 80.6 \approx 178$  %.
- Moving from the (2.16 m<sup>2</sup>, 151.2 L) to the (4.32 m<sup>2</sup>, 302.4 L) system, thus increasing the size of each aspect of the system by 2 or 200 %, leads to:
  - An increase of the transparent covering convective losses by  $951.9 / 389.6 \approx 244$  %.
  - An increase of the storage tank convective losses by  $203.5 / 80.6 \approx 252$  %.

This analysis shows that the energy losses of the system, as calculated by the model, increase disproportionately with the increase of the system capacity. This occurs because, in addition to increasing the thermal exchange surfaces, there is an increase of the temperatures in the collectors and the tank accordingly. The increased

system losses eventually reduce the efficiency of the larger systems and can limit their energy performance. Although effort has been made to explain this behaviour of the system in the model, it is not within the scope of this study to reduce heat losses of larger systems. Given the behaviour of the system, it would be agreeable to select a system combination with reasonable energy performance and efficiency, at low cost and low space requirements.

Consequently, the combination of the **2.16 m<sup>2</sup> collector area, 151.2 L storage tank** would be acceptable for the application to the office sector in Greece, in terms of its energy performance and the very low percentage (8 %) of the roof space covered by the collectors.

If solar systems with similar proportions of collector area and storage size per m<sup>2</sup> of heated floor area (0.08 m<sup>2</sup> collector/m<sup>2</sup> floor and 5.6 L/m<sup>2</sup> floor respectively) were to be applied massively within the office sector in Greece, significant fractional energy savings could result for the country. At the same time, this choice offers low space requirements, in terms of both roof space coverage and storage capacity, which could make it technically applicable to a greater extent in the Greek offices.

Furthermore, the application to office blocks would require sufficient roof space for the solar collectors to produce heat for the total number of floors. Since the roof space (considering flat roof) is normally equal to the floor area of one floor, in this case the coverage of 8 % of the roof space for collectors to supply heat to each floor would make it theoretically possible for collectors to be installed on the roof to supply up to 12 floors in total, which is higher than the majority of office building blocks in Greece.

#### 4.5. Impact of collector tilt angle

After selecting the collector area and the storage tank size of the active solar system, one very important aspect to be considered is the tilt angle of the solar collectors. The initial design of the system features solar collectors tilted at 30° from horizontal. Changing the tilt angle of the panels inside the model is a procedure that requires accurate trigonometric calculations to determine the final coordinates of all the vertices of the zones `collec_low`, `collec_mid`, `collec_hi` and `col_casee` after tilting the panel by the desired angle. Moreover, the respective flow network nodes need to be updated, especially regarding their reference height attributes to support buoyancy

calculations in the programme. The trigonometric functions used to calculate the vertices of the tilted panels are listed in the Appendix.

The studied scenarios include the selected system combination (2.16 m<sup>2</sup> collector area, 151.2 L storage volume) with the solar collectors tilted at 40° and 50° from horizontal consecutively, and the simulated results are compared as follows:

**Scenario 4.5.1.**

<b>2.16 m<sup>2</sup> collector area (8% roof space)</b>	<b>40° tilt angle</b>
<b>151.2 L tank (70 L/m<sup>2</sup>)</b>	<b>Kastoria (Zone D)</b>

**Scenario 4.5.2.**

<b>2.16 m<sup>2</sup> collector area (8% roof space)</b>	<b>50° tilt angle</b>
<b>151.2 L tank (70 L/m<sup>2</sup>)</b>	<b>Kastoria (Zone D)</b>

	Kastoria (Zone D)	Q <sub>total</sub>		Q <sub>aux</sub>		Solar fraction	Solar fraction difference
		kWh	kWh/m <sup>2</sup> ·a	kWh	kWh/m <sup>2</sup> ·a		
<b>Scenario 4.4.1.</b>	2.16 m <sup>2</sup> , 151.2 L, 30°	1115.7	41.32	740.9	27.44	33.6 %	0 %
<b>Scenario 4.5.1.</b>	2.16 m <sup>2</sup> , 151.2 L, 40°	1115.7	41.32	710.6	26.32	36.3 %	+ 2.7 %
<b>Scenario 4.5.2.</b>	2.16 m <sup>2</sup> , 151.2 L, 50°	1115.7	41.32	680.1	25.19	39.0 %	+ 5.4 %

Table 23: Yearly simulated results comparison with different tilt angles

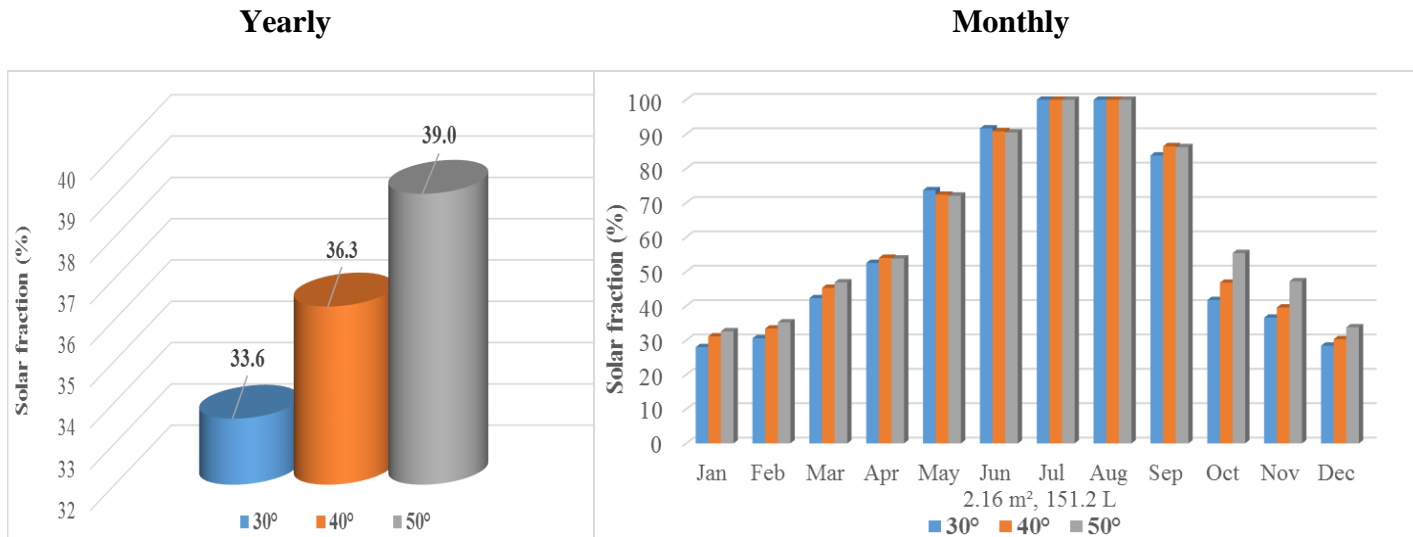


Figure 24: Yearly and monthly solar fraction comparisons with different tilt angles

The results shown in Table 23 and Figure 24 indicate the significant impact the tilt angle of collectors has on the active solar system energy performance. Indeed, the impact of tilt angle alterations is noticeable, especially comparing with the impact the previous changes had on the system. The yearly performance improves from 30° to 40° and, subsequently, from 40° to 50° tilt angle from horizontal. It is remarkable that the (2.16 m<sup>2</sup>, 151.2 L) system with a 50° angle can reach a yearly solar fraction percentage (39 %) in Kastoria, which could not be achieved even when applying a larger system with the previous tilt angle (30°). This indicates how powerful tool is the inclination angle when installing solar collectors, which could lead to cost- and space-effective solutions, instead of applying a larger system capacity.

Following a more in-depth approach for the monthly breakdown of the system performance when increasing the tilt angle from 30° to 40° and thereafter to 50°, Figure 25 collates the solar fraction percentages with the total heating demand loads for each month.

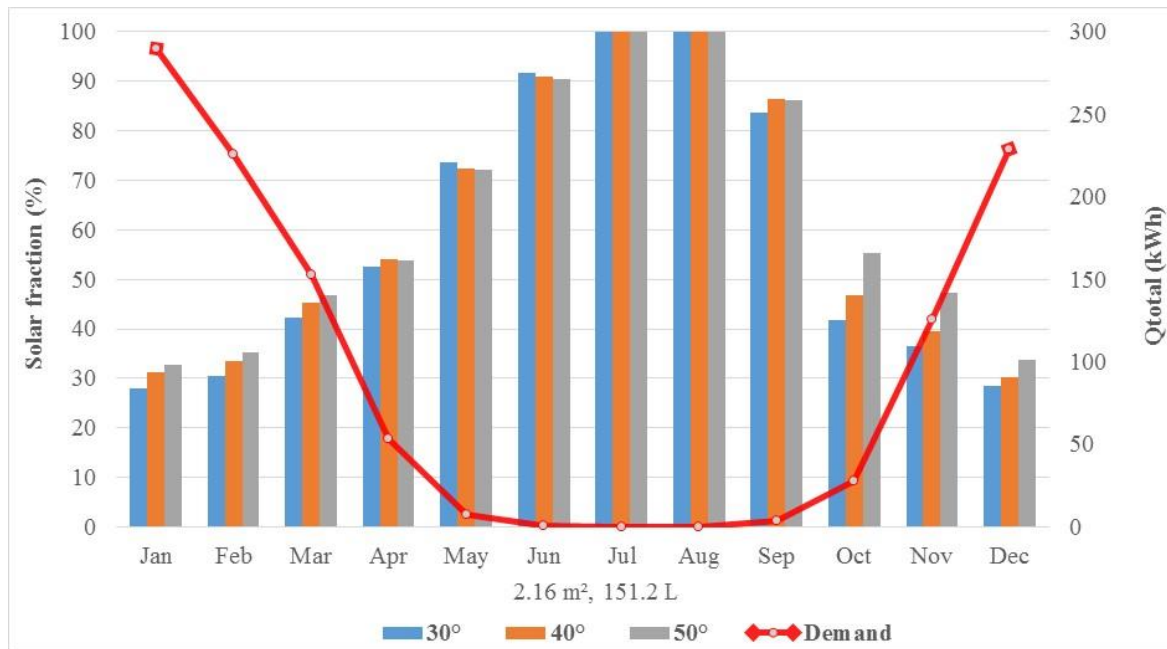


Figure 25: Monthly solar fractions for different tilt angles and collation with heating demands

As can be derived from Figure 25, the angle of 50° performs better during the winter and early spring (until the beginning of April) as well as autumn months (from October until the winter), in relation to 40° and 30° angles. Nevertheless, April and September follow a similar pattern, which indicates that the angle of 40° performs better, while there is a slight reduction in performance with the 50° angle. Moreover, the 30° angle seems to be the most favourable from the examined angles only for May and June. Certainly, July and August do not require heating demands by any means, so that the tilt angle alterations do not make any difference.

On the one hand, the fact that the tilt angle of 50° performs better for all the months for which the heating demand of the building is high (basically January, February, March, November, December), makes it more advantageous on a yearly basis in relation to the other angles. On the other hand, the fact that the 50° angle does not perform better than the others during the warmer months of the year, does not make any difference in total, since the demands during these months are fairly low. Ultimately, the tilt angle of 50° seems to be the most favourable on a yearly basis from the examined angles for Kastoria area.

The high performance of the 50° tilted panel during the winter is attributed to the sun's position low on the horizon. The lower the sun is on the horizon, the more vertically inclined needs the panel to be for maximum exploitation of the solar source.

The opposite occurs in the summer, when the sun is high in the sky and the solar panel needs to be more inclined towards the horizontal. This phenomenon can be depicted in Figure 26 below, with the whole range of the sun's position from the winter to the summer solstice and the panel's possible inclination.

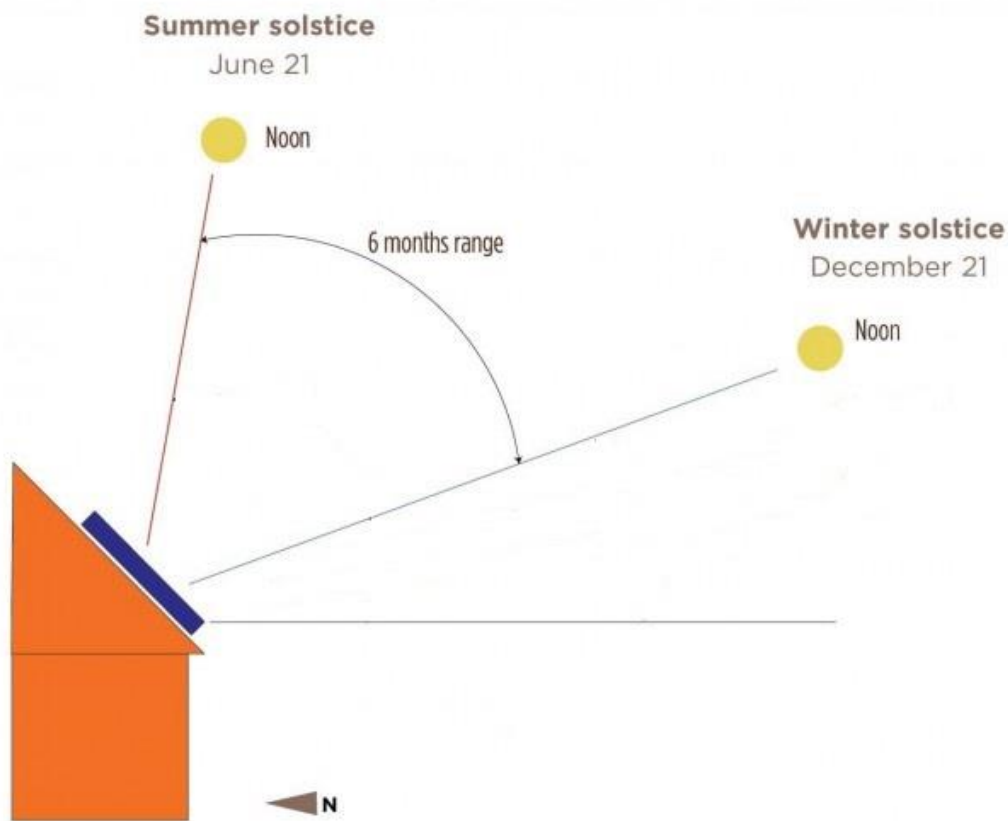


Figure 26: Solar panel inclination depending on the sun's position (Source: BeNature, 2015)

Certainly, the sun's path in the sky from winter to summer and vice versa is a function of the geographical location, thusly it is dependent on the latitude. However, it is not always straightforward to find the optimum tilt angle for a specific location. It is more within the scope of this study to provide model-tested examples accompanied with reasonable explanations for the simulated results, rather than exactly obtaining the optimum tilt angle for a specific area.

Therefore, since the building demands are mostly shifted to the winter, it is apparent that a slightly more vertically than horizontally inclined panel would gain great advantage of the winter performance, which could be reflected onto the yearly performance as well. As long as this observation is verified by our model, the signs show we are on the right track.

Consequently, the tilt angle of **50°** will be followed from now on to the implementation of the active solar system in the Greek office sector. This approach will be attended for all the range of climates in Greece, given the fact that the largest latitude difference between the studied areas is at around 5° (section 3.3), which does not justify a different approach for the tilt angle of the collectors in different areas of the country.

#### 4.6. Conclusion

In conclusion, this chapter has analysed and subsequently explained the response of the model from a different point of view during each stage of the procedure. The whole set of model tests has been carried out for the climatic zone D of Greece, represented by the weather of Kastoria. This zone features colder climatic characteristics in comparison with the rest of the zones (TEE, 2012). The resulting solar system for this climate will have sufficient capacity for the rest of the country as well.

After all, the selected combination for the active solar system features **2.16 m<sup>2</sup>** of collector area (**8 %** roof space coverage or *0.08 m<sup>2</sup> collector/m<sup>2</sup> floor*), a storage tank capacity of **151.2 L** (**70 L/m<sup>2</sup>** of collector area and *5.6 L/m<sup>2</sup> floor*) and a tilt angle for the collectors adjusted at **50°** from horizontal.

According to the simulation results at this point, this system could be able to contribute to around 39 % of the yearly thermal energy required for space heating of the two offices in Kastoria. The rest 61 % needs to be provided by the conventional (auxiliary) heating system already installed in the offices.

The same system will thereafter be implemented in more case study scenarios (Chapter 5), before these results are extrapolated to the whole office building stock of Greece (Chapter 6).

## 5. Energy performance at different building exposure

### 5.1. Introduction

This chapter introduces some basic scenarios which primarily concern the building side in correlation to its surrounding climatic conditions, rather than the active solar system itself. More specifically, after having selected the combination for the solar system to be used, our focus is maintained on the exposure conditions of the building to the outside. The impact of the exposure is studied based on the type of the exposure:

- Building orientation, which changes the side of building exposure to the same climatic conditions.
- Climatic zones, where the impact of different climatic conditions at different locations is studied for the same building orientation.
- Exposure of the building surfaces, where the impact of different climatic conditions is studied for different types of building surfaces exposure (internal / external / ground) for the same building orientation.

After the impact of the above exposure scenarios has been investigated, an “average” scenario of the simulated cases is regarded as the representative scenario for each climatic zone of Greece. This means that after this chapter, the ground will have been prepared for the Chapter 6 and the extrapolation of our analysis to the whole office building stock in Greece.

Before starting our investigation into the building orientation, it is reminded that the selected active solar system to be used from now on is as follows:

**2.16 m<sup>2</sup> collector area (8% roof space)**

**50° tilt angle**

**151.2 L tank (70 L/m<sup>2</sup>)**

**All climatic zones**

### 5.2. Building orientation

This section studies the impact of the building orientation on the heating demands of the building and the fractional thermal energy savings offered by the active solar system. Therefore, it is important to understand that the orientation of the building structure firstly affects the main heating demands in the base case model ( $Q_{total}$ ),

subsequently the auxiliary heating demands in the presence of the solar system ( $Q_{aux}$ ) and accordingly the solar coverage fractions.

The orientation of the building is tested with the windows facing to each of the four cardinal points consecutively. At the same time, the solar collectors are always facing to the south (azimuth angle  $180^\circ$  from north), since the location of the building is in the northern hemisphere.

The starting point of the simulations is the south orientation for the windows, which has already been executed for the selected system ( $2.16 \text{ m}^2$ ,  $151.2 \text{ L}$ ,  $50^\circ$ , Kastoria) in the previous chapter. The rest of the orientation scenarios are also run for the climate of Kastoria (Zone D) and the results come up as follows, where the average values of the four orientations are calculated as well:

<b>Kastoria (Zone D)</b>	<b>Orientation (windows)</b>	<b><math>Q_{total}</math></b>		<b><math>Q_{aux}</math></b>		<b>Solar fraction</b>
		<b>kWh</b>	<b>kWh/m<sup>2</sup>·a</b>	<b>kWh</b>	<b>kWh/m<sup>2</sup>·a</b>	
	<b>South</b>	1115.7	41.32	680.1	25.19	39.0 %
	<b>North</b>	1871	69.30	1030.8	38.18	44.9 %
	<b>East</b>	1379.9	51.11	801.1	29.67	41.9 %
	<b>West</b>	1530.8	56.70	908.3	33.64	40.7 %
	<b>Average</b>	<b>1474.4</b>	<b>54.61</b>	<b>855.1</b>	<b>31.67</b>	<b>42.0 %</b>

*Table 24: Yearly simulated results comparison with different orientations of building for Kastoria*

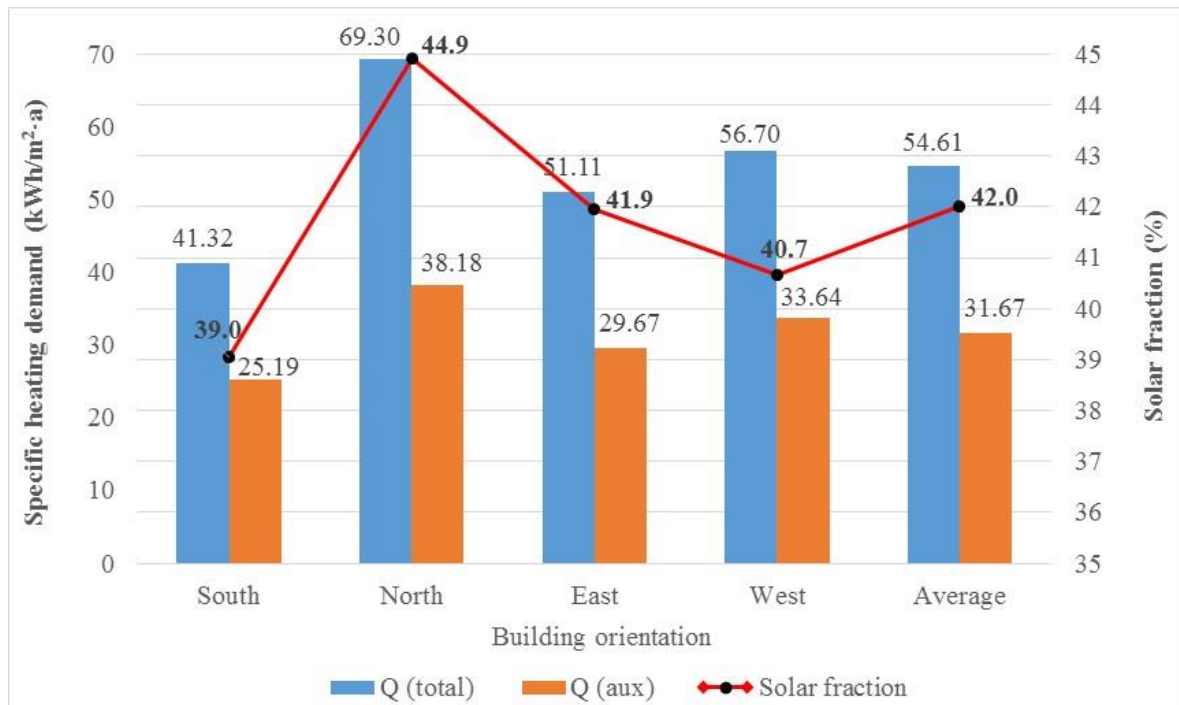


Figure 27: Specific heating demands before and after the implementation of the active solar system and respective yearly solar fractions with different orientations of building for Kastoria

As can be observed from the results, there is a significant increase of the total heating demands from the south to the north facing windows, from 41.32 kWh/m<sup>2</sup>·a to 69.30 kWh/m<sup>2</sup>·a for Kastoria. This is attributed to the passive solar gains, which are obviously much more significant for the case of south-facing windows, since the building is located in the northern hemisphere. Moreover, it is reminded that the façade is external while the back wall of the corridor is internal (section 3.2.4) in this set of simulations, which results in even more reduced impact of the solar gains from the south side of the building (internal), when it is north-oriented (Figure 28). This makes the differences in heating demands more extreme between the scenarios of south- and north-facing windows.

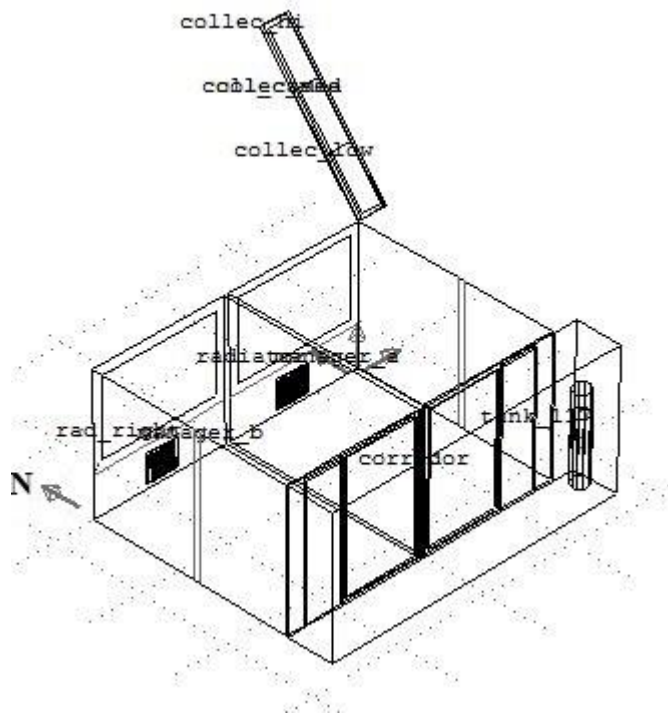


Figure 28: ESP-r model with north-facing windows

After the active solar system has been implemented, the residual heating demands (auxiliary) are reduced to 25.19 kWh/m<sup>2</sup>·a, with a solar coverage of 39 %, for the south-oriented building. The respective heating demand (auxiliary) for the north orientation stands at 38.18 kWh/m<sup>2</sup>·a, as predicted by the model. Nonetheless, the solar fraction percentage comes to almost 45 % for the north orientation.

This interesting result showcases the greater impact the active solar collector system has on the coverage of the building heating demands for the north orientation compared to the south orientation. This can be explained through the reduced passive solar gains the building has when it is oriented to the north, which makes the impact of the active solar gains from the collectors more visible. In other words, in the scenario of the north orientation the active solar system has more “opportunities” to deliver its captured energy into the building without being overlapped by the passive solar gains to the same extent as in the scenario of the south orientation.

Accordingly, east and west orientation lie in the middle between south and north orientation, in terms of both total heating demands ( $Q_{total}$ ) and auxiliary heating demands after the implementation of the active solar system ( $Q_{aux}$ ), as well as solar fraction percentages. To explain the higher demands of the west compared to the east orientation, we can take a look at the picture of the west-oriented building (Figure 29).

The side wall of manager\_b office, which is of internal boundary (section 3.2.4), faces to the south so that it cannot take maximum advantage of the solar gains from the south. Moreover, the side wall of manager\_a office is external and faces to the north in this case, where there are no available direct solar gains.

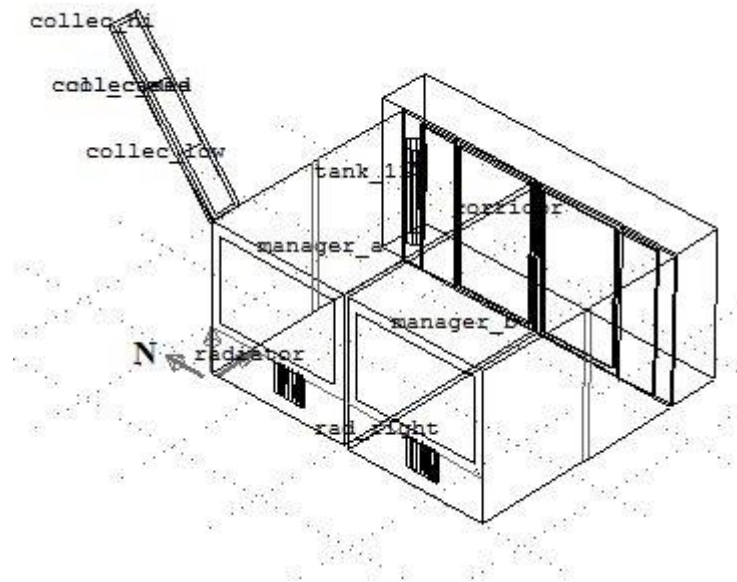


Figure 29: ESP-r model with west-facing windows

Finally, the average heating demands before and after the implementation of the active solar system ( $Q_{total}$ ,  $Q_{aux}$ ) are calculated for the four building orientations and a resulting average solar fraction is estimated at around 42 % for Kastoria.

However, there is the need to choose a real case orientation from the simulated to be as close as possible to the calculated average results from the worst-case side (higher demands, lower solar fraction). Namely, for the chosen orientation:

- The total heating demands ( $Q_{total}$ ) need to be at least as much as the calculated average total heating demands ( $54.61 \text{ kWh/m}^2 \cdot \text{a}$ ).
- The auxiliary heating demands after the active solar system implementation ( $Q_{aux}$ ) need to be at least as much as the calculated average auxiliary heating demands ( $31.67 \text{ kWh/m}^2 \cdot \text{a}$ ).
- The respective solar fraction percentage needs to be lower than the calculated average solar fraction (42 %).

The orientation for which the results comply with these three characteristics is the west. This orientation presents total heating demands ( $Q_{total}$ ) of 56.70 kWh/m<sup>2</sup>·a and auxiliary heating demands after the implementation of the active solar system ( $Q_{aux}$ ) of 33.64 kWh/m<sup>2</sup>·a, covering eventually 40.7 % of the yearly heating demands of the offices in Kastoria by solar.

As a result, the **west** orientation can be representative of all the four simulated orientations for the building in Kastoria. This orientation will be used from now on to represent the average case for the office building orientations in each of the climatic zones of Greece.

### 5.3. Climatic zones

After having tested the model response for the active solar system selection and the building orientation in Kastoria (Zone D), it is now time to trust the model for the different climatic zones of Greece, as introduced in section 1.2. The chosen cities of Iraklion, Athens, Thessaloniki and Kastoria to represent the climatic zones A, B, C and D respectively have also been introduced in section 3.3, where a number of their basic climatic characteristics has been presented as well.

Following the rationale that the west orientation of the building can be representative of an average orientation case for the office buildings in the rest of the climatic zones, as it was proven for Kastoria (Zone D), the simulation results for the west orientation of building in all the climatic zones of Greece are presented below:

West orientation	City (Climatic Zone)	$Q_{total}$		$Q_{aux}$		Solar fraction
		kWh	kWh/m <sup>2</sup> ·a	kWh	kWh/m <sup>2</sup> ·a	
	<b>Iraklion (Zone A)</b>	201.5	7.46	84.8	3.14	57.9 %
	<b>Athens (Zone B)</b>	386	14.30	202	7.48	47.7 %
	<b>Thessaloniki (Zone C)</b>	892.3	33.05	544.7	20.17	39.0 %
	<b>Kastoria (Zone D)</b>	1530.8	56.70	908.3	33.64	40.7 %

Table 25: Yearly simulated results comparison between the climatic zones of Greece for west orientation of building (low demand)

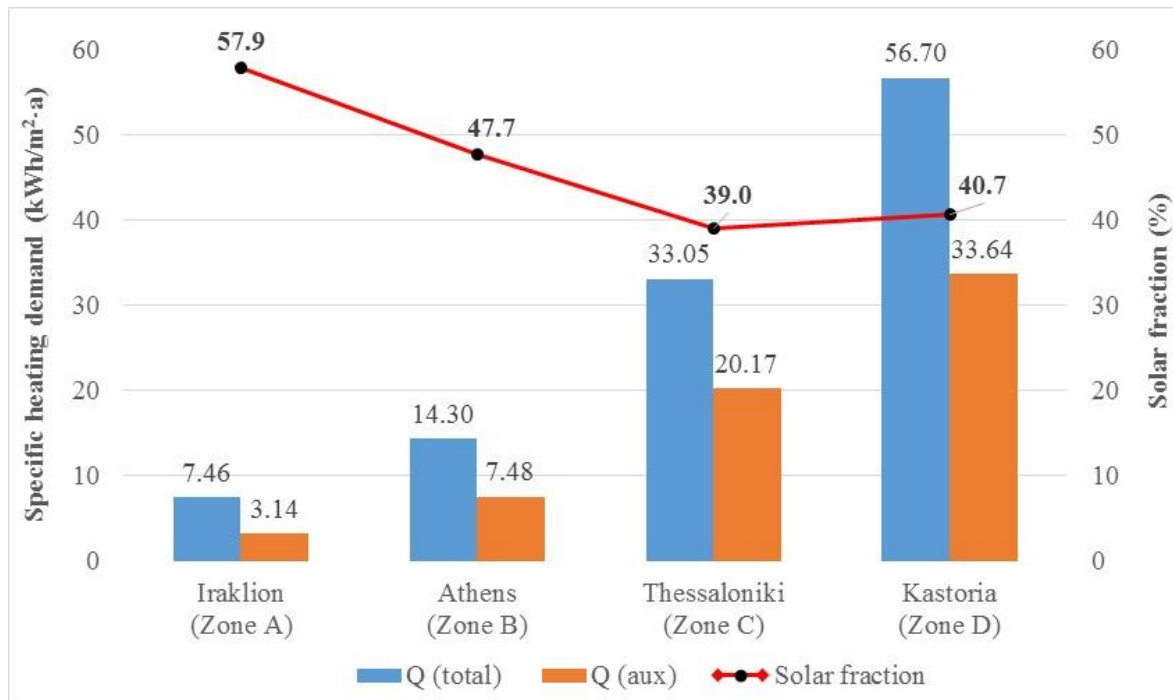


Figure 30: Specific heating demands before and after the active solar system implementation and respective yearly solar fractions for all the climatic zones of Greece with west orientation of building (low demand)

The results show remarkable differences between the climatic zones of Greece in the total heating demands as well as the heating demand reduction achieved with the same active solar system. While this *low demand* scenario (office part of a block of offices) for Kastoria (Zone D) was already estimated at 56.70 kWh/m<sup>2</sup>·a ( $Q_{total}$ ) for the west (average) orientation of the windows, the same scenario for Thessaloniki (Zone C) resulted in 33.05 kWh/m<sup>2</sup>·a, for Athens (Zone B) 14.30 kWh/m<sup>2</sup>·a and for Iraklion (Zone A) as low as 7.46 kWh/m<sup>2</sup>·a. The differences of the total heating demands ( $Q_{total}$ ) between the climatic zones are reasonable, as we are moving from the coldest zone D to the warmest zone A. This is perceptible from Figure 31 below, which shows the differences of the yearly mean dry bulb temperature between the climatic zones and how it is significantly reduced when moving from zone A to zone D.

Accordingly, the yearly heating demand reduction achieved with the same active solar system for the same office building is the highest for the warmest zone A, reaching almost 58 %, while it becomes lower when moving to the colder zones B and C, achieving around 47.7 % and 39 % respectively. Nevertheless, it is very interesting that the yearly thermal energy savings achieved by the same solar system in zone D stands at nearly 40.7 %, above than that of the warmer zone C. This is attributed to the

higher mean value of the direct solar radiation for zone D compared to zone C and even to zone B. This increases the thermal energy production by the solar collectors leading to a higher solar fraction in zone D than zone C. However, comparing zone D to zone B, it is obvious that the higher direct solar radiation in zone D is not sufficient to compensate for the much colder climate of zone D, so that the solar fraction there still remains well below that of zone B.

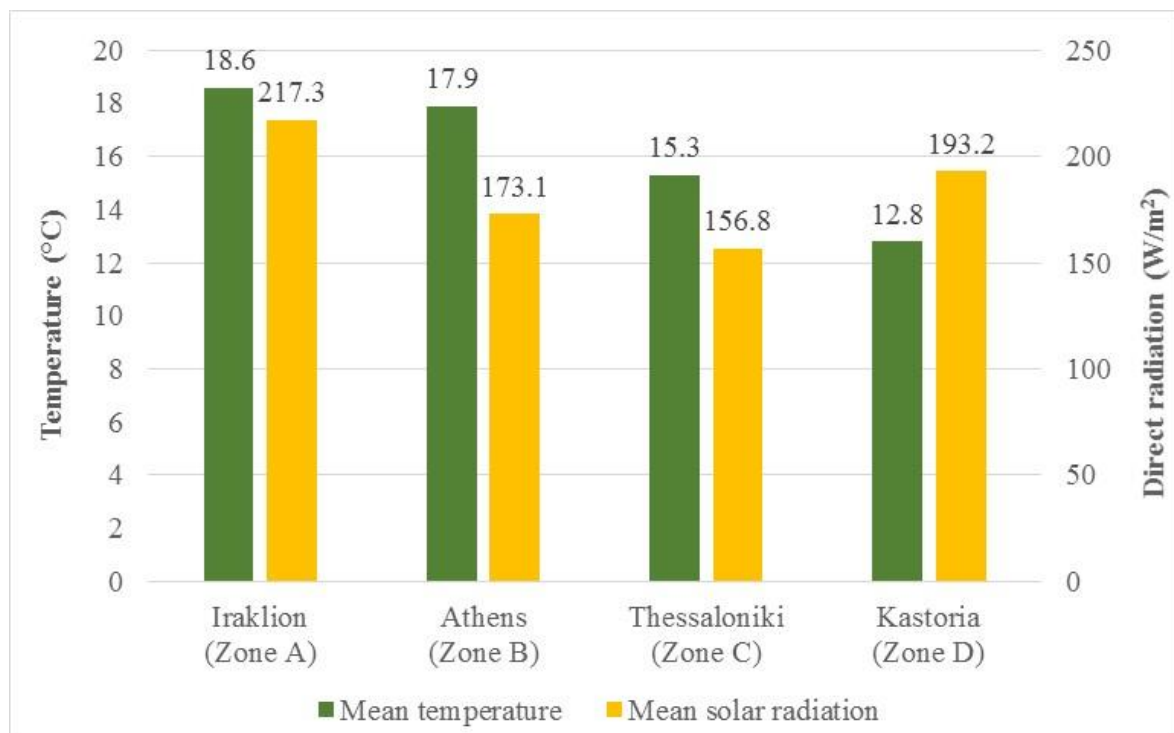


Figure 31: Yearly mean values of temperature and direct solar radiation in each climatic zone

#### 5.4. Exposure of building surfaces

##### Low demand building

It is reminded that in all the above simulated scenarios the office building is considered as part of an office block and the building surfaces connections are such (section 3.2.4), so as to emulate a *low demand* office building in Greece. In this case, the manager\_a office was semi-exterior and the manager\_b office interior from the sides. Both the façades were facing to the outside.

The simulated results have been presented for the two offices as a whole so far, by estimating the specific heating demand for the total heating area of the two offices (27 m<sup>2</sup>). Before executing a fairly *higher demand* scenario later in this section, in

terms of building surfaces exposure to the outer environment, the previous results for the west orientation of the building in all the climatic zones are shown again, for each office room specifically this time (heated floor area = 13.5 m<sup>2</sup>), so as to discern the impact of the building surfaces exposure on the heating demands.

West orientation	City (Climatic Zone)	Office	Q <sub>total</sub>		Q <sub>aux</sub>		Solar fraction
			kWh	kWh/m <sup>2</sup> ·a	kWh	kWh/m <sup>2</sup> ·a	
Iraklion (Zone A)		A	145.0	10.74	66.7	4.94	54.0 %
		B	56.5	4.19	18.1	1.34	68.0 %
Athens (Zone B)		A	269.2	19.94	151.1	11.19	43.9 %
		B	116.8	8.65	50.9	3.77	56.4 %
Thessaloniki (Zone C)		A	616.0	45.63	401.4	29.74	34.8 %
		B	276.3	20.47	143.2	10.61	48.2 %
Kastoria (Zone D)		A	1053.1	78.00	673.5	49.89	36.0 %
		B	477.7	35.39	234.9	17.40	50.8 %

Table 26: Yearly simulated results comparison between the two office rooms in all the climatic zones of Greece for the west orientation of building

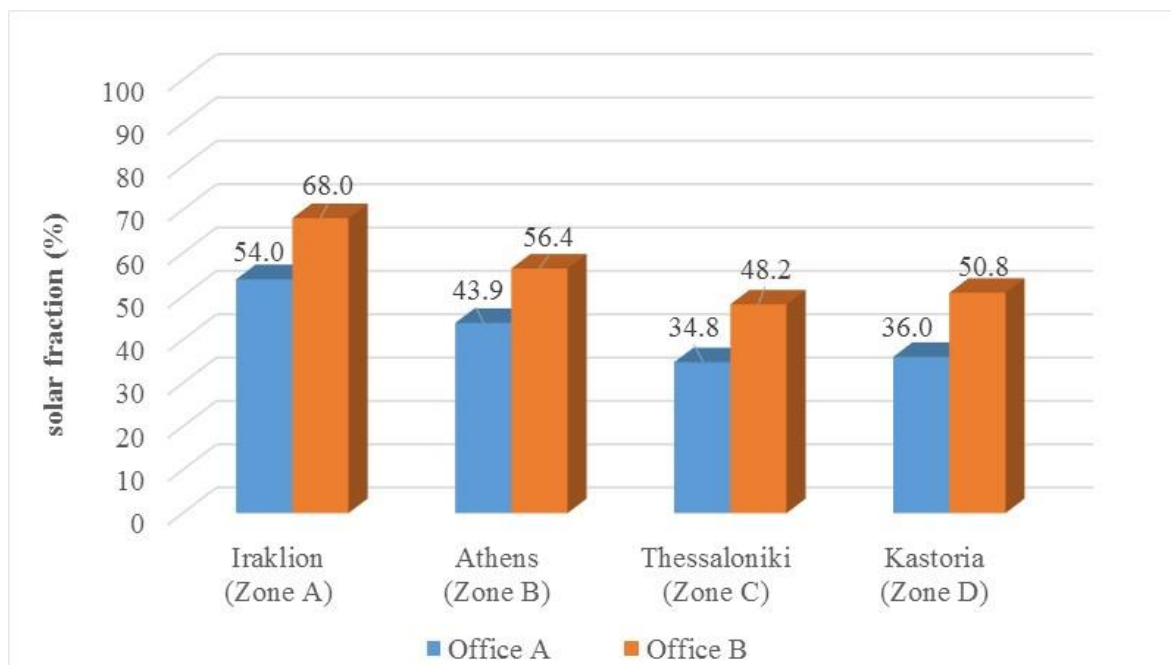


Figure 32: Yearly solar fraction comparisons between the two office rooms in all the climatic zones of Greece for the west orientation of building

As can be observed from the results for all the climates, office room A (manager\_a) has higher heating demands than office B (manager\_b), as anticipated. For example, in Kastoria the semi-external office A has a total heating demand of 78 kWh/m<sup>2</sup>·a compared to the much lower value of 35.39 kWh/m<sup>2</sup>·a (less than half) for the internal office B. Apparently, the impact of the building surfaces exposure appears directly to the heating demands, especially after the implementation of the active solar system. Particularly for Kastoria, the heating demand (auxiliary) after the solar system has been implemented becomes 49.89 kWh/m<sup>2</sup>·a for office A, while for office B this value reaches 17.40 kWh/m<sup>2</sup>·a, almost 1/3 of that for office A.

This impact is also reflected to the solar fraction percentages of the two offices. For the above example for Kastoria, the heating demand reduction by the solar system is at 36 % for office A, while it stands at 50.8 % for office B, showing the significant impact of the fact that office B is internal to a greater extent than office A. The same phenomenon is depicted in Figure 32 for the rest of the climatic zones as well.

This *low demand* scenario will be considered from now on for the two offices as a whole again, since the separate presentation of results for each office room was made only to understand the impact of the building surfaces exposure. The results for the *low demand* scenario are summarized for the two offices as a whole in Table 25 and Figure 30 of section 5.3.

### **High demand building**

It is now time to present the *higher demand* building scenario for the office buildings in Greece, which features a greater exposure of the building surfaces to the outer environment.

Specifically, in this scenario, the office building is considered as *detached*; the side walls of the two offices are considered as exterior, as well as the back wall of the corridor, the façade and the ceiling of the building. The floor is now connected to the ground. This can resemble a *high demand* scenario for the Greek office building stock, which can commonly be met in lower density urban areas or in the countryside.

The simulation results for this *high demand* scenario come up as below for the different climatic zones of Greece and west (average) building orientation:

West orientation	City (Climatic Zone)	$Q_{total}$		$Q_{aux}$		Solar fraction
		kWh	kWh/m <sup>2</sup> ·a	kWh	kWh/m <sup>2</sup> ·a	
	<b>Iraklion (Zone A)</b>	1236.2	45.79	822.4	30.46	33.5 %
	<b>Athens (Zone B)</b>	1702.1	63.04	1249.1	46.26	26.6 %
	<b>Thessaloniki (Zone C)</b>	2657.8	98.44	2066.3	76.53	22.3 %
	<b>Kastoria (Zone D)</b>	3789.3	140.34	2863.8	106.07	24.4 %

Table 27: Yearly simulated results comparison between the climatic zones of Greece for west orientation of building (high demand)

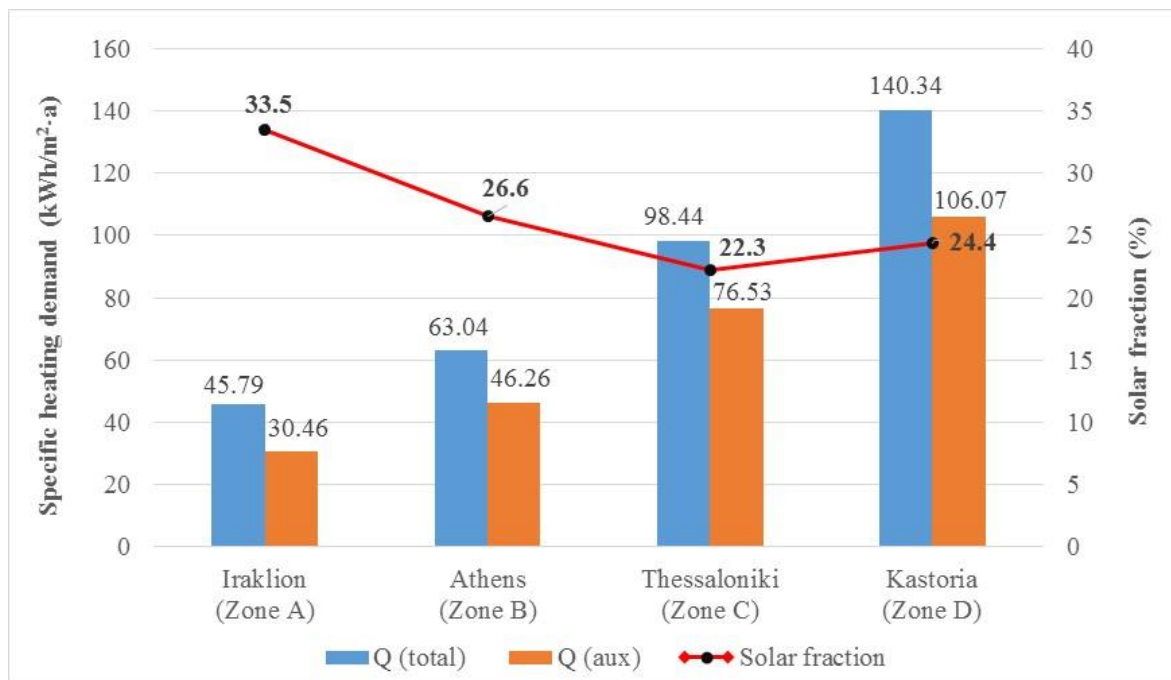


Figure 33: Specific heating demands before and after the implementation of the active solar system and respective yearly solar fractions for all the climatic zones of Greece with west orientation of building (high demand)

It is apparent from the results that in the case of a *high demand* building due to a high level of exposure of the structural surfaces to the outside, the thermal energy demand reduction achieved with the solar system becomes considerably lower for all the climates. This is the same conclusion extracted when office A and B of the *low demand* building were separately examined, where the solar fraction percentages were much lower for the “more exposed” office A. Thusly, the higher the building demands due to external exposure, the lower the solar fractional energy savings achieved by the solar system.

In the *high demand* office building particularly examined, the solar fractions have dropped to nearly 33.5 % for the warmest zone A, 26.6 % for zone B, 22.3 % for zone C and 24.4 % for zone D, which are remarkably lower than the 57.9 %, 47.7 %, 39 % and 40.7 % achieved respectively in the *lower demand* building. However, again the colder zone D shows a higher solar coverage than zone C, owing to its high solar radiation levels as discussed earlier in section 5.3.

## 5.5. Conclusion

In conclusion, this chapter studied thoroughly how the correlation of the building with the outer environment determined the energy performance of the active solar system in various scenarios. The impact of factors such as building orientation, weather characteristics and exposure of the building to the outside was notable on the degree of solar thermal energy utilisation.

After all, one of the building orientations (west) had to be chosen to represent the “average” orientation case, so as to be used afterwards to emulate the *low demand* and the *high demand* office building for the range of basic climates in Greece. The so-called *low demand* and *high demand* building scenarios were basically determined by the level of exposure of the structural surfaces to the outside. Ultimately, these are the most important outputs after this chapter ends, which will be used to extrapolate our results to the whole office building stock in Greece. For this reason, the results for the *low demand* and *high demand* building cases are summarized in Tables 28 and 29 below.

City	Climatic Zone	$Q_{total}$ (kWh/m <sup>2</sup> ·a)	$Q_{aux}$ (kWh/m <sup>2</sup> ·a)	Solar fraction
<b>Iraklion</b>	<b>A</b>	7.46	3.14	57.9 %
<b>Athens</b>	<b>B</b>	14.30	7.48	47.7 %
<b>Thessaloniki</b>	<b>C</b>	33.05	20.17	39.0 %
<b>Kastoria</b>	<b>D</b>	56.70	33.64	40.7 %

Table 28: *Low demand office building*

<b>City</b>	<b>Climatic Zone</b>	<b>Q<sub>total</sub></b> <b>(kWh/m<sup>2</sup>·a)</b>	<b>Q<sub>aux</sub></b> <b>(kWh/m<sup>2</sup>·a)</b>	<b>Solar fraction</b>
<b>Iraklion</b>	<b>A</b>	45.79	30.46	33.5 %
<b>Athens</b>	<b>B</b>	63.04	46.26	26.6 %
<b>Thessaloniki</b>	<b>C</b>	98.44	76.53	22.3 %
<b>Kastoria</b>	<b>D</b>	140.34	106.07	24.4 %

*Table 29: High demand office building*

## **6. Extrapolation to office building stock in Greece**

### **6.1. Introduction / Disclaimer**

This chapter will endeavour to refer to the whole office building stock in Greece, by extrapolating the previously simulated results for the active solar system to the total number of office buildings in the country. This is part of an effort to describe and predict what the effects would be for the non-residential office/commercial sector of Greece if a typical active solar thermal installation, like the one suggested therein, was to be applied massively.

These effects are appraised in terms of thermal energy savings and CO<sub>2</sub> emissions abatement for the whole country, respecting one particular sub-sector of services; the office/commercial sector, including both private and public offices. It is important to note that this endeavour expresses the author's personal standpoint, based on the simulation results and the relevant data/clues, where possible. Otherwise, when assumptions have to be made due to the lack of data, these are stated clearly in advance. Therefore, the current venture constitutes the author's personal work and estimations by any means, and has to be treated as accordingly.

### **6.2. Overview of office sector in Greece**

The total floor area of the office buildings in Greece can be estimated using a number of relevant sources. Firstly, the average floor area per capita in the country stands at 12 m<sup>2</sup>/cap for the services (non-residential) sector (Entranze, 2016). Using the Greek population number given for 2015 (UN, 2015) at around 10,955,000 residents, this results in nearly 131.5 million m<sup>2</sup> building floor area in the services (non-residential) sector in total.

The number of offices (both private and public included) can be extracted from the previous number, taking into account that 19 % of the floor area of non-residential buildings is occupied by offices (Entranze, 2016). This translates into:

$$0.19 \cdot 131,500,000 \approx 25 \text{ million m}^2 \text{ total floor area of offices in Greece}$$

In addition to the total floor area of office buildings in Greece, it is very useful to know the distribution of them between the four climatic zones of the country. There are sufficient data for this (Gaglia et al., 2007: 1163), where the above estimated

number can be crosschecked as well, with negligible deviation. Therefore, the data from this source will be used for the estimation of the office area share by climatic zone, as presented in Table 30.

<b>Climatic zones</b>	<b>Floor area (m<sup>2</sup>)</b>	<b>Distribution percentage</b>
<b>A</b>	2,641,015	10.34 %
<b>B</b>	14,004,147	54.82 %
<b>C</b>	8,513,392	33.33 %
<b>D</b>	385,581	1.51 %
<b>Greece (total)</b>	<b>25,544,135</b>	<b>100 %</b>

Table 30: Distribution of office buildings in Greece (2002–2010) by climatic zone (Source: Gaglia et al., 2007: 1163)

The average annual thermal energy consumption for space heating of the office/commercial buildings is nearly 70 kWh/m<sup>2</sup>·a in 2010 for Greece in total (Gaglia et al., 2007: 1167). This results in a total thermal energy demand yearly of around:

$$(70 \text{ kWh/m}^2\cdot\text{a}) \cdot (25,544,135 \text{ m}^2) \approx 1.788 \cdot 10^9 \text{ kWh} \quad \text{OR} \quad \mathbf{6.44 \text{ PJ}}$$

At this point, this estimation can be crosschecked by the 2012 European Commission report (Pardo et al., 2012: 60), which states that the thermal energy demand for space heating in offices in Greece for 2009 was 6.5 PJ (PetaJoules).

It is important that the data can be crosschecked from multiple sources, so that their quality is assured. Now, we can combine these two sources (Gaglia et al., 2007; Pardo et al., 2012) which are in accordance with each other, so that we can estimate the average annual total energy consumption share *by use* for the offices in Greece. This will be useful in our analysis later:

- Space heating: 6.5 PJ  $\Leftrightarrow$  70 kWh/m<sup>2</sup>·a (area = 25,544,135 m<sup>2</sup>)
- Water heating (Pardo et al., 2012: 60): 2.6 PJ  $\Rightarrow$  28 kWh/m<sup>2</sup>·a
- Space cooling (Pardo et al., 2012: 60): 15.3 PJ  $\Rightarrow$  166 kWh/m<sup>2</sup>·a
- Electricity (Gaglia et al., 2007: 1167): 71 kWh/m<sup>2</sup>·a

As a result, the **total** energy consumption in the Greek offices annually stands at nearly:

Total energy consumption (offices) =  $70 + 28 + 166 + 71 = 335 \text{ kWh/m}^2\cdot\text{a}$

This number can also be verified from a different source (Papamanolis, 2015: 394) with negligible deviation (by taking the weighted average for the four climatic zones for the total demands of offices).

This analysis will be important for our assumption to be based on, in order to estimate the thermal energy share *by fuel* for the space heating of offices in Greece, due to the lack of available data specifically on this. Our assumptions and the procedure to estimate the energy share *by fuel* is described analytically in the following section.

### 6.2.1. Analysis and assumptions for the estimation of share by fuel for the thermal energy used for space heating of offices in Greece

There are available data for the total energy consumption by fuel in services (non-residential) sector in Greece for the period 2000-2013 (Iatridis and Karamani, 2015: 32). If we compare the data for 2009, they are the same as presented in “Total unit consumption per  $\text{m}^2$  in non-residential” (Entranze, 2016). However, the most recent data for 2013 will be used (Iatridis and Karamani, 2015: 32), according to which for the total energy consumption in services in Greece:

- 82 % comes from electricity
- 9 % from oil
- 7 % from gas
- 2 % from renewable sources

The **assumption** that needs to be made here, due to the lack of more specific data, is that a similar total energy share by fuel is followed in the offices sector as well, which is part of the services sector. Thereupon, from the total of  $335 \text{ kWh/m}^2\cdot\text{a}$  in the offices:

- $0.82 \cdot 335 = 274.7 \text{ kWh/m}^2\cdot\text{a}$  comes from electricity
- $0.09 \cdot 335 = 30.15 \text{ kWh/m}^2\cdot\text{a}$  from oil
- $0.07 \cdot 335 = 23.45 \text{ kWh/m}^2\cdot\text{a}$  from gas

- $0.02 \cdot 335 = 6.7 \text{ kWh/m}^2\cdot\text{a}$  from renewable sources

Consequently, we can match the total energy share *by fuel* with the energy share *by use* in the Greek offices, as summarized in Table 31:

Total energy share by fuel in offices (kWh/m <sup>2</sup> ·a)		Total energy share by use in offices (kWh/m <sup>2</sup> ·a)	
Electricity	274.7	Space heating	70
Oil	30.15	Water heating	28
Gas	23.45	Space cooling	166
Renewable	6.7	Electricity	71
<b>Total</b>	<b>335</b>	<b>Total</b>	<b>335</b>

Table 31: Summary of total energy share by fuel (based on assumption and data) and by use (based on data) for the office sector in Greece

Attempting to match the above data, if electrical energy use (71 kWh/m<sup>2</sup>·a) and space cooling (166 kWh/m<sup>2</sup>·a) totally come from electricity, then the remaining electricity as a fuel is nearly  $274.7 - 71 - 166 = 37.7 \text{ kWh/m}^2\cdot\text{a}$  for the space and water heating needs.

Therefore, considering space and water heating demands together, as a total of  $70 + 28 = 98 \text{ kWh/m}^2\cdot\text{a}$ , these will have to be met by the remaining  $37.7 \text{ kWh/m}^2\cdot\text{a}$  of electricity,  $30.15 \text{ kWh/m}^2\cdot\text{a}$  of oil,  $23.45 \text{ kWh/m}^2\cdot\text{a}$  of gas and  $6.7 \text{ kWh/m}^2\cdot\text{a}$  of renewable sources. As a result, the share by fuel for (**space + water**) heating for the offices in Greece can be estimated as below:

- $37.7 / 98 \approx \mathbf{38 \% \text{ electricity}}$
- $30.15 / 98 \approx \mathbf{31 \% \text{ oil}}$
- $23.45 / 98 \approx \mathbf{24 \% \text{ gas}}$
- $6.7 / 98 \approx \mathbf{7 \% \text{ renewables}}$

Since there are no particular data available for the space heating and water heating separately in the office sector, we will **assume** that the above distribution of fuels for (space + water) heating together can be similarly applied to each one.

Therefore, the **assumed** share by fuel for **space heating** in the office sector in Greece is presented in the pie chart below:

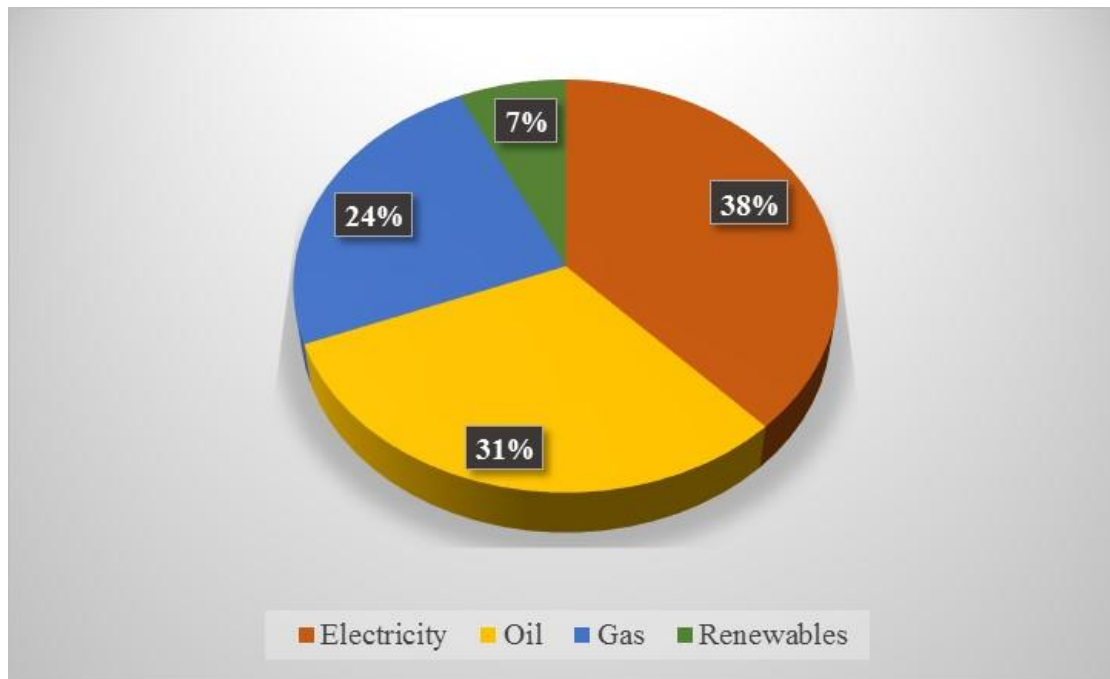


Figure 34: Estimation (based on assumptions) of share by fuel for the energy used for space heating of the offices in Greece

### 6.3. Realisation of active solar system for space heating of offices in Greece

The analysis for the active solar system application to the office buildings in different areas of Greece resulted in two different main result sets; one for a *low demand* and one for a *high demand* office building, as presented in Tables 28 and 29 of section 5.5 respectively. The general idea to approximate the typical office building in Greece is to consider a **combined** scenario, where the average of the *low demand* and the *high demand* building scenarios is calculated and regarded to be closer to the actual building.

This final combined scenario (Table 32) represents the typical (average) office building demand loads in Greece and, at the same time, approximates the performance of the active solar system of 2.16 m<sup>2</sup> collector area (**8 %** roof space coverage or 0.08 m<sup>2</sup> collector/m<sup>2</sup> floor), 151.2 L storage tank (**70 L/m<sup>2</sup>** of collector area and 5.6 L/m<sup>2</sup> floor) and 50° tilt angle of panels, as integrated to this building.

Climatic Zone	City	Q <sub>total</sub> (kWh/m <sup>2</sup> ·a)	Q <sub>aux</sub> (kWh/m <sup>2</sup> ·a)	Solar fraction
A	Iraklion	26.63	16.80	36.9 %
B	Athens	38.67	26.87	30.5 %
C	Thessaloniki	65.75	48.35	26.5 %
D	Kastoria	98.52	69.86	29.1 %
<b>GREECE</b>	<b>Total</b>	<b>47.35</b>	<b>33.64</b>	<b>29.0 %</b>

Table 32: Final combined scenario for the average office demands and the performance of the active solar system in Greece (average of low and high demand scenarios)

The combined scenario derives from taking the average values between the *low demand* (Table 28) and *high demand* (Table 29) building scenario for the Q<sub>total</sub> and Q<sub>aux</sub> in each climatic zone, and then calculating the final solar coverage fraction using the equation (4.1).

The total average specific demands for the whole of Greece (Table 32) constitutes the *weighted average* of the specific demands of each climatic zone, depending on the respective proportion of the floor area of offices from Table 30. For example, the total specific heating demand of the offices in Greece, as calculated from our base case model before implementing a solar system, stands at:

$$\text{Total specific heating demand (weighted average)} = 26.63 \cdot 0.1034 + 38.67 \cdot 0.5482 + 65.75 \cdot 0.3333 + 98.52 \cdot 0.0151 \approx \mathbf{47.35 \text{ kWh/m}^2\cdot\mathbf{a}}$$

For the whole country, this number translates into:

$$(47.35 \text{ kWh/m}^2\cdot\mathbf{a}) \cdot (25,544,135 \text{ m}^2) = 1.209515 \cdot 10^9 \text{ kWh} \approx \mathbf{4.35 \text{ PJ}}$$

---

### Matching with the real case heating demands

The resulting heating demands of total office buildings for the whole country yearly is around 4.35 PJ or 47.35 kWh/m<sup>2</sup>·a. It is reminded that our model includes thermal insulation of external walls, well-insulated ceiling (roof), double glazing and emulates a good management control system over the heating loops, the ventilation, the lighting and the power systems. However, this is not the current state of office buildings in Greece, which require a total of around **6.5 PJ** of thermal energy for space heating (Pardo et al., 2012: 60) or **70 kWh/m<sup>2</sup>·a** (Gaglia et al., 2007: 1167).

This difference is reasonable and implies that the Greek office building stock needs to be subject to significant improvements and renovations until it reaches the starting point where our model simulations correspond to. More specifically, a number of Energy Conservation Measures (ECMs) is proposed to be implemented to reduce the thermal energy requirements of non-residential buildings in Greece (Gaglia et al., 2007). After the implementation of various ECMs, such as thermal insulation of external walls and roofs, double glazing or a successful building management system, the thermal energy demand can be reduced up to approximately 600 GWh annually for Hellenic office/commercial buildings (Gaglia et al., 2007: 1171). This reduction is equal to 2.16 PJ, which means that the total thermal demands for space heating of offices yearly after the implementation of the ECMs are reduced to:

$$\text{After ECMs: } 6.5 - 2.16 = \mathbf{4.34 \text{ PJ}} \quad (\mathbf{33 \% \text{ reduction}})$$

**This is the same value derived from the above final combined scenario, which shows that our model approximates the real case thermal energy demands of Greek offices, after the respective Energy Conservation Measures (ECMs) have been implemented to the current office building stock. This is reasonable since our model features the characteristics implied by the proposed ECMs (Gaglia et al., 2007), such as thermal insulation of external walls and ceilings (roofs), double glazing or a successful management control system over the heating and ventilation of the building.**

---

Thereafter, the effect of the proposed active solar system [2.16 m<sup>2</sup> collector area (8 % roof space coverage or 0.08 m<sup>2</sup> collector/m<sup>2</sup> floor), 151.2 L storage tank (70 L/m<sup>2</sup> of collector area and 5.6 L/m<sup>2</sup> floor) and 50° tilt angle of panels] in the current study starts from the point of total space heating demands for Greek offices of around **4.35 PJ** annually or **47.35 kWh/m<sup>2</sup>·a**.

From this point, the estimated final thermal energy demand for space heating after the implementation of the active solar system drops at **33.64 kWh/m<sup>2</sup>·a**, featuring yearly thermal energy savings of nearly **29 %** for the total office sector of Greece. This would finally lead to a total thermal energy demand for space heating of approximately **3.09 PJ**, after the solar systems have been installed to the Hellenic office buildings.

The final thermal energy demand reduction percentages for each climatic zone stand at almost 37 % for zone A, 30.5 % for zone B, 26.5 % for zone C and finally 29.1 % for the coldest zone D. Apparently, zone D again shows a higher solar coverage percentage compared to zone C in this final combined scenario, for the reasons that have already been discussed in section 5.3. Figure 35 below summarizes the results for this final combined scenario, if realised within the Hellenic office building stock.

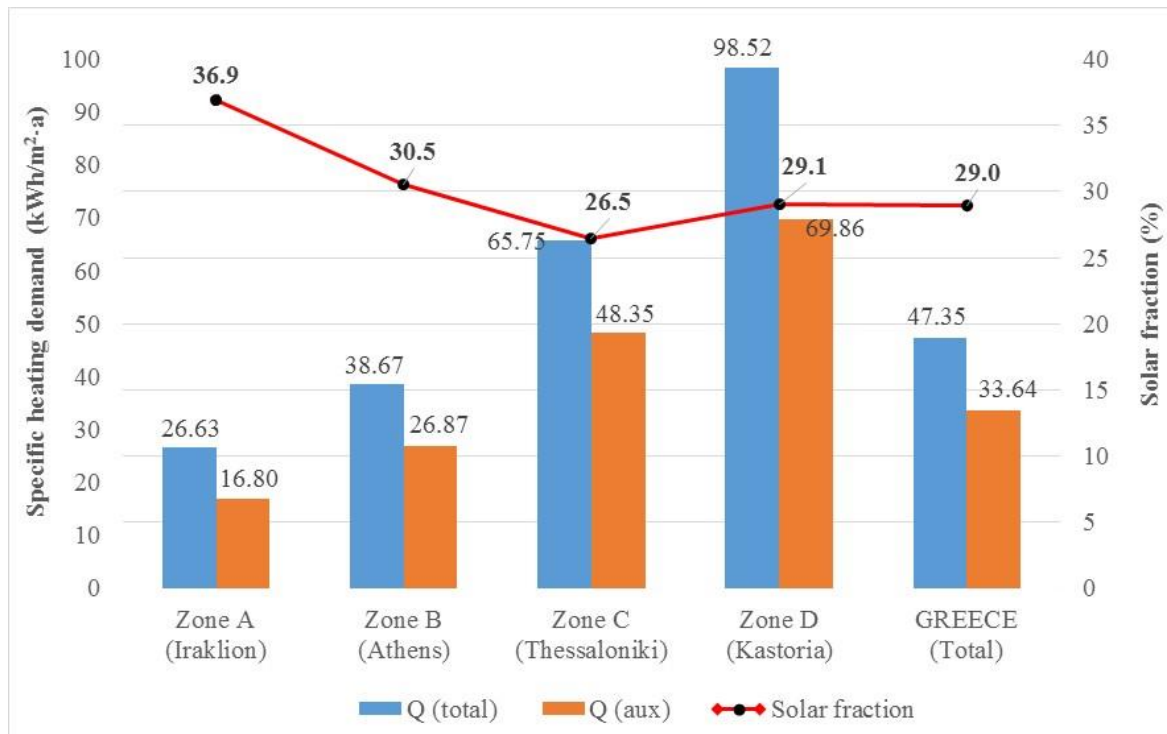


Figure 35: Specific heating demands before and after the active solar system implementation and respective yearly solar fractions for each climatic zone and total of Greece in the final combined scenario after extrapolation to the whole office sector

#### 6.4. Environmental performance appraisal and conclusions

The corresponding CO<sub>2</sub> emissions savings, after the implementation of the suggested solar space heating system for the Hellenic offices, have been calculated based on the share by fuel estimations for the space heating of offices, as concluded in section 6.2.1. This distribution is summarized in Table 33 below, where the specific CO<sub>2</sub> emissions factor considered for each fuel type is stated as well.

Firstly, for the electricity use, the estimations of emissions are based on 1.05 kg CO<sub>2</sub>/kWh of electrical energy generation in Greece (Gaglia et al., 2007: 1171).

Respectively, for the thermal energy production from oil, the estimations are based on 0.265 kg CO<sub>2</sub>/kWh (Gaglia et al., 2007: 1171; AEA, 2010: 9), while for the thermal energy produced from gas, 0.185 kg CO<sub>2</sub>/kWh (AEA, 2010: 9). Lastly, for the energy produced from renewable sources during their operation stage of life cycle, the CO<sub>2</sub> emissions are considered as zero.

<b>Fuel</b>	<b>Percentage share (%)</b>	<b>Specific emissions factor (kg CO<sub>2</sub> per kWh)</b>
<b>Electricity</b>	38	1.05
<b>Oil</b>	31	0.265
<b>Gas</b>	24	0.185
<b>Renewables</b>	7	0
<b>TOTAL</b>	100	0.52555

*Table 33: Percentage share by fuel for office space heating and specific CO<sub>2</sub> emissions factors used*

Regarding the share by fuel presented in Table 33, the equivalent specific CO<sub>2</sub> emissions factor, for the current situation of the space heating of offices in Greece is calculated at:

$$0.38 \cdot 1.05 + 0.31 \cdot 0.265 + 0.24 \cdot 0.185 + 0.07 \cdot 0 = \mathbf{0.52555 \text{ kg CO}_2 \text{ per kWh}}$$

This value is used for the estimation of the final CO<sub>2</sub> emissions abatement achieved after the implementation of the active solar space heating system in the office buildings of the whole country. The calculations are based on the final combined scenario of our simulations presented in Table 32, from which the total yearly thermal energy demand reduction (in kWh or PJ) and the equivalent CO<sub>2</sub> emissions abatement (in kt) per year derive for each climatic zone separately and then for the country as a whole, depending on the corresponding floor area of office buildings. These results are presented in Table 34 and Figure 36 below.

Climatic Zone	City	Floor area (m <sup>2</sup> )	Total thermal energy demand reduction per year (PJ)	CO <sub>2</sub> emissions abatement per year (kt)
A	Iraklion	2,641,015	0.09	13.6
B	Athens	14,004,147	0.60	86.8
C	Thessaloniki	8,513,392	0.53	77.8
D	Kastoria	385,581	0.04	5.8
<b>GREECE</b>	<b>Sum (total)</b>	<b>25,544,135</b>	<b>1.26</b>	<b>184</b>

Table 34: Final total thermal energy demand reduction and CO<sub>2</sub> emissions abatement per year after the implementation of the active solar system in the offices of whole Greece

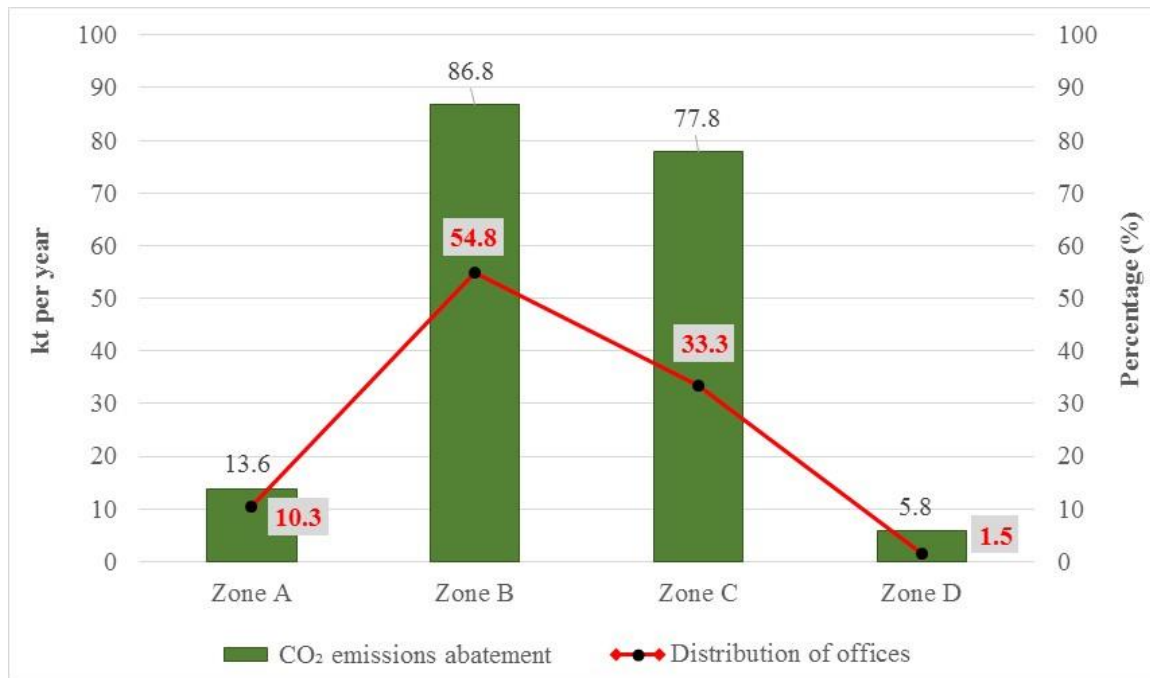


Figure 36: CO<sub>2</sub> emissions abatement in kilotonnes (kt) per year compared to the office floor area distribution in each climatic zone, after the implementation of the active solar system in the total number of offices

Certainly, the CO<sub>2</sub> emissions savings are proportionate to the thermal energy demand reduction for each climatic zone, which depends on the difference between  $Q_{\text{total}}$  and  $Q_{\text{aux}}$  in the final combined scenario (Table 32) and the corresponding office floor area in each zone.

It appears from the results that the *determinant* factor for the total CO<sub>2</sub> emissions abatement in each climatic zone is the total office buildings floor area. This can be

noticed from Figure 36, where the total CO<sub>2</sub> emissions savings are presented in parallel with the total office floor area distribution in each climatic zone.

The CO<sub>2</sub> savings are the highest (86.8 kt) for the climatic zone B, where the capital Athens is located, mainly because almost 55 % of the Greek offices are located in this zone. Zone C follows with 77.8 kt CO<sub>2</sub> savings, while accommodating 1/3 of the total office floor area of the country. Eventually, zone A and D present significantly lesser CO<sub>2</sub> emissions savings (13.6 kt and 5.8 kt respectively), since they accommodate a much smaller percentage of the total offices (10.3 % and 1.5 % respectively).

Ultimately, the CO<sub>2</sub> emissions abatement calculated for the whole office building stock of Greece, if the proposed active solar space heating system was to be applied massively, are approximately **184 kt** per year. This corresponds to a total thermal energy demand reduction of 1.26 PJ for the space heating of offices in the country, or nearly **29 %**.

## 7. Final discussion

To sum up, the installation of a closed loop forced circulation active solar system with flat plate collectors, storage capacity and closed radiator heating loop, featuring:

- *0.08 m<sup>2</sup> collector area / m<sup>2</sup> heated floor area*
- *70 L storage volume / m<sup>2</sup> of collector area or 5.6 L storage volume / m<sup>2</sup> heated floor area*
- *50° tilt angle of collectors and south orientation (180° azimuth angle from north)*

to the whole office building stock in Greece, of a total floor area of 25,544,135 m<sup>2</sup>, would result in a total solar collector area of nearly *2.05 million m<sup>2</sup>* and a storage capacity of roughly *143 million L* in total.

Compared to the total surface of glazed collectors, which was already operating in Greece in 2007 and reached approximately 3.57 million m<sup>2</sup> (Giakoumi and Iatridis, 2009: 21), the present venture for the office buildings would require almost 57 % more collector area to be added to the existing throughout the country.

If this system was to be applied massively to the total office building sector throughout Greece, a number of buildings would firstly need to be subject to significant improvements (Energy Conservation Measures or ECMs) as proposed by Gaglia et al. (2007), such as thermal insulation of external walls and roofs, double glazing and a successful building management system over the heating and ventilation controls.

After these upgrades have been implemented to the Hellenic office building stock, the currently proposed active solar system would be able to be applied massively with considerable outcomes. It is important that this system, as simulated in this study, would not require any further improvements in the heating system of the office buildings, such as the installation of an underfloor or wall-integrated heating loop. On the contrary, it is proven that the integration within the existing radiator heating loop would be feasible and would lead to remarkable results.

More specifically, after the essential fabric upgrades implied by the ECMs, the proposed active solar system would result in further thermal energy savings of 29 % for space heating and equivalent CO<sub>2</sub> emissions abatement of 184 kt in total within the Hellenic office building sector.

## **8. Proposals for further investigation**

The proposals for further research work to follow would include:

- The integration of an underfloor or wall-integrated heating system, instead of conventional radiators, which would offer a higher exchanging surface between the heating system and the room space. This would lead to more beneficial performance of the low temperature active solar system.
- The use of different technologies of solar collectors, such as evacuated tube collectors, which feature higher efficiency than flat plate collectors.
- The reduction of thermal losses through different parts of the system, such as the transparent covering of collectors or the storage tank, which would result in higher solar coverage fraction with the same system.
- A financial evaluation of the proposed active solar system application, in terms of installation/maintenance costs, potential revenues from incentive schemes and payback periods.
- An investigation into the potential of active solar space heating applications in other parts of the non-residential (services) sector of Greece, such as schools, hotels or hospitals.
- An investigation into the potential of active solar space heating applications in other sectors of Greece, such as in residential or industrial contexts.

## 9. References

AEA, (2010). *2010 Guidelines to Defra / DECC's GHG Conversion Factors for Company Reporting*. Produced by AEA for the Department of Energy and Climate Change (DECC) and the Department for Environment, Food and Rural Affairs (Defra). Version 1.2.1 FINAL.

Angrisani, G., Entchev, E., Roselli, C., Sasso, M., Tariello, F. and Yaïci, W. (2016). Dynamic simulation of a solar heating and cooling system for an office building located in Southern Italy. *Applied Thermal Engineering*, 103, pp. 377-390.

ArchiEXPO. (2016). *Electric hot water tank / solar / free-standing - WHPS BA DS - Fondital*. [online] Available at: <http://www.archiexpo.com/prod/fondital/product-78780-1529022.html> [Accessed 24 Aug. 2016].

BeNature. (2015). *Ideal solar panel angle: 3 factors to consider*. [online] Available at: <http://benature.tv/ideal-solar-panel-angle-3-factors-to-consider/> [Accessed 16 Aug. 2016].

Chwieduk, D.A. (2016). Active solar space heating. In: Wang, R. and Ge, T. eds. *Advances in solar heating and cooling*. Amsterdam: Elsevier, pp. 151-202.

CIBSE, (2001). *Guide B2 - Ventilation and Air Conditioning*. London: CIBSE.

DOE. (2016). *Active Solar Heating*. [online] Available at: <http://energy.gov/energysaver/active-solar-heating> [Accessed 21 Jul. 2016].

Duarte, C., Van Den Wymelenberg, K. and Rieger, C. (2013). Revealing occupancy patterns in an office building through the use of occupancy sensor data. *Energy and Buildings*, 67, pp. 587-595.

Duffie, J. and Beckman, W. (2013). *Solar Engineering of Thermal Processes*, 4<sup>th</sup> edition, Hoboken: Wiley.

EnergyPlus (n.d.). *Weather Data / EnergyPlus*. [online] Available at: <https://energyplus.net/weather> [Accessed 1 Jul. 2016].

EnergyPlus Support. (2016). *Yahoo groups*. [online] Available at: [https://beta.groups.yahoo.com/neo/groups/EnergyPlus\\_Support/info](https://beta.groups.yahoo.com/neo/groups/EnergyPlus_Support/info) [Accessed 2 Jul. 2016].

Entranze. (2016). *Average floor area per capita. Share of non-residential in total buildings floor area. Total unit consumption per m<sup>2</sup> in non-residential*. [online] Available at: <http://www.entranze.enerdata.eu/> [Accessed 19 Aug. 2016].

ESRU. (n.d.). *ESP-r*. [online] Available at: <http://www.esru.strath.ac.uk/Programs/ESP-r.htm> [Accessed 15 Jun. 2016].

ESTIF, (2014). *Solar Thermal Markets in Europe. Trends and Market Statistics*. Brussels: European Solar Thermal Industry Federation.

Gaglia, A., Balaras, C., Mirasgedis, S., Georgopoulou, E., Sarafidis, Y. and Lalas, D. (2007). Empirical assessment of the Hellenic non-residential building stock, energy consumption, emissions and potential energy savings. *Energy Conversion and Management*, 48(4), pp.1160-1175.

Giakoumi, A. and Iatridis, M. (2009). Current state of heating and cooling markets in Greece. Policy development for improving RES-H/C penetration in European Member States (RES-H Policy). CRES, Greece: Intelligent Energy Europe.

GitHub. (2016). *Build software better, together*. [online] Available at: <https://github.com/> [Accessed 19 Jun. 2016]

GreenSpec. (2016). *Green Building Design: Solar hot water collectors*. [online] Available at: <http://www.greenspec.co.uk/building-design/solar-collectors/> [Accessed 20 Jul. 2016].

Iatridis, M. and Karamani, F. (2015). *Energy Efficiency trends and policies in Greece*. [online] Pikermi: Center for Renewable Energy Sources and Saving (CRES), Greece,

p.32. Available at: <http://www.odyssee-mure.eu/publications/national-reports/energy-efficiency-greece.pdf> [Accessed 16 Aug. 2016].

Jaehnig, D. and Weiss, W. (2007). *Design Guidelines - Solar Space Heating of Factory Buildings*. Gleisdorf: AEE INTEC.

Kalidasan, B. and Srinivas, T. (2014). Study on Effect of Number of Transparent Covers and Refractive Index on Performance of Solar Water Heater. *Journal of Renewable Energy*, 2014, pp.1-11.

Lorenzini, G., Biserni, C. and Flacco, G. (2010). *Solar thermal and biomass energy*. Southampton, UK: WIT.

Marcos, J., Izquierdo, M. and Parra, D. (2011). Solar space heating and cooling for Spanish housing: Potential energy savings and emissions reduction. *Solar Energy*, 85(11), pp. 2622-2641.

Marken, C. and Olson, K. (2003). *Part 2: Closed Loop Antifreeze*. SDHW Installation Basics. [online] Ashland: Home Power. Available at: <http://www.uvm.edu/~gflomenh/CDAE106/readings/sdhwinstallparttwo95-42.pdf> [Accessed 20 Jul. 2016].

OME, (2012). SOLAR THERMAL IN THE MEDITERRANEAN REGION. SOLAR THERMAL ACTION PLAN. Nanterre: Observatoire Méditerranéen de l'Energie.

Ozsoy, A., Demirer, S. and Adam, N. (2014). An Experimental Study on Double-Glazed Flat Plate Solar Water Heating System in Turkey. *AMM*, 564, pp.204-209.

Papamanolis, N. (2015). The first indications of the effects of the new legislation concerning the energy performance of buildings on renewable energy applications in buildings in Greece. *International Journal of Sustainable Built Environment*, 4(2), pp. 391-399.

Pardo, N., Vatopoulos, K., Krook-Riekkola, A., Moya, J. and Perez, A. (2012). *Heat and cooling demand and market perspective*. JRC Scientific and Policy Reports. [online] Petten: European Commission, p.60.

Available at:

<http://publications.jrc.ec.europa.eu/repository/bitstream/111111111/26989/1/Idna25381enn.pdf> [Accessed 15 Aug. 2016].

Peuser, F., Remmers, K. and Schnauss, M. (2002). *Solar Thermal Systems. Successful Planning and Construction*. Berlin: Solarpraxis.

Quaschnig, V. (2004). *Technology Fundamentals: Solar thermal water heating*. [online] Erneuerbare Energien und Klimaschutz. Available at: [http://www.volker-quaschnig.de/articles/fundamentals4/index\\_e.php](http://www.volker-quaschnig.de/articles/fundamentals4/index_e.php) [Accessed 21 Jul. 2016].

REUK. (2015). *DIY Solar Water Heating*. [online] Available at:

<http://www.reuk.co.uk/DIY-Solar-Water-Heating.htm> [Accessed 21 Jul. 2016].

Shojaeizadeh, E., Veysi, F., Yousefi, T. and Davodi, F. (2014). An experimental investigation on the efficiency of a Flat-plate solar collector with binary working fluid: A case study of propylene glycol (PG) – water. *Experimental Thermal and Fluid Science*, 53, pp. 218-226.

Sobhy, I., Brakez, A. and Benhamou, B. (2015). Dynamic modeling of thermal behavior of a solar floor heating system for a HAMMAM in Marrakech. *IEEE*. DOI: 10.1109/IRSEC.2015.7455139.

Solar365. (2016). *How to Set Up a Storage Tank for Solar Thermal Space Heating*. [online] Available at: <http://www.solar365.com/solar/thermal/how-set-storage-tank-solar-thermal-space-heating> [Accessed 20 Aug. 2016].

Solar King. (2016). *Forced circulation systems*. [online]

Available at: <http://solarking.me/forced-circulation-systems/> [Accessed 20 Aug. 2016].

Solar Sense. (2013). *Solar Geyser Technology Explained*. [online]

Available at: <http://www.solarsense.co.za/solar-water-heating-explained.php>  
[Accessed 30 Jun. 2016].

Stegou-Sagia, A., Koronaki, I.P. and Sagia, Z. (2010). A Solar Space Heating Plant for Greek Buildings with underfloor heating system. Proceedings of 23rd International Conference on Efficiency, Cost, Optimisation, Simulation and Environmental Impact of Energy Systems. ECOS 2010, Lausanne (Ecole Polytechnique Federale de Lausanne), Switzerland.

Strachan, P. (2000). ESP-r: Summary of Validation Studies. Glasgow: ESRU.

Streicher, W. (2016). Solar thermal technologies for domestic hot water preparation and space heating. In: Stryi-Hipp, G. ed. Renewable heating and cooling. Amsterdam: Elsevier, pp. 9-39.

TEE, (2012). Climatic Data of regions in Greece. T.O.T.E.E. 20701–3/2010 (In Greek). Available at: [http://helapco.gr/pdf/TOTEE\\_20701\\_3\\_Final\\_TEE\\_2nd.pdf](http://helapco.gr/pdf/TOTEE_20701_3_Final_TEE_2nd.pdf)

The Renewable Energy Hub. (2016). *Solar Thermal Information: The different types of solar thermal panel collectors*. [online]  
Available at: <https://www.renewableenergyhub.co.uk/the-different-types-of-solar-thermal-panel-collectors.html> [Accessed 19 Jul. 2016].

Thoubboron, K. (2015). *Solar Water Heating and Solar Space Heaters Explained*. [online] EnergySage. Available at: <http://news.energysage.com/solar-water-heating-and-solar-space-heaters-explained/#more-3421> [Accessed 28 Jun. 2016].

UN, (2015). *World Population Prospects: The 2015 Revision*. Key Findings and Advance Tables. [online] New York: United Nations, Department of Economic and Social Affairs, Population Division, p.26.  
Available at:  
[https://esa.un.org/unpd/wpp/Publications/Files/Key\\_Findings\\_WPP\\_2015.pdf](https://esa.un.org/unpd/wpp/Publications/Files/Key_Findings_WPP_2015.pdf)  
[Accessed 20 Aug. 2016].

Wang, R. and Ge, T. eds., (2016). *Advances in solar heating and cooling*.  
Amsterdam: Elsevier.

Weiss, W. ed., (2003). *Solar Heating Systems for Houses*. A design handbook for  
solar combisystems. London: James & James.

YPEKA, (2010). KENAK – Greek Regulation for the Energy Efficiency of Buildings.  
EK407/B/9.4.2010 (in Greek).

Zerrouki, A., Boumédién, A. and BouhadeF, K. (2002). The natural circulation solar  
water heater model with linear temperature distribution. *Renewable Energy*, 26(4), pp.  
549-559.

## 10. Appendix

The calculation of the vertices coordinates of the tilted solar collectors in ESP-r *cellular\_expl\_sdhw* model is summarized in the following Tables 35-38, expressed as a function of tilt angle ( $t$ ) in degrees ( $^{\circ}$ ) from horizontal.

Vertex	x	y	z
1	1.2	0	3
2	0	0	3
3	0	$1.2 \cdot \cos t$	$1.2 \cdot \sin t + 3$
4	1.2	$1.2 \cdot \cos t$	$1.2 \cdot \sin t + 3$
5	0	$0.01 \cdot \sin t$	$3 - 0.01 \cdot \cos t$
6	1.2	$0.01 \cdot \sin t$	$3 - 0.01 \cdot \cos t$
7	1.2	$1.2 \cdot \cos t + 0.01 \cdot \sin t$	$-0.01 \cdot \cos t + 1.2 \cdot \sin t + 3$
8	0	$1.2 \cdot \cos t + 0.01 \cdot \sin t$	$-0.01 \cdot \cos t + 1.2 \cdot \sin t + 3$

Table 35: Coordinates of vertices for *collec\_low* zone

Vertex	x	y	z
1	1.2	$1.2 \cdot \cos t$	$1.2 \cdot \sin t + 3$
2	0	$1.2 \cdot \cos t$	$1.2 \cdot \sin t + 3$
3	0	$2.4 \cdot \cos t$	$2.4 \cdot \sin t + 3$
4	1.2	$2.4 \cdot \cos t$	$2.4 \cdot \sin t + 3$
5	0	$1.2 \cdot \cos t + 0.01 \cdot \sin t$	$-0.01 \cdot \cos t + 1.2 \cdot \sin t + 3$
6	1.2	$1.2 \cdot \cos t + 0.01 \cdot \sin t$	$-0.01 \cdot \cos t + 1.2 \cdot \sin t + 3$
7	1.2	$2.4 \cdot \cos t + 0.01 \cdot \sin t$	$-0.01 \cdot \cos t + 2.4 \cdot \sin t + 3$
8	0	$2.4 \cdot \cos t + 0.01 \cdot \sin t$	$-0.01 \cdot \cos t + 2.4 \cdot \sin t + 3$

Table 36: Coordinates of vertices for *collec\_mid* zone

Vertex	x	y	z
1	1.2	$2.4 \cdot \cos t$	$2.4 \cdot \sin t + 3$
2	0	$2.4 \cdot \cos t$	$2.4 \cdot \sin t + 3$
3	0	$3.6 \cdot \cos t$	$3.6 \cdot \sin t + 3$
4	1.2	$3.6 \cdot \cos t$	$3.6 \cdot \sin t + 3$
5	0	$2.4 \cdot \cos t + 0.01 \cdot \sin t$	$-0.01 \cdot \cos t + 2.4 \cdot \sin t + 3$
6	1.2	$2.4 \cdot \cos t + 0.01 \cdot \sin t$	$-0.01 \cdot \cos t + 2.4 \cdot \sin t + 3$
7	1.2	$3.6 \cdot \cos t + 0.01 \cdot \sin t$	$-0.01 \cdot \cos t + 3.6 \cdot \sin t + 3$
8	0	$3.6 \cdot \cos t + 0.01 \cdot \sin t$	$-0.01 \cdot \cos t + 3.6 \cdot \sin t + 3$

Table 37: Coordinates of vertices for collec\_hi zone

Vertex	x	y	z
1	1.2	0	3
2	1.2	$3.6 \cdot \cos t$	$3.6 \cdot \sin t + 3$
3	0	$3.6 \cdot \cos t$	$3.6 \cdot \sin t + 3$
4	0	0	3
5	1.2	$-0.1 \cdot \sin t$	$0.1 \cdot \cos t + 3$
6	1.2	$3.6 \cdot \cos t - 0.1 \cdot \sin t$	$0.1 \cdot \cos t + 3.6 \cdot \sin t + 3$
7	0	$3.6 \cdot \cos t - 0.1 \cdot \sin t$	$0.1 \cdot \cos t + 3.6 \cdot \sin t + 3$
8	0	$-0.1 \cdot \sin t$	$0.1 \cdot \cos t + 3$
9	1.2	$1.2 \cdot \cos t$	$1.2 \cdot \sin t + 3$
10	1.2	$2.4 \cdot \cos t$	$2.4 \cdot \sin t + 3$
11	0	$1.2 \cdot \cos t$	$1.2 \cdot \sin t + 3$
12	0	$2.4 \cdot \cos t$	$2.4 \cdot \sin t + 3$
13	1.12	$0.08 \cdot \cos t - 0.1 \cdot \sin t$	$0.1 \cdot \cos t + 0.08 \cdot \sin t + 3$
14	1.12	$3.52 \cdot \cos t - 0.1 \cdot \sin t$	$0.1 \cdot \cos t + 3.52 \cdot \sin t + 3$
15	0.08	$3.52 \cdot \cos t - 0.1 \cdot \sin t$	$0.1 \cdot \cos t + 3.52 \cdot \sin t + 3$
16	0.08	$0.08 \cdot \cos t - 0.1 \cdot \sin t$	$0.1 \cdot \cos t + 0.08 \cdot \sin t + 3$

Table 38: Coordinates of vertices for col\_casee zone